# Austrian Journal of Technical and Natural Sciences

№ 7–8 2018
July – August

PREMIER
Publishing

Vienna 2018

# Austrian Journal of Technical and Natural Sciences

Scientific journal

№ 7–8 2018 (July – August)

ISSN 2310-5607



**Editorial office** Premier Publishing s.r.o.
Praha 8 – Karlín, Lyčkovo nám. 508/7, PSČ 18600

**E-mail:** pub@ppublishing.org

**Homepage:** ppublishing.org

**Austrian Journal of Technical and Natural Sciences** is an international, German/English/Russian language, peer-reviewed journal. It is published bimonthly with circulation of 1000 copies.

The decisive criterion for accepting a manuscript for publication is scientific quality. All research articles published in this journal have undergone a rigorous peer review. Based on initial screening by the editors, each paper is anonymized and reviewed by at least two anonymous referees. Recommending the articles for publishing, the reviewers confirm that in their opinion the submitted article contains important or new scientific results.

Premier Publishing s.r.o. is not responsible for the stylistic content of the article. The responsibility for the stylistic content lies on an author of an article.

Instructions for authors

Full instructions for manuscript preparation and submission can be found through the Premier Publishing s.r.o. home page at:
http://www. ppublishing.org.

Material disclaimer

The opinions expressed in the conference proceedings do not necessarily reflect those of the Premier Publishing s.r.o., the editor, the editorial board, or the organization to which the authors are affiliated.

Premier Publishing s.r.o. is not responsible for the stylistic content of the article. The responsibility for the stylistic content lies on an author of an article.

Included to the open access repositories:



Typeset in Berling by Ziegler Buchdruckerei, Linz, Austria.
Printed by Premier Publishing s.r.o., Vienna, Austria on acid-free paper.

# Section 1. Biology

*Zhurlov Oleg Sergeevich,*
*Institute for Cellular and Intracellular Symbiosis,*
*Ural Branch Russian Academy of Sciences,*
*Orenburg, Russia*
*E-mail: jurlov1968@mail.ru*

*Mushinskiy Alexandr Alekseevich,*
*Institute for Cellular and Intracellular Symbiosis,*
*Ural Branch Russian Academy of Sciences,*
*Orenburg, Russia*
*E-mail: SAN2127@yandex.ru*

## METHODOLOGICAL APPROACHES TO THE STUDY OF MICROBIAL COMMUNITIES DEGRADIATED SOILS OF URBANIZED TERRITORIES

**Abstract:** Anthropogenic transformation of the soil cover of urban areas has a strong effect on the composition of microbial communities in urban soils. Degradation of soil cover in urban conditions is irreversible. The development of common methodical techniques for sampling soil for physico-chemical, microbiological and metagenomic research is necessary to monitor the entire range of indicators that determine the safety of the soil for the population. A single methodical sampling of soil samples will contribute to the effectiveness of assessing the "health" of the soil and the succession of microbial communities of soils in urbanized areas.

**Keywords:** urban soil, bacterial communities, topsoil material.

Urban ecosystems are formed in the soils of settlements and adjacent territories, which differ from natural zonal biogeocenoses [1]. In the conditions of large cities, industrial centers, the change in the ecological state of the environment is systemic [2]. Urban soil, like other components of the urban ecosystem, undergoes pressure of urbotehnogenesis transforming a relatively homogeneous landscape into a large variety of technogenic-altered soils.

Indeed, the generic title "made lands" hides a wide variety of both natural (conditionally undisturbed) and anthropogenically-modified soils [3].

The main differences of «urban» soil, from soils of natural landscapes, are the diversity of the morphological structure, the mosaic nature of the soil contours and the contrast of the physico-chemical and biological properties of soils. Anthropogenic transformation of the soil cover affects not only the structure of the soil horizons and the physico-chemical properties of the soil, but also the composition of microbial communities of urban soil [4].

Anthropogenic modification of "urban" soils causes degradation of the humus horizon. The humus layer of the soil is the main habitat of soil

microbiota and the decrease in the thickness of the humus layer of the soil affects its composition, turning fertile soil into low-productive lands with the dominance of oligotrophic microorganisms.

In addition, the pollution of urban soils with xenobiotics leads to the formation of a chemically-transformed surface horizon of soil [5]. So, with mechanical removal of the upper layers of the soil, the surface, the most valuable in the biocenotic relation, organogenic horizons of the soil (humus horizons) transforms into the so-called urbic horizon (depth ≤ 50 cm). It is formed from dump, mixed and imported soils. The profile of such soils consists of different coloring, thickness, lithology, time of bedding of layers and includes fragments of soil layers, construction and household garbage. In soils of natural landscapes and agrolandscapes, the humus horizon helps to increase the biological activity of soil microflora and plays an important role in maintaining the consistency of physico-chemical properties and soil buffering, migration of nutrients and the ability to bind heavy metals.

However, the change in the state of the humus horizon of the soil (its thickness, chemical composition and microbiocenosis) is not analyzed, despite the fact that this is an important factor in the remediation of technogenic-altered soils.

Moreover, an analysis of the "health" of soils is not possible without an evaluation of the succession of microbial communities. Therefore, the development of a single methodological sampling of soil sampling is necessary to monitor changes in the physicochemical parameters of the soil and the succession of microbial communities, which will provide important information on the ecological and trophic groups of microorganisms forming in urban soils, their variation under anthropogenic load and urban landscape features.

Thus, the anthropogenic transformation of the soil cover leads to a decrease in the enzymatic activity of microorganisms (urease, dehydrogenase, catalase and phosphatase) [6], which is related both to an increase in the concentration of pollutants and to decrease in the humidity of urban soils.

Despite the fact that natural-technogenic urban habitats are characterized by the preservation of the connection with the soil-forming rock, unchanged middle and lower horizons are always determined in the soil profile, but the connection with the vegetation cover is completely broken. The regeneration of anthropogenic-modified soil, with the remaining underlying soil horizons, is impossible with the use of mineral fertilizers alone, without the restoration of the humus horizon (microbial communities of soils) and the restoration of the content of ammonium and nitrate nitrogen [7]. The process of restoring the ecological functions of the soil, in urban conditions, is more complex and depends on a combination of factors of different genesis.

Undoubtedly, a change in the physico-chemical properties of urban soil affects the succession of microbial communities.

The accumulation of toxic species of micromycetes in the soil increases in conditions of technogenic pollution with the introduction of high doses of mineral fertilizers, with soil contamination with pesticides and heavy metals. So, in the soil near the roads there are toxin-producing micromycetes (*A. clavatus, A. ochraceus, A. terreus, A. terricola, A. fumigatus, P. funiculosum, P. rubrum, P. viridicatum, Talaromyces flavus, Botryotrichum piluliferum, Stachybotrys chartarum*) [8]. And many of them can be used for bioindication of soil pollution with oil products and heavy metals. Reducing the toxicity of the soil is one of main tasks facing regeneration of soils in urbanized areas.

Today, the application of methods of molecular genetic analysis in combination with the methods of cultivation bacteria on artificial nutrient media allows a fairly complete characterization of biological diversity of microorganisms contained in soils [9]. However, these methods are used separately from the physico-chemical and classical microbiological methods of soil analysis, often limited to screening

studies with the determination of the dominant phylogenetic groups of bacteria, the composition of the "minor" group of microorganisms, whose role in environmental safety of the soil is no less important, is not analyzed. With help of methods of metagenomic analysis of microbial communities of soils the main (dominant) groups of microorganisms composing microbial communities of soils of natural landscapes – *α-Proteobacteria, Actinobacteria, Acidobacteria, Verrucomicrobia, Bacteroidetes, Firmicutes, Gemmatimonadetes, Chloroflexi* [10]. It was shown that qualitative composition of microbial communities of soils in natural landscapes depends on two physico-chemical indicators of the soil (pH and humidity).

However, our knowledge of effectiveness impact of urbanization on entire ecosystem is very limited [11; 12]. Therefore, the development of methods for geoinformation mapping of microbial communities of soils will facilitate effective monitoring of changes in physico-chemical soil indicators and succession of microbial communities in urban areas.

Microbial communities of soil in urban landscapes, as one of components of the ecosystem, can serve as indicators of environmental changes in the environment.

**Conclusion**

Thus, the study of bacterial communities of urban soils is quite relevant, both in terms of obtaining information on composition of microbial communities and detection of microorganisms-indicators of soil pollution, which is of great practical importance for assessing the risks of soil pollution impact on environment and public health.

The development of scientific and methodological approaches to assessing the state of soils in urban landscapes and monitoring succession of microbial communities on basis of the maps [13], reflecting the most dangerous areas of changes in the geoecology of urban landscapes will help improve the efficiency of reclamation of technogenic contaminated soils.

Moreover, in order to completely restore the biological activity of the soil, it is necessary not only to restore the biodiversity of microbial communities of soils, but also to restore the ecological-trophic groups of microorganisms that are formed under similar conditions in soils of natural landscapes.

**Acknowledgements**

The reported research was funded by Russian Foundation for Basic Research and the government of the region of the Russian Federation, grant № 18–44–560005.

## References:

1. Pickett S. T. A., Cadenasso M. L., Grove J. M., Nilon C. H., Pouyat R. V., Zipperer W. C. et al. Urban ecological systems: linking terrestrial, ecological, physical and socioeconomic components of metropolitan areas. Annu. Rev. Ecol. Syst. 2001. – 32,– P. 127–157.
2. Vitousek P. M., Mooney H. A., Lubchenco J., Melillo J. P. Human domination on Earth's Ecosystems. Science. 1997. – 5225,– P. 494–499.
3. Pouyat R., Groffman P., Yesilonis I., Hernandez L. Soil carbon pools and fluxes in urban ecosystems. Environ. Pollut. 2002. – 116,– P. 107–118.
4. Kaye J. P., McCulley R. L., Burke I. C. Carbon fluxes, nitrogen cycling, and soil microbial communities in adjacent urban, native and agricultural ecosystems. Glob. Change Biol. 2005. – 11,– P. 575–587.
5. Anderson J. P.E. Soil respiration // Methods of soil analyses / Eds: A. L. Page, R. H. Millar, D. H. Keeney. Madison, Wisc. 1982.– P. 831–871.
6. Cardelli R., Vanni G., Guidi L., Marchini F., Saviozzi A. Antioxidant capacity in urban soils. Landscape and Urban Planning. 2014. – 124,– P. 66–75.

7. Fresquez P. R., Aldon E. F., Lindemann W. C. Enzyme activities in reclaimed coal mine spoils and soils. Landscape and Urban Planning.1987. – 14,– P. 359–367.
8. Svistova I. D., Koretskaja I. I. The accumulation of dangerous soil micromycetes to humans in the zone of influence of the highway «DON». Problems in medical mycology. 2014. – 4,– P. 38–40.
9. Zhurlov O. S., Grudinin D. A., Yakovlev I. G. Phylogenetic 16S metagenomic analysis and antibiotic resistance of psychrotolerant bacteria isolated from the soils of the Batagay Failure. International Journal of Applied and Fundamental Research. 2015.– P. 11–5,– P. 648–651.
10. Lauber C. L., Strickland M. S., Bradford M. A., Fierer N. The influence of soil properties on the structure of bacterial and fungal communities across land-use types. Soil Biol. Biochem. 2008. – 40,– P. 2407–2415. URL: http://doi.org/10.1016/j.soilbio.2008.05.021.
11. Byrne L. B., Bruns M. A., Kim K. C. Ecosystem properties of urban land covers at the aboveground-belowground interface. Ecosystems. 2008. – 11,– P. 1065–1077.
12. Cheng Z., Richmond D. S., Salminen O. S., Grewal P. S. Ecology of urban lawns under three common management programs. Urban Ecosyst. 2008 b. – 11,– P. 177–195.
13. Zhurlov O. S., Grudinin D. A. Theoretical approaches to creating a phylogenetic map of microbial communities of unique landscapes. Advances in current natural science. 2017. – 2,– P. 74–79.

# Section 2. Light industry

*Rasulova M. K.,*
*Tashkent institute of textile and light industry*
*E-mail: mastura_m@mail.ru*

## TREATING METHOD OF COTTON FABRICS TO REDUCE CREASING OF SPECIAL CLOTHING

**Abstract:** the article covers the research of creasing resistance of cotton fabric produced from local raw materials and treated with a modified urea-formaldehyde oligomer of the appropriate concentration and describes the optimal concentration of the oligomer for the treatment of cotton fabric based on the drying method.

**Keywords:** cotton fabric, creasing (resistance to creasing), modified urea-formaldehyde oligomer, drying method, product life period, concentration, washing.

Clothing is subject to many complex factors destroying it during its use. Most important of those factors are mechanical stimuli, such as stretching, abrasion and creasing [1].

Ever expanding variety of newly created and modified materials is used in the production of clothing. In assessing of the operational properties of clothing, stability of the initial appearance for the product life period is of increasing importance.

The desire of scientists to improve the performance properties of materials for clothing with its proper quality dictates the need to create new chemically active compounds for this purpose and technology for their application. It becomes necessary to determine the behavior of chemically active compounds with the material treated.

Clothing models' fast changeability imposes strict requirements to preservation of their form at use, which means that the ability of clothing materials (components and complete products alike) to resist deformation and preserve their original form after the external deforming force no longer affects it [2].

To increase the stability of the deformation to be set, it is advisable to the technological solutions use as a plasticizing medium used in final finishing of textile materials. Commonly, a cotton fabric is easily creased.

Textile materials are frequently exposed to direct contact with water. In everyday use, they are subject to washing, creasing due to exposure to rain, etc. On that basis, it is necessary to find make textile materials resistant to creasing.

Chemical processing technology in terms of giving and preserving the shape of clothing is most viable to that end. When assessing the operational properties of clothing, stability of the initial appearance for the product life period is of increasing importance.

To improve resistance to creasing, shrinkage capacities and to preserve form of cotton products, chemical processing of fabrics is used. When assessing the performance properties of clothing, stability of the initial appearance in the product life period is of increasing importance. The performance properties of clothing fabrics require the creation of new

finishing chemically active agents and technologies for their application. It becomes necessary to determine the behavior of chemically active agents in the material being processed.

The main principle of the developed method of crease-proof treating is that a technological solution based on a modified urea-formaldehyde oligomer is introduced into the steam medium during the steaming stage.

Urea-formaldehyde oligomer consists of the following components: water, urea, cystamin, sulfuric acid, cretonaldehyde [3].

It was determined, that during treating with modified urea-formaldehyde oligomer of appropriate concentration is sorbed on the surface of the cloth fibers, plasticizes them, transferring the polymer from vitrified to highly elastic state, penetrating into the fibers due to partial pressures at the interphase boundary.

Cotton fabric produced from local raw materials was chosen as the subject of the research of textile materials' resistance to creasing, used in the manufacture of special clothes with a surface density of 218 g/m$^2$ of twill interlacing and 5 variants of fabrics treated with a technological solution of the modified urea-formaldehyde oligomer of various concentrations under laboratory conditions. The consumption of technological consumption was 15–60 ml per sample of 150x250 mm, 15 ml interval. Drying was carried out in three ways: natural, contact and convective.

The treated fabrics were tested for creasing resistance on the fabric crease tester of Central Research Institute Of Cotton Industry, mark SMT ("CMT"), at a specific pressure of 0.1 MPa, load duration of 11 min., lay duration of 10 min. The fabric creasing resistance was characterized by the sum of recovery angles by warp and by weft [4].

Measurement of recovery angles was carried out after lagging the prepared samples under standard conditions with 60% relative humidity at 18–20 °C for 16 hours. The results of the research are shown in Table 1 and in the form of a diagram in Figure 1.

Research shown that the fabric treated with the use of traditional methods has a creasing resistance somewhat lesser (an average of 21°) compared to the fabric treated with modified urea-formaldehyde oligomer.

Table 1.– Creasing resistance of cotton fabric treated with a modified urea-formaldehyde oligomer

| № | Drying Method | Modified urea-formaldehyde oligomer concentration,%. | | | | |
|---|---|---|---|---|---|---|
| | | 1 | 3 | 5 | 10 | 15 |
| 1. | Natural | 52.1/61.1 | 62.2/70.0 | 72.6/78.8 | 77.7/72.5 | 70.0/67.7 |
| 2. | Contact | 57.6/62.7 | 67.8/68.5 | 75.0/73.3 | 77.7/65.5 | 66.1/64.4 |
| 3. | Convective | 57.5/58.3 | 69.4/64.4 | 74.1/74.1 | 71.7/62.2 | 65.2/61.8 |

*Note: numerator is warp, denominator is weft*

Therefore, the best effect was obtained by treating the cotton fabric with a modified urea-formaldehyde oligomer of 5% and 10% concentration.

Washing is carried out after a certain period of clothes usage. Clothes tear from the mutually overlapping interactions of wear and washing. The products made from natural fibers are the most frequently washed, many of which are more likely to tear from washing than wear. Tear from washing happens due to the destruction occurring both in the "rough" structure of the material and in the "fine" structure of the fibers. The destruction of external links in the "rough" structure of materials is mainly due to mechanical stimuli.

After treating with modified urea-formaldehyde oligomer, samples were washed 5 times according to standard procedures [5]. After washing the samples in a soapy solution, they are rinsed and dried at room temperature.

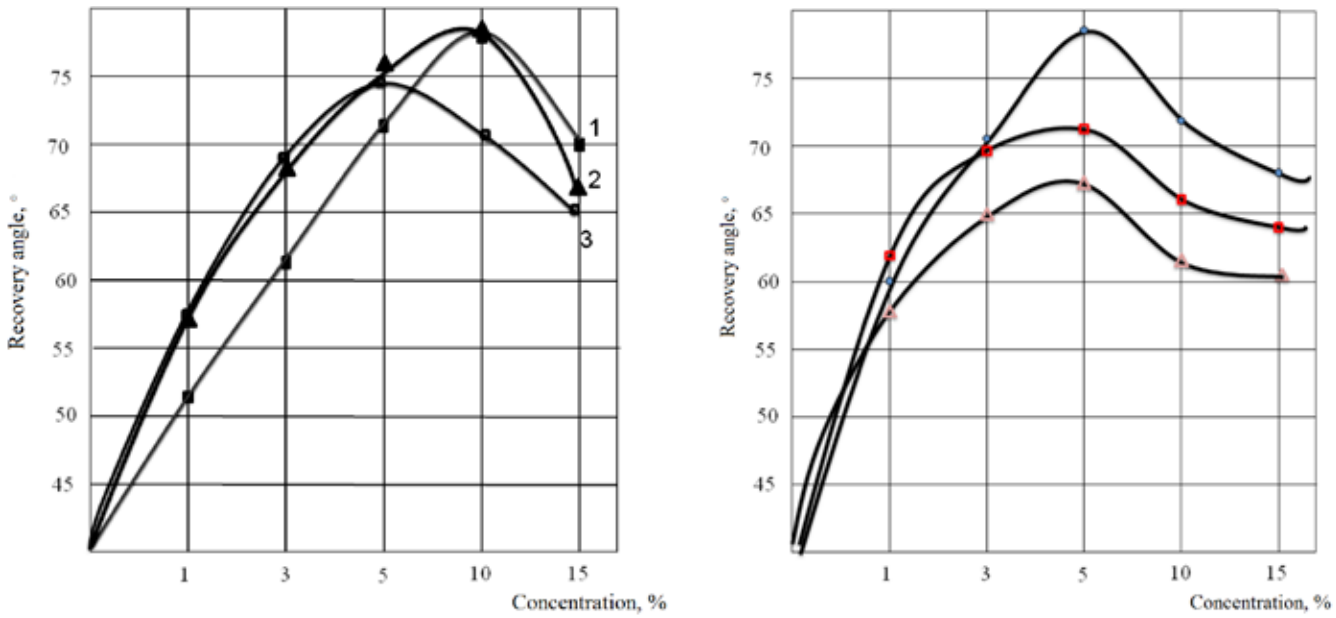


a) b)

Figure 1. The parameters of recovery angles in warp – (a) and in weft – (b), depending on the drying conditions of the samples: 1 – natural, 2 – contact and 3 – convective

After each wash, the samples were again tested for creasing resistance on the fabric crease tester of Central Research Institute Of Cotton Industry, mark SMT ("CMT"), at a specific pressure of 0.1 MPa, load duration of 11 minutes, lay duration of 10 min.

The parameters of recovery angles after washing are shown in (Table 2) and in the form of diagrams (Figures 2 and 3).

Table 2.– Creasing resistance of cotton fabric clothing treated with a modified urea-formaldehyde oligomer after washing

| № | Washed | Modified urea-formaldehyde oligomer concentration,%. | | | | |
|---|---|---|---|---|---|---|
| | | 1 | 3 | 5 | 10 | 15 |
| 1. | 1 time | 52.1/61.1 | 62.2/70.0 | 72.6/78.8 | 77.7/72.5 | 70.0/67.7 |
| 2. | 2 times | 52.0/61.5 | 62.3/70.0 | 72.5/78.7 | 76.5/72.0 | 70.2/67.5 |
| 3. | 3 times | 51.8/61.3 | 62.1/69.8 | 72.0/78.5 | 76.0/72.1 | 70.5/67.0 |
| 4. | 4 times | 51.9/61.2 | 62.0/69.8 | 72.6/78.4 | 75.8/72.1 | 69.7/66.8 |
| 5. | 5 times | 51.6/61.0 | 62.0/69.5 | 72.4/77.7 | 75.5/72.0 | 69.7/67.0 |

*Note: numerator is warp, denominator is weft*

Based on the foregoing, the following conclusions can be drawn: to ensure the best resistance to creasing of clothes made from cotton fabrics the most viable are: treatment with a 10% concentration of the modified urea-formaldehyde oligomer with natural and contact drying and contact and convective drying and the best resistance was obtained at 5% concentration. Therefore, based on drying method, it is possible to select the optimum concentration of oligomer for treating cotton fabric.

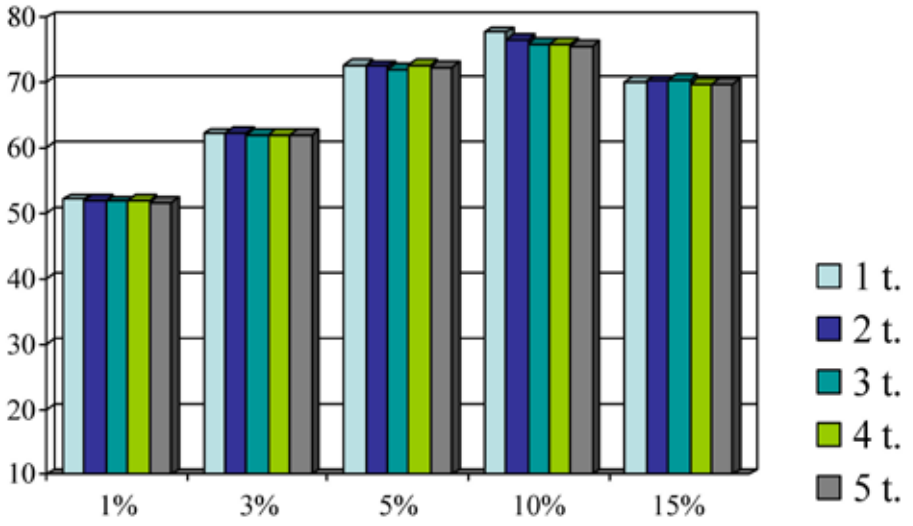


Figure 2. Recovery angles in warp after washing

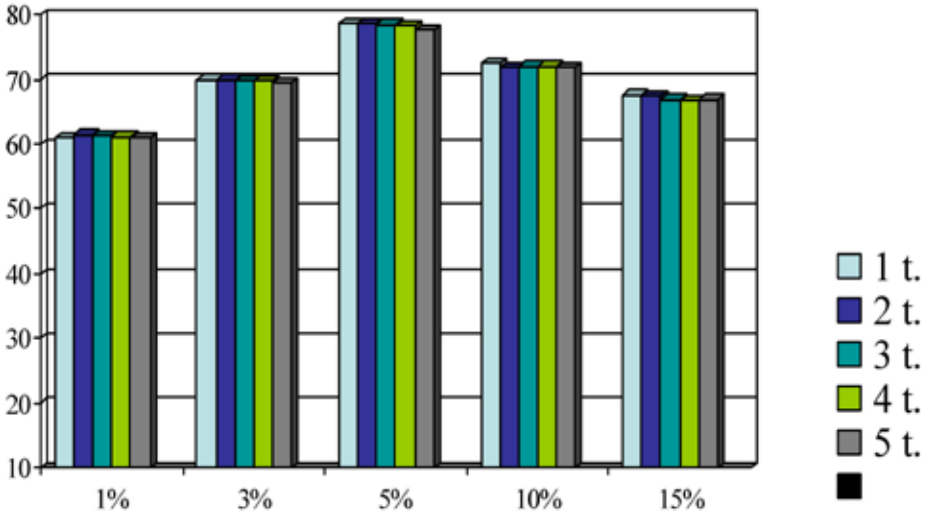


Figure 3. Recovery angles in weft after washing

## References:

1. Бузов Б. А., Модестова Т. А., Алыменкова Н. Д. Материаловедение швейного производства.– М.: «Академия», 2004.
2. Садыкова Ф. Х. Текстильное материаловедение и основы текстильных производств: Учебник для вузов.– М.: Легпромбытиздат, 1989.
3. Расулова М. К., Атабаева М., Кадыров Т. Ж. Повышение формоустойчивости хлопчатобумажных тканей, обработанных модифицированным олигомером. Журнал «Проблемы текстиля» 2012. – № 4.
4. Жерницын Ю. В. Методическое указание по выполнению научно-исследовательских и лабораторных работ по испытанию продукции текстильного назначения.– Ташкент, 2007.
5. ГОСТ 30157.1–95. Полотна текстильные. Методы определения изменения размеров после мокрых обработок или химической чистки. Режимы обработок.

# Section 3. Mathematics

*Dergachev Victor Mikhaylovich,*
*associate professor,*
*candidate physical. mat. sciences*
*Moscow polytechnical university,*
*Lelyavin Sergey Nikitovich,*
*associate professor,*
*candidate physical. mat. sciences*
*The Moscow state technical*
*university of N. E. Bauman*
*E-mail: lel@internets.ru*

## CREATION OF STABLE SIMPLICIAL COMPLEXES OF THE P. I

**Abstract:** A design of the classifying space [1, 7–12] it is very useful at the solution of various problems of algebraic topology.

In language of simplicial sets creation of simplicial analogs of varieties of Grassmann $G_N(A)$ and Shtifel $V_{N,K}(A)$ for an associative ring which are used in creation of functors is carried out: $F_G : G'_N(A) \to FNA(a_0,...,a_n)$, $F_V : V'_{N,K}(A) \to FNA_k(b_0,b_1,...,b_n)$ and stable simplicial complexes $\widehat{GL}(A),\widehat{G}(A),\widehat{V}(A)$.

**Keywords:** simplex, subalgebra, morphism, retraction, flag, functor.

**Theorem 1.** Let $NA(a_0,a_1,...,a_n)$ a nilpotent subalgebra for a nilpotent set of tops $(a_0,a_1,...,a_n)$ from $G_N(A)$ and $\Sigma_{n+1}$ a permutation group of $n+1$ elements, then for any substitution $\sigma \in \Sigma_{n+1}$ equality is fair: $NA(a_0,a_1,...,a_n) = NA\left(a_{\sigma(0)},a_{\sigma(1)},...,a_{\sigma(n)}\right)$ [7, 19–20].

Let's construct simplicial analogs of varieties of Grassmann $G_N(A)$ and Shtifel $V_{N,K}(A)$ for an associative ring, according to work [2, 103–109].

**Corollary 1.** Let $\left(a_{i_0},...,a_{i_k}\right) \subset (a_0,a_1,...,a_n)$ the investment of nilpotent subsets of tops from $G_N(A)$, then be available an investment of nilpotent subalgebras: $NA\left(a_{i_0},...,a_{i_k}\right) \subset NA(a_0,a_1,...,a_n)$ [7, 19–20].

**Corollary 2.** Let $\left(b_{i_0},...,b_{i_k}\right) \subset (b_0,...,b_n)$ the investment – nilpotent subsets of tops from $V_{N,K}(A)$, then be fair in the same party an investment $K$ – nilpotent subalgebras:

$NA_k\left(b_{i_0},...,b_{i_k}\right) \subset NA_k(b_0,...,b_n)$ [7, 19–20].

Owing to a **corollary 1.**: to an inclusion map of simplexes in $G'_N(A)$:

$j : \left(a_{i_0},...,a_{i_k}\right) \subset (a_0,...,a_n)$ there corresponds the investment of nilpotent subalgebras:

$NA\left(a_{i_0},...,a_{i_k}\right) \subset NA(a_0,a_1,...,a_n)$, owing to existence of a contravariant functor

$F : (a_0,...,a_n) \to FNA(a_0,...,a_n)$ we have display of retracts of admissible flags:

$F_G(j) : FNA(a_0,...,a_n) \to FNA\left(a_{i_0},...,a_{i_k}\right)$ also we have a contravariant functor $F_G$, which is associated with the simplicial scheme $G'_N(A)$ [1, 7–12].

**The remark.** Corresponds to any conditionally minimum simplex $\sigma^n \in D$ he, $\sigma^n = \bigcup_{i=1}^{k} \sigma^{n_i}$, $\sigma^{n_i}, i = 1,...,k$ at various minimum simplexes for $\sigma^n$ in $D$ [4, 165–166].

**Definition 1. (Grassmaniana.)** $\left(a_0, a_1, ..., a_n, F^n\right)$ – set is called

$n$ – dimensional simplex in a complex $G_N(A)$ we will also designate it through $\sigma_G^n$,
where $(a_0, a_1, ..., a_n)$ – a nilpotent set of tops from $G'_N(A)$, $F^n$ – the flag from $FNA(a_0, a_1, ..., a_n)$, number $n$ designates not dimension of a flag $F^n$.

Display $d_G$ of transition to subsimplexes in a complex $G_N(A)$:
if $j : \left(a_{i_0}, ..., a_{i_k}\right) \subset (a_0, ..., a_n)$ the investment of nilpotent sets of tops in $G'_N(A)$, then $d_G : \left(a_0, a_1, ..., a_n, F^n\right) \to \left(a_{i_0}, ..., a_{i_k}, F^k\right)$. Condition of transitivity for displays $d_G, F_G$, is also apparently carried out. The constructed simplicial $G_N(A)$ set is Grasmanian, similarly we build a simplicial complex $V_{N,K}(A)$: if $NA_k(b_0, b_1, ..., b_n)$, $K$ – a nilpotent subalgebra of algebra $End\left(A^N\right)$, $D_k$ – a subset $K$ – admissible flags for a subalgebra $NA_k(b_0, b_1, ..., b_n)$, $F \in D_k$ - any $K$ – an admissible flag at top $b_0 = \left(u_1^0, ..., u_k^0, Q_0\right)$, $D_k^* \subset D_k$

– a set $K$ – admissible flags at top $b_0$,
which have the same filtration on the module $Q_0$, as a flag $F$, then owing to the **theorem 1.** and **remarks:** there is the single minimum flag $F_{inf} \in D_k^* \subset D_k$.

We have display $p_k : D_k \to \tilde{D}_k$, which compares to each flag $F \in D_k$ a minimum flag $F_{inf} \in D_k^* \subset D_k$, where $\tilde{D}_k$ – a set of minimum flags $F_{inf}$ for flags $F \in D_k$.

So, $K$ – admissible flags $D_k$ corresponds to each subset owing to the constructed display $p_k$, the set of minimum flags $\tilde{D}_k \subset D_k$, so is defined an investment it is $i : \tilde{D}_k \subset D_k$. Easily possible to show that for any flag $F_{inf}$ fairly $p_k\left(i\left(F_{inf}\right)\right) = F_{inf}$, as $i\left(F_{inf}\right) = F_{inf}$ and because of the design of a flag $F_{inf}$, apparently that $p_k\left(F_{inf}\right) = F_{inf}$.

Thus, the composition $p_k \circ i$ is an identity mapping, i.e. $p_k : D_k \to \tilde{D}_k$ – a retraction on a subset.

**Definition 2. (Simplicial great number of Shtifel.)**

Owing to the perfect analogy to a complex $G_N(A)$ the contravariant functor $F_k$ (similar to a functor $F : NA(a_0, ..., a_n) \to FNA(a_0, ..., a_n)$ ) from category $K$ – nilpotent subalgebras of algebra $End\left(A^N\right)$ in category of retracts $K$ – admissible (minimum) flags is had:

$$F_k : NA_k(b_0, ..., b_n) \to F_k NA_k(b_0, ..., b_n).$$

Let's define a contravariant functor $F_V$ from the simplicial scheme $V'_{N,K}(A)$ in category of retracts $K$ – admissible flags $F_k NA_k(b_0, ..., b_n)$, to everyone $K$ – in we will
deliver to a nilpotent set of tops $(b_0, b_1, ..., b_n)$ in $V'_{N,K}(A)$ compliance $K$ – a nilpotent subalgebra of $NA_k(b_0, b_1, ..., b_n)$, which owing to existence of a contravariant functor $F_k$ there corresponds the retract $K$ – admissible flags $F_k NA_k(b_0, b_1, ..., b_n)$, then we have display on objects of categories: $F_V : (b_0, b_1, ..., b_n) \to F_k NA_k(b_0, b_1, ..., b_n)$.

Owing to a **corollary 2.**: to an inclusion map $K$ – a nilpotent set of tops (simplexes in $V'_{N,K}(A)$) $j : \left(b_{i_0}, ..., b_{i_k}\right) \to (b_0, b_1, ..., b_n)$ there corresponds the investment $NA_k\left(b_{i_0}, ..., b_{i_k}\right) \subset NA_k(b_0, b_1, ..., b_n)$, $K$ – nilpotent subalgebras to which owing to existence of a functor $F_k$ there corresponds display of retracts $K$ – admissible (minimum) flags: $F_V(j) : F_k NA_k(b_0, b_1, ..., b_n) \to F_k NA_k\left(b_{i_0}, ..., b_{i_k}\right)$ then we have the contravariant functor $F_V$, associated with the simplicial scheme $V'_{N,K}(A)$.

Let's construct the simplicial $V_{N,K}(A)$, set associated with a functor $F_V$. Let $\left(b_0, b_1, ..., b_n, F_1^n\right)$ is $n$ – a measuring simplex in a complex $V_{N,K}(A)$, we will designate it through $\sigma_V^n$, where $\left(b_0, b_1, ..., b_n, F_1^n\right)$ is $n$ – a measuring simplex (a nilpotent set of tops) in $V'_{N,K}(A)$, $F_1^n$ – some minimum flag from a retract $F_k NA_k(b_0, b_1, ..., b_n)$. The number $n$ is not dimension of a flag $F_1^n$.

Display $d_V$ of transition to subsimplexes in a complex here $V_{N,K}(A)$: if $j:(b_{i_0},...,b_{i_k})\to(b_0,b_1,...,b_n)$ the investment $K$ – nilpotent subsets of tops in $V'_{N,K}(A)$, then $d_V:(b_0,b_1,...,b_n,F_1^n)\to(b_{i_0},...,b_{i_k},F_1^k)$, where $K$ – a flag is image $K$ – a flag $F_1^n$ at display of retracts:

$$F_V(j):F_kNA_k(b_0,b_1,...,b_n)\to F_kNA_k(b_{i_0},...,b_{i_k}).$$

Transitivity conditions for displays $d_V,F_V$ are satisfied:

$$F_V(j_1)\circ F_V(j_2):F_kNA_k(b_0,b_1,...,b_n)\to F_kNA_k(b_{i_0},...,b_{i_k}),$$

$$d_V(j_1)\circ d_V(j_2):(b_0,b_1,...,b_n,F_1^n)\to(b_{i_0},...,b_{i_{k_1}},F_1^{k_1}),$$

where $j_1:(b_{i_0},...,b_{i_{k_1}})\to(b_{i_0},...,b_{i_{k_2}})$,

$j_2:(b_{i_0},...,b_{i_{k_2}})\to(b_0,b_1,...,b_n)$ serial investments in the simplicial scheme $V'_{N,K}(A)$.

The Constructed Set $V_{N,K}(A)$ are a simplicial greatnumberofShtifel.Display $p:V_{N,K}(A)\to G_N(A)$ was defined still at tops (zero-dimensional simplexes). Let's continue it on the arbitrariest $n$ – dimensional simplexes. For this purpose we will define display $p$ according to the common definition of display of one simplicial set associated with a functor in another [2, 103–109].

We will deliver to each $n$ – dimensional simplex in Shtifel $\sigma_V^n=(b_0,...,b_n,F_1^n)$ in compliance a $n$ – dimensional simplex in Grassmann $\sigma_G^n=(a_0,...,a_n,F_1^n)$ as follows: $K$ – the nilpotent set of tops $(b_0,...,b_n)$ is displayed on a nilpotent set of tops $(a_0,...,a_n)$ identically, so homomorphisms of projection $\varphi_i,\psi_i\in NA_k(b_0,...,b_n)$ do not change, and the homomorphisms $G_i$, transferring basis $u_1^0,...,u_k^0$ of the module $P_0=\{u_1^0,...,u_k^0\}$ to basis $u_1^i,...,u_k^i$ of the module $P_i=\{u_1^i,...,u_k^i\}$ are ignored, i.e. $G_i=0,i=1,...,n$. At the same time $K$ – the nilpotent algebra $NA_k(b_0,...,b_n)$ is naturally displayed on nilpotent algebra $NA(a_0,...,a_n)$, and a set $K$ – admissible flags $D_k$ for $K$ – nilpotent algebra $NA_k(b_0,...,b_n)$ naturally invests in a set of admissible flags $D$ for a subalgebra $NA(a_0,...,a_n)$, i.e. the minimum flag $F_1^n$ will be at the same time an element of a set of admissible flags $D\leftrightarrow F_1^n\in D$: everyone $K$ – the admissible flag of a set $D_k$ is an admissible flag of a set $D$.

For a flag $F_1^n\in D$ is available in a set of conditionally minimum flags $FNA(a_0,...,a_n)\subset D$, $F_1^n$ – some conditionally minimum flag.

Thus, it is defined: $p:V_{N,K}(A)\to G_N(A)$, $\left[(b_0,...,b_n,F_1^n)\to(a_0,...,a_n,F_1^n)\right]$ display of a simplicial set Shtifelya $V_{N,K}(A)$,, associated with a functor $F_V$ in the simplicial great number of Grassmann $G_N(A)$, associated with a functor $F_G$, which is display of the simplicial sets associated with functors.

To each morphism of simplexes $d_V:(b_0,b_1,...,b_n,F_1^n)\to(b_{i_0},...,b_{i_k},F_1^k)$ in a complex $V_{N,K}(A)$ to the answering investment $j:(b_{i_0},...,b_{i_k})\subset(b_0,...,b_n)$, $K$ – nilpotent sets of tops in a complex $V'_{N,K}(A)$, there corresponds the similar morphism of simplexes in a complex $G_N(A)$: $d_G:(a_0,...,a_n,F^n)\to(a_{i_0},...,a_{i_k},F^k)$, where $F^n,F^k$ images $K$ – flags $F_1^n,F_1^k$ respectively. And to each display of retracts $K$ – admissible flags: $F_V(j):F_kNA_k(b_0,...,b_n)\to F_kNA_k(b_{i_0},...,b_{i_k})$ the corresponding display of retracts answers: $F_G(j):FNA(a_0,...,a_n)\to FNA(a_{i_0},...,a_{i_k})$ admissible flags so the following charts, apparently, are commutative:

$$\begin{array}{ccccc}
F_kNA_k(b_0,...,b_n) & \xrightarrow{F_V(j_2)} & F_kNA_k(b_{i_0},...,b_{i_{k_2}}) & \xrightarrow{F_V(j_1)} & F_kNA_k(b_{i_0},...,b_{i_{k_1}}) \\
{\scriptstyle p}\downarrow & & {\scriptstyle p}\downarrow & & {\scriptstyle p}\downarrow \\
FNA(a_0,...,a_n) & \xrightarrow{F_G(j_2)} & FNA(a_{i_0},...,a_{i_{k_2}}) & \xrightarrow{F_G(j_1)} & FNA(a_{i_0},...,a_{i_{k_1}}),
\end{array}$$

$$\begin{array}{ccccc}
(b_0,...,b_n,F^n) & \xrightarrow{d_V(j_2)} & (b_{i_0},...,b_{i_{k_2}},F_1^{k_2}) & \xrightarrow{d_V(j_1)} & (b_{i_0},...,b_{i_{k_1}},F_1^{k_1}) \\
{\scriptstyle p}\downarrow & & {\scriptstyle p}\downarrow & & {\scriptstyle p}\downarrow \\
(a_0,...,a_n,F^n) & \xrightarrow{d_G(j_2)} & (a_{i_0},...,a_{i_{k_2}},F^{k_2}) & \xrightarrow{d_G(j_1)} & (a_{i_0},...,a_{i_{k_1}},F^{k_1}),
\end{array}$$

$$j_1:(b_{i_0},...,b_{i_{k_1}})\subset(b_{i_0},...,b_{i_{k_2}}),j_2:(b_{i_0},...,b_{i_{k_2}})\subset(b_0,...,b_n).$$

Let's use definition of general linear group $GL(n,A)$ and stable simplicial complexes $\widehat{GL}(A),\widehat{G}(A),\widehat{V}(A)$ according to works [1, 7–12] and [5, 118–126].

**Definition 3.** (Stabilization 1. (on the II item $Q$ in $G_N(A),V_{N,K}(A)$).

On on zero-dimensional simplexes we will construct an investment: $i_1^G:(P,Q)\to(P,Q\oplus A)$. We will continue this investment to a simplicial investment of complexes: $\widehat{i}_1^G:G_N(A)\to G_{N+1}(A)$ adding the module $A$, as a direct item to all terms of filtration of flags, similarly we define stabilization 1. in the Shtifelya complex: $V_{N,K}(A)$: $\widehat{i}_1^V:V_{N,K}(A)\to V_{N+1,K}(A)$, $i_1^V:(e_1,...,e_k,Q)\to(e_1,...,e_k,Q\oplus A)$

According to work [6, 567–572] straight lines limits of these stabilization set stable complexes on the II item $\widehat{G}_p(A),\widehat{V}_k(A)$.

**Definition 4.** (Stabilization 2. (on the I item in $G_N(A),V_{N,K}(A)$).

At a set of tops we define investments: $i_2^G:(P,Q)\to(P\oplus A,Q)$,

$i_2^V:(e_1,...,e_k,Q)\to(e_1,...,e_k,y,Q)$, $y$ – forming the module we $A$. Continue these displays to simplicial investments, adding the module $A$ to all terms of filtrations of flags.

Stable simplicial complexes $\widehat{G}(A)$ and $\widehat{V}(A)$, being direct limits of stabilization 1. and 2 [6, 567–572], there are simplicial complexes of Grassmann and Shtifel [5,118–126]. As display $p:V_{N,K}(A)\to G_N(A)$ switches with both stabilization, we receive a simplicial map of stable complexes: $p:\widehat{V}(A)\to\widehat{G}(A)$.

## References:


1. Dergachev V. M., Lelyavin S. N. The universal stratification and algebraic K – groups. Col. Scientific searching in the modern world. Makhachkala: Research Center Aprobation 2014.– No. 6.– P. 7–12.
2. Dergachev V. M., Lelyavin S. N. The universal object in algebraic K – theories. Col. A new word in science and practice. Novosibirsk: CRNS 2014.– No. 11.– P. 103–109.
3. Dergachev V., Lelyavin S. Design to algebraic K-functors. Austrian Journal of Technical and Natural Sciences – No. 3–4. 2015. (March–April),– P. 20–22.
4. Dergachev V. M., Lelyavin S. N. To creation of the infinite algebraic K – theories. International scientific conference. Fundamental and applied problems of mechanics.,– M., 2017. (October 24–27),– P. 165–166.
5. Dergachev V., Lelyavin S. The construction of the algebraic K-theory via simplicial analogues of manifolds Grassmann and Stiefel. Oxford Journal of Scientific Research, 2015.– No. 1. (9) (January-June).– Volume IV.– P. 118–126.
6. Dergachev V., Lelyavin S. Universal bundle in algebraic K – theory. Australian Journal of Scientific Research, 2014.– No. 1. (5) (January-June).– Volume IV.– P. 567–572.
7. Dergachev V., Lelyavin S. Creation of the infinite algebraic K – functors of the p. II. Austrian Journal of Technical and Natural Sciences.– No. 3–4. 2018. (March–April).– P. 17–20.

*Sadikaj Ndriçim,*
*Duka Anila,*
*MSc in Mathematics, the Faculty of Technical Sciences,*
*University "Ismail Qemali" Vlora, Albania,*
*E-mail: ndsadikaj@gmail.com, duka.anila@gmail.com*
*Nikollaq Gjika,*
*MSc in Physics, the Faculty of Technical Sciences,*
*University "Ismail Qemali" Vlora, Albania*
*E-mail: ngjika40@gmail.com*

# STRING INTERACTIONS IN RIEMANN SURFACES

**Abstract:** Interactions and the forces that mediate them make the world interesting. In this paper we will look at String interactions in Riemann surfaces. The world-sheets of interacting open strings are recognized to be Riemann surfaces, and interaction processes are seen to construct the moduli spaces of these surfaces. Conformal mapping is used to provide canonical presentations for interacting light-cone world-sheets.

**Keywords:** string, interactions, world-sheet, conformal map.

**1. Introduction**

Interactions arise very elegantly in string theory because they are described by processes in which strings join and split. In these processes, the world-sheets of free strings combine to form a single world-sheet, which represents the interaction. The goal is to turn a picture of a set of interacting strings into a number which gives the probability for that event to occur. Doing so involves three steps:

1. Drawing the string diagram and calculating the conformal map which gives a canonical representation of that diagram.

2. Using conformal field theory to calculate the scattering amplitude from the canonical representation.

3. Using formula to turn the scattering amplitude into a cross section.

**2. String interactions and global world-sheets**

Strings can interact in a rather limited number of ways. Two possible interactions of open strings go as follows: an open string can split into two open strings, and two open strings can join to form a single open string.

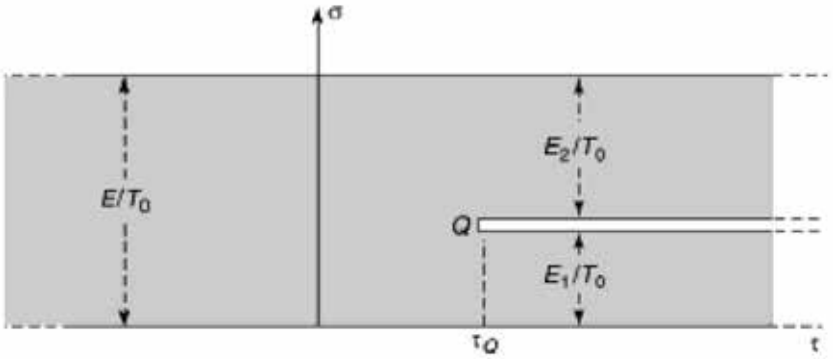


Figure 1. The basic open string interaction

String diagrams are representations of the string interactions. The focus of the string diagram is the $(\tau, \sigma)$ world-sheet. Interactions must be analyzed using a specic gauge, since gauge choices affect the world-sheet description. In this gauge

$$X^0(\tau, \sigma) = c\tau$$

and strings are parameterized using the energy $E$ that they carry:

$$\sigma \in [0, E / T_0] = [0, 2\pi\alpha' E]$$

where $T_0$ is the string tension. Since energy must be conserved and the energy of a string determines its σ length, the interactions must conserve the total σ length. Somewhat more complicated processes are also possible. The string diagrams are universal; the information about the specic particles only enters in step $(2)$ of the amplitude calculation. We select a Lorentz frame, use light-cone coordinates, and, with the above version of the light-cone gauge choice applied to each of the three strings, we have each string is parameterized by

$$\sigma \in \left[0, \frac{2\pi}{\beta}\right] = \left[2\pi\alpha' p^+\right]$$

where $p^+$ is the momentum carried by the string.

**3. World-sheets as Riemann surfaces**

If we take $\omega = \tau + i\sigma$, then we have the world sheet as a Riemann surface. The simplest world-sheet is that of a freely propagating open string. As shown in figure 2, the world-sheet for a string with light-cone momentum $p^+$ is the strip $0 \le Im(\omega) \le 2\pi\alpha' p^+$.

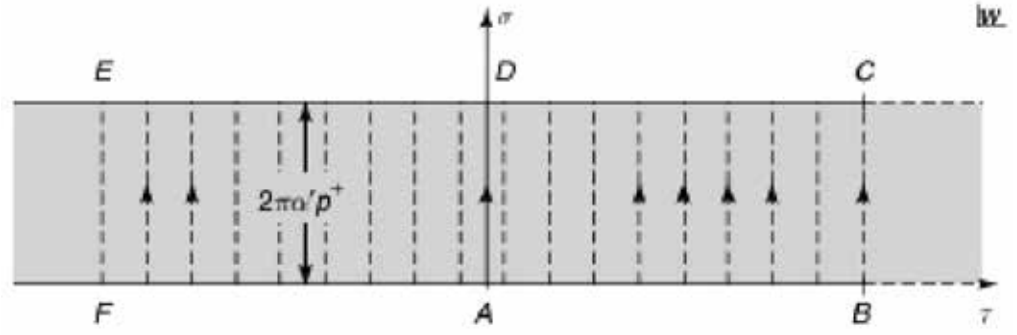


Figure 2. An open string moving from $\tau = \infty$ to $\tau = +\infty$

The strings are the vertical segments of constant $\tau$. If we using the exponential function

$$z = \exp\frac{\omega}{2\pi\alpha' p^+}.$$

As shown in the figure 2, the strings that approach the innite past approach the point $z = 0$. The two boundaries of the strip are mapped to the real line. The boundary $\sigma = 0$ is mapped to the positive half of the real line, while the boundary $2\pi\alpha' p^+$ is mapped to the negative half of the real line. The angle between the boundaries at the innite past has been changed.

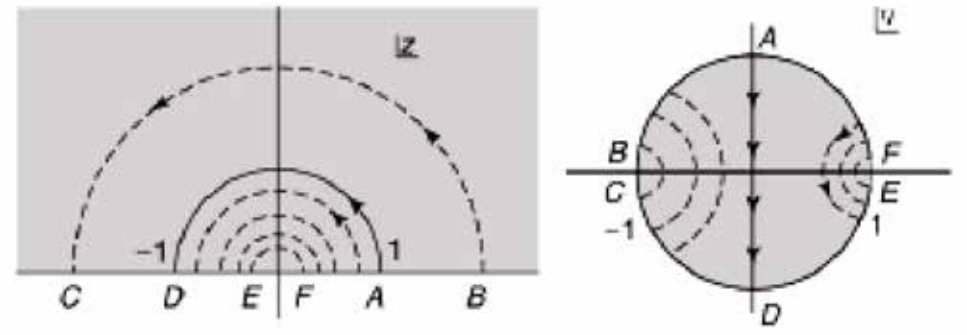


Figure 3. Left: the innite strip is mapped into H via the exponential map. Right: $\bar{H}$ is mapped onto the unit η disk via a linear fractional transformation

The boundaries make zero angle in the strip picture, they make an angle of 180° in the z-picture. The strip has been mapped into $\bar{H}$, and the strings appear as semicircles centered at $z = 0$. The string at $\tau = 0$ is the unit semicircle. The strings in the far future are very large semicircles on the $z$-plane. They grow without bound as the strings approach the infinite future. There is another useful presentation for the Riemann surface of a free open string. We can map $\bar{H}$ onto the unit disk in the η plane via the transformation

$$\eta = \frac{1+iz}{1-iz}.$$

This mapping, illustrated in the right side of (Figure 3), takes the real line $\mathrm{Im}(z) = 0$ into the unit circle.

**4. Schwarz-Christoffel map**

Following the intuition developed above, this surface should be conformally equivalent to a disk with three punctures on the boundary. The maps relating polygons and $\bar{H}$ are called Schwarz-Christoffel maps.

Suppose we have a polygon in the complex w-plane. Let the polygon have n sides and therefore n vertices, denoted by $P_1, P_2, \ldots, P_n$. The Schwarz-Christoffel map $\omega(z)$ takes $z \in \bar{H}$ into the polygon. The situation is illustrated in (Figure 4). We choose the boundary of the polygon to be oriented so that the interior of the polygon lies to the left of the oriented boundary. The mapping takes the real line in the $z$-plane, oriented in the direction of increasing values, into the oriented polygon boundary.

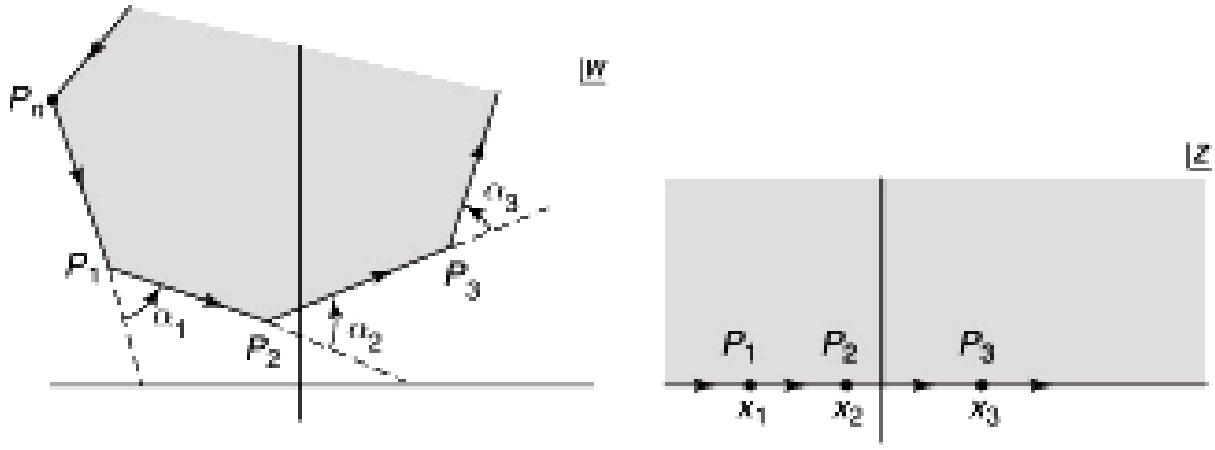


Figure 4. The Schwarz-Christoffel map $\omega(z)$ takes $\bar{H}$ onto the polygon

The polygon has turning angles $a_i$ at the vertices $P_i$. By denition, we restrict turning angles to the interval $[-\pi, \pi]$. The angles $\pi$ and $-\pi$ give completely different types of corners. We claim that the differential equation for the mapping function $\omega(z)$ is

$$\frac{d\omega}{dz} = A\left(z - x_1\right)^{\frac{\alpha_1}{\pi}} \left(z - x_2\right)^{\frac{\alpha_2}{\pi}} \ldots \left(z - x_{n-1}\right)^{\frac{\alpha_{n-1}}{\pi}}$$

Since a polygon is closed, the turning angles must sum to $2\pi$.

**5. String interaction**

Let us consider the process where two open strings join to form an intermediate string, which then splits into two open strings. The incoming strings are strings three and four, and the outgoing strings are strings one and two. The string diagram is shown in (Figure 5).

Note that the interaction point $Q_1$ occurs at $\tau = T_1$, and $Q_2$ occurs at $\tau = T_2$. The time interval between interactions is $T = T_1 - T_2$. We now use a Schwarz-Christoffel map to take this diagram into $\bar{H}$. The special points on the boundary of the string diagram are ordered as $(P_1 Q_1 P_2 P_3 Q_2 P_4)$.

At the points $P_i$ the turning angles are $+\pi$, and at the interaction points $Q_i$ the turning angles are $-\pi$. We therefore have

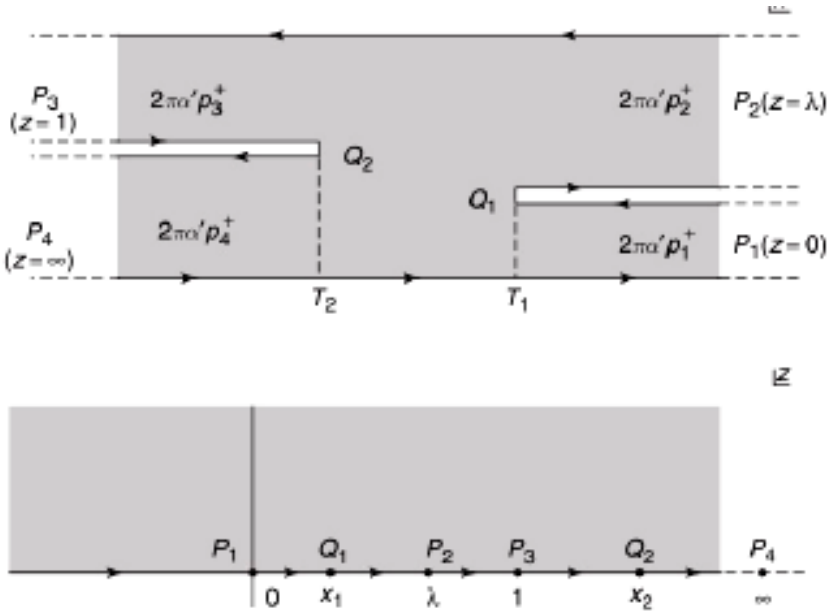


Figure 5. Top: a light-cone string diagram showing strings three and four joining to form an intermediate string that then splits into strings one and two. Bottom: the light-cone diagram is mapped into $\bar{H}$

$$\frac{d\omega}{dz} = A\left[\frac{1}{z}\frac{x_1 x_2}{\lambda} + \frac{1}{z-\lambda}\frac{(\lambda - x_1)(\lambda - x_2)}{\lambda(1-\lambda)} - \frac{1}{z-1}\frac{(1-x_1)(x_2-1)}{1-\lambda}\right]$$

This last equation, together with those previous, fixes the values of the unknown parameters.

**6. Veneziano amplitude**

Consider $\bar{H}$ punctured at $x_1$, $x$, $x_3$, and $x_4$ with $x_1 < x < x_3 < x_4$, as shown in (figure 6).

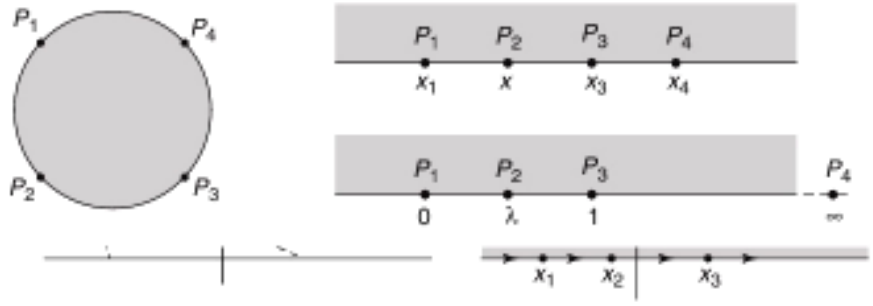


Figure 6. The scattering amplitude for four open string tachyons

At $x_1$ we introduce the tachyon with spacetime momentum $p_1$, at x the tachyon with momentum $p_2$, and at $x_3$ and $x_4$ the tachyons with momenta $p_3$ and $p_4$, respectively. Writing the scattering amplitude $A(p_1, p_2, p_3, p_4)$ as an integral

$$A(p_1, p_2, p_3, p_4) = \int g_0^2 d\mu,$$

the measure $d\mu$ must include a dx since we will integrate over $x$. We simplify the measure by choosing $x_1 = 0$, $x = \lambda$, $x_3 = 1$, and $x_4 = \infty$.

The Veneziano amplitude is given by

$$A(p_1, p_2, p_3, p_4) =$$

$$= g_0^2 \int_0^1 d\lambda \lambda^{2\alpha' p_2 p_1} (1-\lambda)(1-\lambda)^{2\alpha' p_2 p_3}$$

Thus the relevant invariants are

$$s = -(p_1 + p_2)^2 t = -(p_3 + p_4)^2$$

Using this relation, and the corresponding one for $t$, the Veneziano

amplitude is written as

$$A(p_1, p_2, p_3, p_4) = g_0^2 \int_0^1 d\lambda \lambda^{-\alpha(s)-1} \lambda^{-\alpha(t)-1}$$

**7. Conclusion**

We are at a stage where in we can understand what strings are, what they do, how to do what ever it is they do and finally how they form particles. Even though we did not talk about strings forming massive particles like electrons or protons or quarks etc, they are very much part and parcel of string theory.

## References:


1. Zwiebach B. A First Course in String Theory, Second Edition, 2009.
2. Becker K. M. Becker J. H. Schwarz: String Theory and M-theory, a modern introduction. 2007.
3. Krichever I. M., Novikov S. P. Virasoro-Gelfand-Fuks type algebras, Riemanfi surfaces, operator's theory of closed strings. 1988.
4. Collins C. John: Light-cone Variables, Rapidity and All that. 1997.
5. Veneziano G. Construction of a crossing-symmetric, Regge-behaved amplitude for linearly rising trajectories. 1968.

# Section 4. Mechanical engineering

*Vasenin Valery Ivanovitch,*
*associate professor, candidate of technical sciences,*
*department of "Materials, technologies and design of machinery"*
*State National Research Polytechnical University of Perm*
*E-mail: vaseninvaleriy@mail.ru*
*Bogomjagkov Aleksey Vasilievitch,*
*senior teacher*

## STUDY OF THE WORK OF THE GATING SYSTEM WITH SPRUES OF DIFFERENT HEIGHT

**Abstract:** The results of theoretical and experimental study with employment Bernoulli's equation of multi-gate system with 2 sprues of different height are given. Even though Bernoulli's equation is derived for the gating system with one gate and one sprue. The different heights of the sprues are taken into account by including their values in the head loss from each sprue to a zero point gate. He calculation is carried out by the method of successive approximations. Both in the calculation and in the experiment, the fluid velocities in the gates increase as they approach to a zero point gate from the sprues, in which they reach a maximum value.

**Keywords:** sprue, collector, gate, head, zero point, resistance coefficient, flow coefficient, flow velocity, fluid flow rate.

**Introduction**

Previously, *L*-shaped, *P*-shaped, branched, combined, cross, longline, ring-shaped (horizontal and vertical) gating systems (GS), as well as a two-ring system and *L*-shaped system with a collector of variable section were theoretically and experimentally studied. In the calculations of multi-gate GS, the Bernoulli's equation (BE) was used, although it was derived for a flow with a constant flow rate (mass) [1, p. 10; 2, p. 205], which means it should be used for GS with a single gate. Consequently, the Bernoulli's equation works with a flow with variable rate, although it is not clear why it does. And the possibility of using BE in the calculation of GS with a flow rate varying from maximum to zero in the collector (runner) *has not been theoretically proved*. In all the listed GS, only one sprue was used. However, several sprues are also can be used in gating systems ([3] for example). In articles [4–6], gating systems with sprues of equal height were studied. This article is devoted to the theoretical and experimental study of multi-gate gating systems with sprues of different heights.

**Research technique**

The gating system (shown in figure below) consists of 2 sprues of different heights, a collector and 7 gates. The internal diameter of the sprues is 175 mm. Fluid levels $H_1$ and $H_2$ – vertical distances from sections 1–1 and 16–16 to the horizontal axis of the collector – were maintained constant by con-

tinuously adding water to the sprues and draining its excess through special gaps in the sprues: $H_1 = 0.3680$ m, $H_2 = 0.4715$ m. Fluid pours out from the gates into castings. In the sections of the collector 5–5, …, 12–12, piezometers are installed for measuring the head: 500 mm glass tubes of 4.5 mm inner diameter. The time of the fluid outflow from each gate was 50–100s – depending on the number of simultaneously working gates and the volume of water pouring from the gate is about 8 liters. These time and weight limitations provided a deviation from the mean velocity value ±0.005 m/s. The flow rate for each gate was determined at least 7 times.

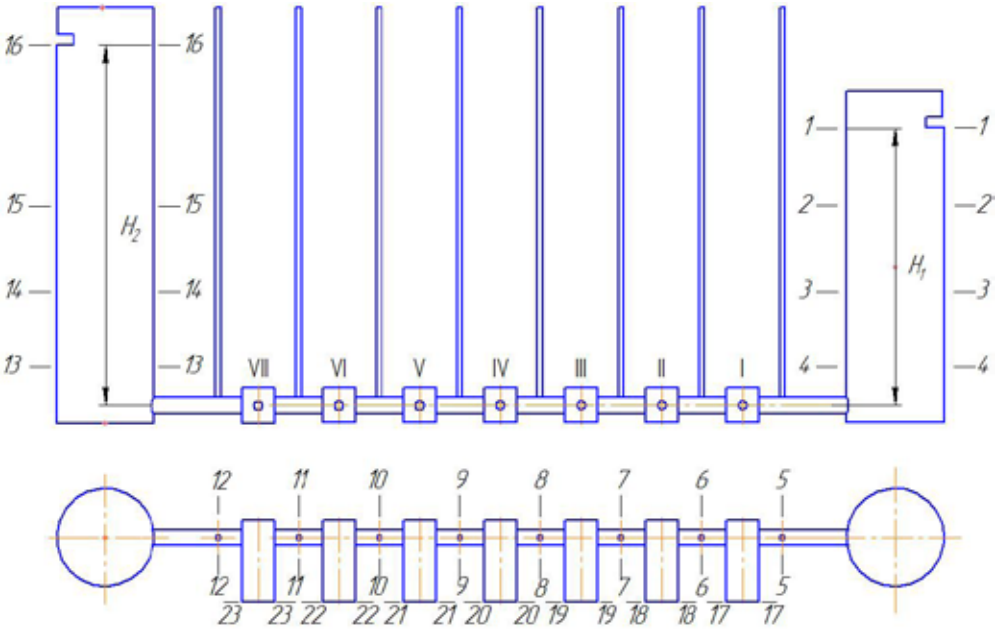


Gating system

**Main body**

Firstly, properties of GS at work of only one gate I will be calculated in the condition of opening the hydraulic system in section 12–12. Bernoulli's equation formulated for the sections 1–1 and 17–17 of GS:

$$H_1 = \alpha \frac{v_{17}^2}{2g} + h_{1-17}, \qquad (1)$$

$\alpha$ – is the coefficient of uneven velocity distribution over the flow section (Coriolis coefficient); and $\alpha = 1.1$ [2, p. 108]; $v_{17}$ – speed of metal in section 17–17, m/s; $g$ – acceleration of gravity; $g = 9.81$ m/s$^2$; $\gamma$ – specific weight of fluid metal, N/m$^3$; $h_{1-17}$ – loss of head when the fluid flows from section *1–1* to section 17–17, m. These loss of head

$$h_{1-17} = \left(\zeta_{sb} + \lambda \frac{l_0}{d_{sb}}\right)\alpha \frac{v_5^2}{2g} + \left(\zeta_g + \lambda \frac{l_g}{d_g}\right)\alpha \frac{v_{17}^2}{2g}, \qquad (2)$$

$\zeta_{sb}$ and $\zeta_g$ – coefficients of the local resistance of the metal inlet from the sprue to the collector and the rotation from the collector to the gate I; $v_5$ – fluid velocity in section *5–5* of collector, m/s; $d_{sb}$ and $d_g$ – hydraulic diameters of the collector and gate I, m; $\lambda$ – coefficient of friction loss; $l_0$ – distance between sprue and gate I, m; $l_g$ – length of gate, m. The flow rate in the GS at downwards discharge is determined by the speed of the metal $v_{17}$ in the outlet section 17–17 of gate I and its sectional area $S_g$:

$$Q_{17} = v_{17} S_g . \qquad (3)$$

The remaining fluid velocities in the GS channels are determined from the equation of continuity of the flow:

$$Q_{17} = v_5 S_{sb} = v_{17} S_g , \qquad (4)$$

$S_{sb}$ – is the sectional area of collector, m$^2$. Velocity $v_5$ shall be expressed (2) through velocity $v_{17}$, and

by using the equation of continuity of the flow (4), we obtain the following equation:

$$h_{1-17(17)} = \alpha \frac{v_{17}^2}{2g}\left[\left(\zeta_{sb} + \lambda \frac{l_0}{d_{sb}}\right)\left(\frac{S_g}{S_{sb}}\right)^2 + \zeta_g + \lambda \frac{l_g}{d_g}\right] \quad (5)$$

The equation in square brackets shall be denoted as $\zeta_{1-17(17)}$ – coefficient of resistance of the system from section 1–1 to section 17–17, deduced to the fluid velocity in this section:

$$\zeta_{1-17(17)} = \left(\zeta_{sb} + \lambda \frac{l_0}{d_{sb}}\right)\left(\frac{S_g}{S_{sb}}\right)^2 + \zeta_g + \lambda \frac{l_g}{d_g}. \quad (6)$$

Now (1) can be reduced to:

$$H_1 = \alpha v_{17}^2 (1 + \zeta_{1-17(17)})/2g. \quad (7)$$

And the coefficient of flow of the system from section 1–1 to section 17–17, deduced to the speed $v_{17}$,

$$\mu_{1-17(17)} = \left(1 + \zeta_{1-17(17)}\right)^{-1/2}. \quad (8)$$

Velocity

$$v_{17} = \mu_{1-17(17)} \sqrt{2gH_1/\alpha}. \quad (9)$$

Flow $Q_{17}$ is determined using equation (3). This gating system has gates with length of $l_g = 0.0495$ m, distance between gates is $l = 0.1190$ m, distance between the sprue and the first gate is $l_0 = 0.1220$ m. Diameters of gates and collector: $d_g = 0.00903$ m, $d_{sb} = d_5 = ... = d_{12} = 0.01603$ m. Let us assume that the friction loss coefficient is $\lambda = 0.03$ as in [7, 8]. The coefficient of local resistance of the inlet from the sprue to the collector is $\zeta_{sb} = 0.3$ [9]. Coefficient of local resistance at 90° rotation from the collector to the gate (with a change in sectional areas) is $\zeta_g = 0.334$ [10]. The results of calculations using relations (6), (8), (9) and (3), and experiments (in the denominator) are given in (Table 1) (flow rate is shown as $cm^3/s$). For the gate I, at the hydraulic system section 5–5, BE looks like this:

$$H_2 = \alpha \frac{v_{17}^2}{2g} + h_{16-17(17)}. \quad (10)$$

Head loss

$$h_{16-17(17)} = \alpha \frac{v_{17}^2}{2g}\left[\left(\zeta_{sb} + \lambda \frac{l_0 + 6l}{d_{sb}}\right)\left(\frac{S_g}{S_{sb}}\right)^2 + \zeta_g + \lambda \frac{l_g}{d_g}\right] \quad (11)$$

For gates IV and VII the calculations are done similarly. As can be seen from Table 1, the calculated values of velocities and flow are higher than the experimental ones.

Table 1. The performance of GS with one sprue and one gate

| Parameters | Working gates | | | | | |
|---|---|---|---|---|---|---|
| | I* | I** | IV* | IV** | VII* | VII** |
| $\zeta$ | 0.552 | 0.686 | 0.619 | 0.619 | 0.686 | 0.552 |
| $\mu$ | 0.803 | 0.770 | 0.786 | 0.786 | 0.770 | 0.803 |
| $v$ | 2.057 / 1.98 | 2.233 / 2.18 | 2.014 / 1.95 | 2.279 / 2.17 | 1.973 / 1.88 | 2.328 / 2.19 |
| $Q$ | 131.72 / 126.80 | 143.02 / 139.61 | 128.95 / 124.88 | 145.96 / 138.97 | 126.35 / 120.40 | 149.09 / 140.25 |

* *Supplied by sprue of $H_1$ height*

** *Supplied by sprue of $H_2$ height*

Next, the fluid flow rate in the system with no open gates shall be found. BE for sections 1–1 and 16–16 will be written as the equation [2, p. 216]:

$$H_2 - H_1 = \alpha \frac{v_5^2}{2g} \zeta_{16-1(5)}, \quad (12)$$

$v_5$ – is the metal velocity in the section 5–5 of collector, m/s; $v_5 = v_{12}$; $\zeta_{16-1(sb)}$ – is the coefficient of resistance of the system from section 16–16 to section 1–1, deduced to the fluid velocity in the collector. This coefficient can be calculated by using the following equation $\zeta_{16-1(sb)} = \zeta_{sb} + \lambda(2l_0 + 6l)/d_{sb} + \zeta_s$. $\zeta_s$ – is the coefficient of local resistance of the inlet from the collector to the sprue. This is the so-called entrance from

the pipe to the tank of large dimensions – a special case of sudden expansion of the flow, when, as in this case, $S_s >> S_{sb}$. $\zeta_{sb} = 1$ [2, c. 187]. Calculation results are: $\zeta_{16-1(5)} = 3.093$, $\mu_{16-1(5)} = 0.569$, $v_5 = 0.773$ m/s, $Q_5 = 155.92 \cdot 10^{-6}$ m$^3$/s. In the experiment: $Q_5^e = 155.84 \cdot 10^{-6}$ m$^3$/s.

Gate I work shall be calculated. BE for sections 1–1 and 17–17 is already been found – it is equation (1). And in the (2) equation of head loss local resistance coefficient of the rotation from collector to the gate $\zeta_g$ should be replaced by $\zeta_{17}$ – the coefficient of resistance to the branch of the flow from the collector section 6–6 to the gate I with the outlet section 17–17. BE for sections 16–16 and 1–1 is the (12) formula. Then, head loss should be deduced to the following equation:

$$h_{16-1} = \left(\zeta_{sb} + \lambda \frac{l_0 + 6l}{d_{sb}}\right)\alpha \frac{v_6^2}{2g} + \left(\zeta_5 + \lambda \frac{l_0}{d_{sb}} + \zeta_s\right)\alpha \frac{v_5^2}{2g}, \quad (13)$$

$\zeta_5$ – is the coefficient of resistance to the flow of fluids from section 6–6 to section 5–5 with branching of the flow from the collector section 6–6 to the gate I. The coefficients of resistance due to the branch of the flow from the collector to the gate will be calculated by the formulas for tees [1, p. 112–115]. Equation of coefficient of resistance to the passage in the collector when a part of the flow branches into the gate is as follows:

$$\zeta_{ps} = 0{,}4\left(1 - v_{ps} / v_{sb}\right)^2 / \left(v_{ps} / v_{sb}\right)^2, \quad (14)$$

and the equation of coefficient of resistance to the branching of part of the flow into the gate is

$$\zeta_{brn} = \left[1 + \tau\left(v_g / v_{sb}\right)^2\right] / \left(v_g / v_{sb}\right)^2, \quad (15)$$

$v_{sb}$ and $v_{ps}$ – is the velocities of the metal in the collector before and after the branching of part of the flow into the gate, m/s; $v_g$ – fluid velocity in the gate, m/s; $\tau$ – coefficient. In this case: $S_g / S_{sb} = 0.317$ $\tau = 0.15$ [11]. Coefficient $\zeta_{ps}$ is deduced to the velocity of passing flow $v_{ps}$ [in this case to $v_5$], and $\zeta_{brn}$ – to the velocity in gate $v_g$ [to $v_{17}$].

The value of the branched flow in the section 6–6 of gate I is unknown. Let us denote the following values as: $v_{5/6} = v_5 / v_6$. $Q_5 = v_{5/6} \cdot Q_6$. Flow rate in gate I: $Q_{17} = v_{17} S_g = \left(1 - v_{5/6}\right) Q_6 = \left(1 - v_{5/6}\right) v_6 S_{sb}$, and $v_{17} / v_6 = \left(1 - v_{5/6}\right) S_{sb} / S_g$ – is the $v_g / v_{sb}$ ratio in equation (15). Let us assume that $v_{5/6} = 0.5$. In equation (14) it is shown that $\zeta_5 = 0.4$, and $\zeta_{17} = 0.552788$ – according to (15).

By using $v_{5/6}$ ratio, from (13) we deduce that: $\zeta_{16-1(5)} = \left(\zeta_{sb} + \lambda \frac{l_0 + 6l}{d_{sb}}\right)\left(\frac{1}{v_{5/6}}\right)^2 + \zeta_5 + \lambda \frac{l_0}{d_\kappa} + \zeta_s$. We determine: $\zeta_{16-17(17)} = 1.468266$, $\mu_{16-17(17)} = 0.636508$, $v_{17} = 1.845857$ m/s, $Q_{17} = 118.212506 \cdot 10^{-6}$ m$^3$/s, $\zeta_{16-1(5)} = 9.086588$, $\mu_{16-1(5)} = 0.331741$, $v_5 = 0.450737$ m/s, $Q_5 = 90.966157 \cdot 10^{-6}$ m$^3$/s. Flow rate in the system: $Q = Q_6 = Q_5 + Q_{17} = 209.178664 \cdot 10^{-6}$ m$^3$/s. Ratio $v_{5/6} = 0.434873$. And we assumed that $v_{5/6} = 0.5$. Let us accept $v_{5/6} = 0.434873$, and, by repeating the calculation, we find that $v_{5/6} = 0.390640$. By using similar approximations for a given ratio $v_{5/6} = 0.2673069$ we determine $v_{5/6} = 0.26730694$. Thereon, the $v_5 / v_6$ ration calculation may be concluded since the resulting value differs from the given value by only 0.00000004. Let us accept $v_{5/6} = 0.267307$. The results of calculations and experiments are given in Table 2. We calculate the work of gates IV and VII similarly. Note that at work of gate I $v_5 / v_6 = 0.267$, for gate IV $v_8 / v_9 = 0.371$, and for gate VII $v_{11} / v_{12} = 0.456$. And at work of one gate with two sprues with a height of $H_1 = 0.3680$ m and $H_2 = 0.4715$ m in comparison to the work with one sprue with a height of $H_2 = 0.4715$ m the flow rate is 1.30 times greater for gate I, 1.48 times for gate II, and 1.69 times greater for gate VII. The calculated values of the fluid velocities at the gates are higher than the experimental values, and the theoretical velocities in the collector are lower than the experimental velocities.

Table 2. The performance of GS with two sprues and one gate

| Parameters | Working gates | | |
|---|---|---|---|
| | I | IV | VII |
| $\zeta_{16-17(17)}$ | 0.852 | – | – |
| $\zeta_{16-20(20)}$ | – | 0.874 | – |
| $\zeta_{16-23(23)}$ | – | – | 0.836 |
| $\zeta_{16-1(5)}$ | 30.329 | 11.738 | 5.664 |
| $\mu_{16-17(17)}$ | 0.735 | – | – |
| $\mu_{16-20(20)}$ | – | 0.731 | – |
| $\mu_{16-23(23)}$ | – | – | 0.738 |
| $\mu_{16-1(5)}$ | 0.182 | 0.292 | 0.420 |
| $v_{17}$ | 2.131 | – | – |
| $v_{20}$ | 2.09 – | 2.119 | – |
| $v_{23}$ | – | 2.08 – | 2.140 |
| $v_5$ | 0.247 | 0.397 | 2.12 0.571 |
| | 0.29 | 0.45 | 0.61 |
| $Q$ | 186.27 | 215.72 | 252.29 |
| | 192.37 | 224.02 | 258.88 |

When any one of the 7 gates is working, the right sprue is completely filled with fluid, which pours out through the gap in this sprue. If there are 2 or more gates, the right sprue is not filled with fluid up to the height of the gap, and the water does not pour out of it. Specifically, when gates I–II work $H_5 = 0.336$ m, I–IV – $H_5 = 0.228$ m, I–VII – $H_5 = 0.188$ m. Those $H_5$ values are calculable (we shall not describe it here). And at work of two or more gates, the fluid was poured into the right sprue to the height of $H_1 = 0.3680$ m.

Let us analyze the work of a system with two gates, I and II. It is clear that one of the gate there should be located at a point of confluence of flows (either a watershed point, or a zero point). The fluid flows to this point from both sides. In a system of two gates, the zero point is, apparently, in the gate II. However, calculations showed that $v_6 / v_5 = 0$. However, calculations showed that. In the experiment, section 6–6 was supplied with a tinted manganese fluid, and the tinted water was poured from the gate I, and not from the gate II. That is, the confluence of flows takes place in the gate I. Let us compile BE for sections *1–1* and *17–17*:

$$H_1 = \left(\zeta_{sb} + \lambda \frac{l_0}{d_{sb}}\right)\alpha \frac{v_5^2}{2g} + \left(\zeta_{gc} + \lambda \frac{l_g}{d_g}\right)\alpha \frac{v_{17}^2}{2g}. \quad (16)$$

BE for sections *16–16* and *18–18*:

$$H_2 = \left(\zeta_{sb} + \lambda \frac{l_0 + 5l}{d_{sb}}\right)\alpha \frac{v_{12}^2}{2g} + \left(\zeta_{18} + \lambda \frac{l_g}{d_g}\right)\alpha \frac{v_{18}^2}{2g}. \quad (17)$$

BE for sections *16–16* and *17–17*:

$$H_2 = \left(\zeta_{sb} + \lambda \frac{l_0 + 5l}{d_{sb}}\right)\alpha \frac{v_{12}^2}{2g} + \left(\zeta_6 + \lambda \frac{l}{d_{sb}}\right)\alpha \frac{v_6^2}{2g} + \left(\zeta_{gc} + \lambda \frac{l_g}{d_g}\right)\alpha \frac{v_{17}^2}{2g}. \quad (18)$$

The fluid enters the gate I from two sides: on the left from section *6–6* and on the right from section 5–5, from parallel pipelines. In this case, the coefficient of local resistance of rotation from the collector to the gate I $\zeta_{gc} = 0.218$ [12], is less than $\zeta_g = 0.334$ [10] coefficient of the fluid supplied to the gate from

one side. In $\zeta_{gc}$ "c" index means that the coefficient was determined by the supply of fluid to the gate from two sides (on the confluence of flows).

In equations (17) and (18) $\zeta_6$ – is the coefficient of resistance to the flow of fluids from section 7–7 to section 6–6 when part of the flow branches from the collector to the gate II; $\zeta_{18}$ – is the coefficient of resistance of branching of flow from the collector to the gate II with an output section 18–18. The value of the branched part of the flow from section 7–7 to gate II is unknown. Let us denote the following values as: $\nu_{6/7} = \nu_6 / \nu_7$. $Q_6 = \nu_{6/7} \cdot Q_7$. Flow rate in the gate II $Q_{18} = \nu_{18} S_g = (1-\nu_{6/7}) Q_7 = (1-\nu_{6/7}) \nu_7 S_{sb}$, and $\nu_{18} / \nu_7 = (1-\nu_{6/7}) S_{sb} / S_g$ – is the ration $\nu_g / \nu_{sb}$ in equation (15). Let us assume, that $\nu_{6/7} = 0.5$. By using equation (14) we determine, that $\zeta_6 = 0.4$; at $\nu_{6/7} = 0.5$ $\nu_{17} / \nu_7 = 1.575657$, and $\zeta_{18} = 0.552788$ – by using equation (15).

It is necessary to somehow connect the work of the sprues through the flow in the gate I – the place of confluence. We proceed as follows: arbitrarily set the ratio of the velocities $\nu_5$ and $\nu_6$ – $\nu_{6/5} = \nu_6 / \nu_5$. Flow rate in section *17–17* of the gate I $Q_{17} = \nu_{17} S_g = (\nu_5 + \nu_6) S_{sb} = (\nu_5 + \nu_{6/5} \nu_5) S_{sb} = (1+\nu_{6/5}) \nu_5 S_{sb}$, and $\nu_5 = \nu_{17} S_g / (1+\nu_{6/5}) S_{sb}$. Similarly we determine that $\nu_6 = \nu_{17} S_g / (1+1/\nu_{6/5}) S_{sb}$. And $\nu_7 = \nu_6 / \nu_{6/7}$. Now equations (16)–(18) can be deducted as follows:

$$H_1 = \alpha \frac{\nu_{17}^2}{2g} \left[ \left( \zeta_{sb} + \lambda \frac{l_0}{d_{sb}} \right) \left( \frac{S_g}{S_{sb}(1+\nu_{6/5})} \right)^2 + \zeta_{gc} + \lambda \frac{l_g}{d_g} \right]. \quad (19)$$

$$H_2 = \alpha \frac{\nu_{18}^2}{2g} \left[ \begin{array}{l} \left( \zeta_{sb} + \lambda \frac{l_0 + 5l}{d_{sb}} \right) \left( \frac{S_g}{S_{sb}(1+1/\nu_{6/5})} \right)^2 + \\ + \zeta_{18} + \lambda \frac{l_g}{d_g} \end{array} \right]. \quad (20)$$

$$H_2 = \alpha \frac{\nu_{17}^2}{2g} \left[ \begin{array}{l} \left( \zeta_{sb} + \lambda \frac{l_0 + 5l}{d_{sb}} \right) \left( \frac{S_g}{S_{sb}(1+1/\nu_{6/5})\nu_{6/7}} \right)^2 + \\ \left( \zeta_6 + \lambda \frac{l}{d_{sb}} \right) \left( \frac{S}{S(1+1/\nu_{6/5})} \right)^2 + \zeta_{gc} + \lambda \frac{l_g}{d_g} \end{array} \right]. \quad (21)$$

Equations in square brackets are the coefficients of local resistances, respectively $\zeta_{1-17(17)}$, $\zeta_{16-18(18)}$ and $\zeta_{16-17(17)}$. We calculate that: $\zeta_{1-17(17)} = 0.406096$, $\mu_{1-17(17)} = 0.843320$, $\nu_{17} = 2.160576$ m/s, $\zeta_{16-18(18)} = 1.378562$, $\mu_{16-18(18)} = 0.648400$, $\nu_{18} = 1.88034$ m/s, $\zeta_{16-17(17)} = 0.462899$, $\mu_{16-17(17)} = 0.826785$, $\nu_{17(16-17)} = 2.397656$ m/s. Velocities in the collector: $\nu_5 = 0.457074$ m/s, $\nu_6 = 0.228537$ m/s, $\nu_7 = 0.825222$ m/s. Ratio of velocities $\nu_{6/7} = 0.276940$. Ratio $\nu_{6/5} = 0.5$ is unchanged (at the current calculation method). It was assumed that $\nu_{6/7} = 0.5$.

We shall determine two ratios – $\nu_{6/5} = 0.5$ and $\nu_{6/7} = 0.5$. We need a criterion for finding these ratios by the method of successive approximations. The confluence of the flows takes place in the gate I. There are two parallel hydraulic lines – from the section *1–1* to the gate I and from the section *16–16* to the gate I. Head losses (taking $H_1$ and $H_2$ into account) should be equal in these lines. From section *1–1* to gate I it will be as follows: $h_{1-1} = H_1 - \left( \zeta_{sb} + \lambda \frac{l_0}{d_{sb}} \right) \alpha \frac{\nu_5^2}{2g}$, and from section *16–16* to gate I it will be $h_{16-1} = H_2 - \left( \zeta_{sb} + \lambda \frac{l_0 + 5l}{d_{sb}} \right) \alpha \frac{\nu_{12}^2}{2g} - \left( \zeta_6 + \lambda \frac{l}{d_{sb}} \right) \alpha \frac{\nu_6^2}{2g}$.

We should make derivation $\Delta h = h_{1-1} - h_{16-1} \to 0$. For the aforementioned example $h_{1-1} = 0.006188$ m, $h_{16-1} = 0.021054$ m, and $\Delta h = 0.088634$ m. When $\nu_{6/7} = 0.276940$ and $\nu_{6/5} = 0.5$ by calculation $\nu_{6/7} = 0.251126$, $\Delta h = 0.038365$. By changing $\nu_{6/5}$ and $\nu_{6/7}$, we calculate that $\nu_{6/5} = 1.087535$ and $\nu_{6/7} = 0.352347$ $\Delta h = -2.005 \cdot 10^{-7}$ m, and $\nu_{17} = 2.16941634$ m/s, $\nu_{17(16-17)} = 2.16941588$ m/s. Apparently, both the value $\Delta h$, and difference between $\nu_{17}$ and $\nu_{17(16-17)}$ be brought to any preassigned infinitesimal value.

Work of gates I and IV, I and VII is calculated similarly. The results of calculations and experiments are given in the (Table 3).

When gates I, II and III are working, the confluence of the streams takes place in the gate I, both in

calculation and in the experiment. BE for sections 1–1 and 17–17 is already been found – it is equation (16). BE for sections 16–16 and 19–19:

$$H_2 = \left(\zeta_{sb} + \lambda\frac{l_0+4l}{d_{sb}}\right)\alpha\frac{v_{12}^2}{2g} + \left(\zeta_{19} + \lambda\frac{l_g}{d_g}\right)\alpha\frac{v_{19}^2}{2g}. \quad (22)$$

BE for sections 16–16 and 18–18:

$$H_2 = \left(\zeta_{sb} + \lambda\frac{l_0+4l}{d_{sb}}\right)\alpha\frac{v_{12}^2}{2g} + \left(\zeta_7 + \lambda\frac{l}{d_{sb}}\right)\alpha\frac{v_7^2}{2g} + \left(\zeta_g + \lambda\frac{l_g}{d_g}\right)\alpha\frac{v_{18}^2}{2g}. \quad (23)$$

BE for sections 16–16 and 17–17:

$$H_2 = \left(\zeta_{sb} + \lambda\frac{l_0+4l}{d_{sb}}\right)\alpha\frac{v_{12}^2}{2g} + \left(\zeta_7 + \lambda\frac{l}{d_{sb}}\right)\alpha\frac{v_7^2}{2g} + \left(\zeta_6 + \lambda\frac{l}{d_{sb}}\right)\alpha\frac{v_6^2}{2g} + \left(\zeta_{gc} + \lambda\frac{l_g}{d_g}\right)\alpha\frac{v_{17}^2}{2g}. \quad (24)$$

$v_{7/8}$, $v_{6/7}$ and $v_{6/5}$ is defined. The coefficients of resistances $\zeta_7$ and $\zeta_{19}$ are calculated the same way as $\zeta_6$ and $\zeta_{18}$. Let us calculate the coefficients of resistances.

$\zeta_{1-17(17)}$, $\zeta_{16-19(19)}$, $\zeta_{16-18(18)}$ and $\zeta_{16-17(17)}$, flow rate, velocity and fluid flow coefficients. The equation for head losses from section 1–1 to gate I have already been determined. Head loss from section 16–16 to gate I (taking $H_2$ in account):

$$h_{16-1} = H_2 - \left(\zeta_{sb} + \lambda\frac{l_0+4l}{d_{sb}}\right)\alpha\frac{v_{12}^2}{2g} - \left(\zeta_7 + \lambda\frac{l}{d_{sb}}\right)\alpha\frac{v_7^2}{2g} - \left(\zeta_6 + \lambda\frac{l}{d_{sb}}\right)\alpha\frac{v_6^2}{2g}.$$

Results are shown in (Table 3).

When gates I, IV and VII are working, the confluence of the flows takes place in the gate I. However, for gates I–IV it is not gate II. BE for sections 1–1 and 17–17:

$$H_1 = \left(\zeta_{sb} + \lambda\frac{l_0}{d_{sb}}\right)\alpha\frac{v_5^2}{2g} + \left(\zeta_{17} + \lambda\frac{l_g}{d_g}\right)\alpha\frac{v_{17}^2}{2g}.$$

BE for sections 1–1 and 18–18:

$$H_1 = \left(\zeta_{sb} + \lambda\frac{l_0}{d_{sb}}\right)\alpha\frac{v_5^2}{2g} + \left(\zeta_6 + \lambda\frac{l}{d_{sb}}\right)\alpha\frac{v_6^2}{2g} + \left(\zeta_{gc} + \lambda\frac{l_g}{d_g}\right)\alpha\frac{v_{18}^2}{2g}.$$

BE for sections 16–16 and 20–20:

$$H_2 = \left(\zeta_{sb} + \lambda\frac{l_0+3l}{d_{sb}}\right)\alpha\frac{v_{12}^2}{2g} + \left(\zeta_{20} + \lambda\frac{l_g}{d_g}\right)\alpha\frac{v_{20}^2}{2g}.$$

BE for sections 16–16 and 19–19:

$$H_2 = \left(\zeta_{sb} + \lambda\frac{l_0+3l}{d_{sb}}\right)\alpha\frac{v_{12}^2}{2g} + \left(\zeta_8 + \lambda\frac{l}{d_{sb}}\right)\alpha\frac{v_8^2}{2g} + \left(\zeta_{19} + \lambda\frac{l_g}{d_g}\right)\alpha\frac{v_{19}^2}{2g}.$$

BE for sections 16–16 and 18–18:

$$H_2 = \left(\zeta_{sb} + \lambda\frac{l_0+3l}{d_{sb}}\right)\alpha\frac{v_{12}^2}{2g} + \left(\zeta_8 + \lambda\frac{l}{d_{sb}}\right)\alpha\frac{v_8^2}{2g} + \left(\zeta_7 + \lambda\frac{l}{d_{sb}}\right)\alpha\frac{v_7^2}{2g} + \left(\zeta_{gc} + \lambda\frac{l_g}{d_g}\right)\alpha\frac{v_{18}^2}{2g}.$$

At the confluence in gate II flow:

$Q_{18} = v_{18}S_g = (v_6 + v_7)S_{sb}$, $v_6 = v_{18}S_g / (1 + v_{7/6})S_{sb}$, $v_7 = v_{18}S_g / (1 + 1/v_{7/6})S_{sb}$. Head loss from section 1–1 to gate II

$$h_{1-11} = H_1 - \left(\zeta_{sb} + \lambda\frac{l_0}{d_{sb}}\right)\alpha\frac{v_5^2}{2g} - \left(\zeta_6 + \lambda\frac{l}{d_{sb}}\right)\alpha\frac{v_6^2}{2g}.$$

Head loss from section 16–16 to gate II

$$h_{16-11} = H_2 - \left(\zeta_{sb} + \lambda\frac{l_0+3l}{d_{sb}}\right)\alpha\frac{v_{12}^2}{2g} - \left(\zeta_8 + \lambda\frac{l}{d_{sb}}\right)\alpha\frac{v_8^2}{2g} - \left(\zeta_7 + \lambda\frac{l}{d_{sb}}\right)\alpha\frac{v_7^2}{2g}.$$

Results are shown in (Table 3).

When I–V gates work, the flows confluence in gate II, and for gates I–VI and I–VII it is gate III.

Table 3. Parameters of gating system*

| Parameters | Working gates | | | | | | |
|---|---|---|---|---|---|---|---|
| | **I, II** | **I, IV** | **I–III** | **I–IV** | **I–V** | **I–VI** | **I–VII** |
| $v_{17}$ | 2.169 / 2.14 | 2.177 / 2.17 | 2.166 / 1212 | 1.914 / 1.90 | 1.837 / 1.84 | 1.579 / 1.65 | 1.490 / 1.58 |
| $v_{18}$ | 2.077 / 2.04 | | 2.105 / 2.04 | 2.040 / 2.01 | 2.011 / 2.00 | 1.796 / 1.87 | 1.717 / 1.72 |
| $v_{19}$ | | | 1.882 / 1.79 | 1.987 / 1.96 | 1.892 / 1.91 | 1.919 / 1.93 | 1.859 / 1.86 |
| $v_{20}$ | | 2.042 / 2.02 | | 1.789 / 1.75 | 1.724 / 1.70 | 1.868 / 1.85 | 1.851 / 1.82 |
| $v_{21}$ | | | | | 1.499 / 1.44 | 1.679 / 1.74 | 1.685 / 1.65 |
| $v_{22}$ | | | | | | 1.446 / 1.37 | 1.463 / 1.41 |
| $v_{23}$ | | | | | | | 1.241 / 1.30 |
| $Q$ | 271.98 / 267.70 | 270.19 / 268.34 | 394.11 / 381.05 | 495.03 / 488.00 | 574.02 / 569.33 | 658.83 / 666.68 | 724.11 / 726.24 |

**At work of gates I and VII* $v_{17} = 2.179$ *m/s,* $v_{17}^{e} = 2.14$ *m/s,* $v_{23} = 2.156$ *m/s,* $v_{23}^{e} = 2.07$ *m/s*

*At work of gates I, IV and VII* $v_{17} = 2.158$ *m/s,* $v_{17}^{e} = 2.15$ *m/s,* $v_{20} = 2.104$ *m/s,* $v_{20}^{э} = 2.06$ *m/s,* $v_{23} = 1.953$ *m/s,* $v_{23}^{e} = 1.95$ *m/s*

**Results and discussion**

As is evident, the study of work structure of GS was divided into three stages. When all the gates are closed, the fluid pours out from the right sprue, and it is not necessary to add water to this sprue. If one of the 7 gates is open, there is no need to add fluid to the right sprue, it pours out from the gate and out of the gap in this sprue. If there are more than one gate, then when only the left sprue is operating, the fluid from the right sprue does not pour out, and it should be added to the right sprue. All aforementioned can be calculated.

When there are no gates, the difference in heads $H_2 - H_1$ is used for head losses in the collector. When one of the gates is working, the head $H_2$ is expended on the velocity head in this gate and on the head loss from the left sprue to this gate, and the head difference $H_2 - H_1$ is expended on head loss in the collector from the working gate to the right sprue. If two or more gates work, then a zero point gate exists in the system in which confluence of flows from the left and right sprues happens (this has been verified experimentally). And which part of the flow will reach zero point gate from each sprue depends on obtained equal head losses from the sprues to each gate. Equality of head losses is achieved by the method of successive approximations. The height of head in the sprue is calculated in in the head loss from this sprue to the zero point gate.

At the work of one, two, three, four or five gates, the calculated values of the fluid velocity in gates are greater than the experimental ones. For systems of six or seven gates, the experimental velocity is higher

than theoretical. The reason of what causes this is unknown. Potentially, refining of equations (14) and (15) is necessary to determining head losses when a part of the flow branches from the collector into the gate.

Both theoretical and practical fluid velocities in the gates increase as they approach to the zero point gate from sprue, in which they reach a maximum value.

In general, we can assume that a good agreement of the theoretical and experimental data is obtained. And the Bernoulli's equation, deduced for a particular case – for a system with one sprue and one gate – also works in a multi-gate gating system with two sprues of different heights, which means with two different energy sources of different sizes.

**Conclusion**

Usability of Bernoulli's Equation in multi-gate gating systems with sprues of different height was proven both theoretically and experimentally for the first time. The calculation is carried out by the method of successive approximations to obtain equal head losses from the sprues to the gates taken as the zero point (before the confluence of the flows), and in the head losses from each sprue to this gate the head of the fluid in the sprue is taken into the account.

**References:**


1. Меерович И. Г., Мучник Г. Ф. Гидродинамика коллекторных систем.– М.: Наука, 1986.– 144 с.
2. Чугаев Р. Р. Гидравлика.– М.: изд-во "Бастет", 2008.– 672 с.
3. Васенин В. И., Богомягков А. В. Исследование работы уравнения Бернулли в многопитательной литниковой системе // Литейное производство.2017.– № 6.– С. 12–15.
4. Vasenin V. I. Investigation of the work of the gating system with two sprues // Austrian Journal of Technical and Natural Sciences. 2016.– No. 5–6.– P. 6–12.
5. Vasenin V. I., Bogomyagkov A. V. Study of gating system with two sprues // Eastern European Scientific Journal.2018.– No. 3.– P. 410–419.
6. Васенин В. И., Богомягков А. В. Исследование работы литниковой системы с двумя стояками // Литейное производство.2018.– № 8.– С. 10–13.
7. Токарев Ж. В. К вопросу о гидравлическом сопротивлении отдельных элементов незамкнутых литниковых систем // Улучшение технологии изготовления отливок.– Свердловск: изд-во УПИ, 1966.– С. 32–40.
8. Jonekura Koji (et al.) Calculation of amount of flow in gating systems for some automotive castings // The Journal of the Japan Foundrymen's Society.1988.– Vol. 60.– No. 8.– P. 326–331.
9. Васенин В. И., Богомягков А. В., Шаров К. В. Исследование влияния относительной длины питателя на характеристики литниковой системы // Вестник Пермского национального исследовательского политехнического университета. Машиностроение, материаловедение.2013.– Т. 15.– № 2.– С. 48–52.
10. Васенин В. И., Васенин Д. В., Богомягков А. В., Шаров К. В. Исследование местных сопротивлений литниковой системы // Вестник Пермского национального исследовательского политехнического университета. Машиностроение, материаловедение.2012.– Т. 14.– № 2.– С. 46–53.
11. Васенин В. И., Богомягков А. В., Шаров К. В. Исследования L-образных литниковых систем // Вестник Пермского национального исследовательского политехнического университета. Машиностроение, материаловедение.2012.– Т. 14.– № 4.– С. 108–122.
12. Vasenin V. I., Bogomyagkov A. V., Sharov K. V. Definition of the resistance to fluid flow during confluence and rotation of the streams / / Austrian Journal of Technical and Natural Sciences.2018.– No. 5–6.– P. 11–15.

# Section 5. Medicine

*Zefi Gjulio,*
*doct., in Physical Education,*
*the Faculty of Educational Sciences*
*University of Shkodra*
*E-mail: gjuliozefi@yahoo.it*

## WHICH IS THE MOST USEFUL PHYSICAL ACTIVITY FOR OLD PEOPLE?

**Abstract:** A sedentary life combined with the non suitable way of eating increases obesity in old people. It is widely spoken about the health benefits that the elders who take up sport have along with the necessity of living an active life as long as possible. So we should think which are the most useful and effective exercises to keep the body of an old person fit. Dealing with functional training means practising some exercises and movements equal to moving activities of everyday life. This may result in good health benefits for our body enabling us to have a good physical body and improve the quality life.

**Keywords:** functional gymnastics, the physical aerobic activity, muscular strengthening, equilibrium and flexibility, quality life.

**Introduction**

We hear everyday people talking about the improvement of the life conditions, lifespan or healthy aging. The lack of physical activity leads to lots of chronic diseases which are visible in adults and old people such as cardiac problems, stroke, diabetes mellitus, pulmonary illnesses, Alzheimer illness, hypertension and cancer. A sedentary life combined with the non suitable way of eating increases obesity in old people. Exercising regularly is related to obesity as well as the reduction of disabled people and it also affects the improvement of the life quality in old people.

It is often spoken about the health benefits that those who take up sport have along with the necessity of living an active life as long as possible. A question arises: Which is the most useful and effective physical activity to keep the body of an old person fit?

We often hear the term "functional gymnastics" or "functional physical activity" which is recommended to those who are part of the third age. Firstly we must explain some characteristics of doing the "functional gymnastics". Dealing with a "functional physical activity" means doing lots of movements and exercises, this may result in good health benefits for our body and in a good physical appearance. There are several "functional gymnastics" and every year other new methods and exercises are suggested. The fact that they are always in progress makes it difficult for us to choose which the most suitable area for our requests is.

There are lots of meanings attached to the term "functional physical activity" from the rehabilitation to the muscular empowerment, from the corrective one to that which lets you a little bit apart from the real sports activities.

Besides this, there is also the physical activity based on specific exercises for special parts of the body. Nevertheless, gymnastics for old people, whatever it is, should be thought and programmed in advance in order to favour the "muscular-skeletal flexibility", motor skills and general postural position for people who due to their advanced age are slower in motion. So, it is important to put more emphasis on the moves done in their proper way. It is a good thing to constantly practise in every phase of life sticking to appropriate rhythms and the physical requirements. Physical activity extends our lives, it also keeps our mind alive, it encourages the functioning of the organs and the human body apparatus and it is even a very good antidepressant [2, 12–23].

In 2008, the Health Department in the USA, in the annual gazette, has highlighted and recommended the fact that in order to have good health benefits an old person should do at least 150 min aerobic activity with a moderated intensity or 75 min aerobic activity with an optimal intensity, or a combination of these versions per week. Old people should also be committed to increase the activity which includes all groups of the muscles at least twice a week.

The physical activity for old people should favor some main aspects such as breathing, relaxation and muscular extension, a better posture and a better command of their body. The goal an elder must reach is that he/she must be more secure in moving till he/she finally succeeds in being less frightened to walk without being checked.

The physical activity for the third age must predict a lot of stretching exercises which engage the upper and lower limbs, the spinal cord and even the belly. These exercises must be done in accordance with the breathing acts which is very important for a good psycho-physical equilibrium [3, 34–43].

In the gymnastics activity for old people (the functional training), free body exercises as well as exercises with specific equipment may be included. Nowadays, there are numerous studies which have proved that the physical activity is a good equipment to slow down and make the aging process be less problematic. Some of them emphasize that a moderated training performed in a relatively long period of time may take some years to represent pathology related with the aging process.

It is not true that the older a person becomes, the less the need to move is. He/she must keep moving following some basic and good instructions. So, for this reason, it is very important to be suggested a "training" plan. Only by doing this, the physical activity can give its benefits and can also serve as a means of social exchange among old people.

The rational and constant physical exercise affects, as previously mentioned, in the breathing apparatus increasing the function of the respiratory muscles as well as the moving process among the vertebrae of the ribs (the chest cough), enabling the growth and safety of the elasticity of the lungs [4, 8–16].

The effect is visible in the muscular-skeletal system removing the negative effects of the muscular hypertrophies, osteoporosis and arthritis. The functional training has also a great impact on the peripheral and central nervous system increasing the focus and the critical ability. It also improves the functioning of the immune system; it opposes the birth of cardiovascular pathologies, of hypertension, and metabolic diseases such as diabetes.

We must never forget that the elder won't be trained to take part in competitions and at the same time he/she mustn't be considered as a desperate and irresponsible case. For this reason, there are certain helpful and necessary specific trainings in suitable schedules and with nice music in the background without having around any of the "inappropriate" characters for the age and the physical level of the elders. Old people also make up an important human "deposit" for the instructor of physical education, too. Listening to the stories and the experiences they have faced, carrying years of commitment on their shoulders, they can also gain something valuable. In this way, they will not only feel more helpful, but also better psychologically.

The physical activity must be functional which means making the person execute any kind of movement retrieving it independently and automatically in his/her everyday life. This will stimulate old people to acquire a more effective body and movement scheme.

Sometimes the instructors of physical education intend to strengthen a muscular zone by randomly overcoming the physiological aspects which are associated with the aging of the muscle itself. Getting older, the decrease of the number of muscle fibers is more noticeable in those facts. So, the development of general coordinative skills, the respect for the person as a whole and the prevention of accidents are 3 main goals of a functional training (functional gymnastics) which must have the self-perception and stabilization of different parts of the body as basic elements. This is achieved through a progressive way and through equilibrium exercises such as medicine ball exercises, in order to improve the perceptual ability of particular areas as well as of the whole body.

As a conclusion, the functional training aims to create exercises which regard daily movements based on some key points required in the development of every muscular exercise such as: the equilibrium, the reaction (the reactivity), and the growth of the muscular strength. We should never forget the fact that old people don't have the same skills as the younger ones; therefore, care must be taken with the gestures and movements offered to them to accomplish.

The most suitable exercise which may be done by old people can be arranged in 3 groups:

**1. The physical aerobic activity**

It is advisable that different kinds of physical aerobic activities should be used during the week. This kind of activity must last at least 10 min long for each session and must be done with moderate intensity. Some studies have proved that the activity accomplished at least three times a week may reduce the risks of injury and excessive fatigue by producing health benefits for the elders.

**2. Muscular strengthening**

The development of muscular strength and the resistance is progressive and very important to help elders to prevent the bone and muscle soreness. At least two days a week, elders must deal with activities for the muscular strengthening by activating all crucial muscular groups. These kinds of exercises must contain from 8 to 12 repetitions per activity or must be carried out until the old person has difficulties in repeating the exercise without anybody's assistance.

**3. Equilibrium and flexibility**

The use of exercises which keeps or improves the equilibrium can reduce the risk of falls and injuries related to them. The older a person becomes, the more the chances of falling increase, and as a result, even their recovery is more difficult and lasts longer. Equilibrium exercises and the activity to strengthen the musculature must be done at least three times a week with a total of 90 min in addition to walking with moderate intensity for about an hour a week. Good examples of exercises to improve the equilibrium include walking backwards, on the heels, at the tip of the fingers etc. The more the equilibrium is improved, the more the difficulty of the executed exercises is increased.

As far as flexibility is concerned, stretching exercises can help to maintain it. Old people should be trained in order to keep and develop the flexibility at least twice a week for 10 min a day [5].

**Some recommendations for the physical activity for old people**

That a physical activity has as much effect on the organism, it must be developed regularly.

– In order to achieve significant health benefits with a minimum activity, it can be a 2 hours and 30 min aerobic activity with moderated intensity (as for example, walking with resistible rhythm) per week, as well as physical activity to strengthen the muscular at least two days a week.

Or, an hour and 15 min (75 min) aerobic activity with higher intensity (for example jogging, run-

ning) per week and physical activity to strengthen the muscular at least two days a week.

Or a combination of an aerobic activity of moderated intensity with that of a higher intensity equivalent to the above recommendations as well as the physical activity to strengthen the body muscular in general.

– While to increase the level and keep for as long as possible all health benefits achieved through the functional training, we should do 5 hours (300 min) aerobic activity with moderated intensity per week as well as physical activity in order to strengthen the muscular at least twice a week.

Or, a 2 hour and 30 min (150 min) aerobic activity of a higher intensity per week as well as a physical activity to strengthen the muscular at least twice a week.

Or a combination of an aerobic activity of moderated intensity with that of a higher intensity equivalent to the above recommendations, as well as the physical activity to strengthen the body muscular twice a week.

In order to achieve his/her own goals and objectives, an old person needs a plan in which should be included all kinds of physical activities advised for his/her age. This plan should describe in details how, when and where the physical activity will take place. People with chronic problems need a plan which integrates their caring and training. The plan of the physical activity should also foresee the gradual and progressive growth of the physical activity which will take place. There should also be a personal doctor who will advise the elders to participate continuously and adequately in the functional training during the week. The combination of the moderated intensity with the higher one during the practice of the physical training must be followed carefully by the physical education instructor, and even be individualized according to the function abilities of the individuals. Some activities which may improve different physical skills upon the elders can be: bike rides at distances with different rhythms, functional training sessions, dancing (different kinds), swimming, acquagym, tennis, the use of the vacuum cleaner, walking in nature, jogging, callisthenic exercises, transportation of food bags, palates, different types of work in the garden, some yoga exercises and tai chi, chores (washing glasses and floors) etc.

**References:**

1. Bassem Elsawy M. D., e Kim E. Higgins D. O., Methodist Charlton Medical Center, Dallas, Texas 2010 Jan 1; 81 (1): 55–59.
2. Alberto Tomasi, Lara Lucchesi. Igiene prevenzione e sport, CIC Edizioni Internazionali, Roma, 2005; 12–23.
3. Minasso G., Piccolo C. e A., "Ginnastica per la terza età", Roma Edizioni Mediterranee 1983; 43–43.
4. Fox Bowers Foss, "Le basi fisiologiche dell'educazione fisica e dello sport", Roma Il pensiero scientifico editore 1994; 8–16.
5. URL: http://www.health.gov/paguidelines/guidelines

*Rahmatullaeva Nasiba Islambaevna,*
*assistant of the Department of Neurology*
*Andijan State Medical Institute*

*Rakhimbaeva Gulnara Sattarovna,*
*Head of the Department of Nervous Diseases, professor*
*Tashkent Medical Academy*

*Nasirdinova Nargisa Askarovna,*
*associate professor of the Department of Neurology*
*Andijan State Medical Institute*
*E-mail: karimova60@mail.ru*

# LEUKOENCEPHALOPATHY: BINSWANGER'S DISEASE. PECULIARITIES OF CURRENT AND TREATMENT

**Abstract:** The article describes the case of Binswanger's disease, developed relatively at a young age. The disease quickly progressed and ended in a fatal outcome. Neuroimaging and neuropsychological studies confirmed the diagnosis of leukoencephalopathy. Early diagnosis and adequate therapy will slow the progression of the disease.

**Keywords:** vascular dementia, atherosclerosis, lecoencephalopathy, Binswanger's disease, cognitive impairment.

To date, the diagnosis of Binswanger's disease is essentially a "rarity", is rarely established. Previously, such a diagnosis was established only pathoanatomically, but modern methods of neuroimaging can diagnose this disease in vivo.

However, according to neuroimaging methods, most patients simultaneously have two or more pathogenetic types of vascular dementia.

Dermographic changes in the population structure of all developed countries led to a significant increase in the proportion of diseases of the elderly and especially chronic progressive cerebrovascular diseases (CEH). This raises the problem of chronic progressive disorders of cerebral circulation to one of the leading places in modern angioneurology.

Unlike acute disorders of cerebral circulation (CABG), the economic and medical consequences of chronic progressive disorders of cerebral circulation, are not exactly established. There is every reason to believe that they are very significant. Thus, with the present trend towards the middle of this century, half of Europe's population will be over 60 years old. Since in this age group, the prevalence of dementia averages about 6%, and every 5 years this percentage is doubled, then 3–4% of the population will suffer from dementia.

The urgency of the problem is also due to social consequences. Neurological disorders and disorders of higher cortical functions in chronic progressive disorders of cerebral circulation can be the cause of severe disability of patients requiring significant financial costs for the maintenance of such patients, both from the relatives of the patient and the State. As a result of the expansion of the methodological possibilities for studying chronic progressive cerebral vascular diseases, a potential opportunity to prevent or slow the progression of cognitive impairment (CN), including dementia, under the condition of early diagnosis and timely pathogenetic treatment has arisen [Chui N., 2000; Bowler, J., 2002].

Currently, abroad, among progressive progressive disorders of cerebral circulation, isolated progressive vascular leukoencephalopathy (Binswanger's disease), also referred to as subcortical arteriosclerotic encephalopathy (SAE). In the domestic literature SAE is considered as one of the variants of discirculatory encephalopathy in the presence of arterial hypertension (AH) [Shmidt E. V., Maksudov G. A., 1975; Shmidt E. V. 1985; Kalashnikova JI.A, et al., 1998; Shprakh V. V., 1994; Yakhno N. N., Damulin I. V., 1999].

Here is the case of leukoencephalopathy (Binswanger's disease), diagnosed in a middle-aged patient, with a subsequent fatal outcome.

The patient was born in 1967. He was born in the department of neurology with complaints from his relatives for a sharp decrease in his outlook, efficiency, lack of interest in others and difficulty walking due to frequent falls. Before the development of these conditions, the patient often complained of the occurrence of periodic headaches.

From the anamnesis it is revealed that the patient suffers for 4 years. Its disease does not connect with anything. At the beginning of the disease, the patient had headaches, dizziness, transient instability when walking. He noted an increase in irritation, sleep disturbance. Then, against the background of the symptoms of autonomic dystonia, there are impaired coordination – cerebellar ataxia, unsteady gait, increased dizziness. The patient underwent a number of laboratory and instrumental studies, was treated with vasoactive drugs, after which the condition improved moderately. In 2016, the patient, against a backdrop of dizziness, developed stiffness of movements, disorientation in space and time, pseudobulbar syndrome. Since then, the patient described the symptoms have progressed. The patient entered the hospital due to deterioration of the state.

Neurological status: CHMN – smell, hearing preserved, II pair – visus OD = OS0,8, VII – symmetrical face, hypomimous, signs of central lesion of IX–X pair – nasal, periodic buries, XII – deviation of tongue, dysarthria. The motor sphere – muscle tone increased by plastic type, muscle strength on both sides 3.5 points, reflexes brisk, pathological reflexes – upper Rossolimo, Babinsky, Marinescu-Rodovici, proboscis positive from both sides, walks with support. Sensitive sphere – sensitivity disorders could not be identified because of an inadequate state (we could not get a full answer to the questions asked). In the Romberg pose is unstable, the coordinating samples from both sides perform with mild ataxia, positive tests of Stuart-Holmes. Extrapyramidal system: oligobardikinesia, a positive symptom of the "cogwheel", hypomia, slowness of thinking. VNS – On examination, white dermographism, tachycardia, hyperhidrosis distal, significant weight loss are revealed. GNI is emotionally unstable, decreasing memory for current events, disrupting orientation in time and space, a significant decrease in intelligence, performing simple instructions, no more complex reactions, simpler answers to questions, more often using the words "yes", "no."

On MRI, according to literature data, more sensitive to changes in white matter, leukoareosis (LA) is a zone of altered signal intensity (decreased in T1 mode and increased in T2 and FLAIR regimes) localized in the periventricular and deep sections of the hemispheres, as well as in the the brain stem. The conducted studies showed that in the presence of LA on MRI in periventricular white matter a certain spectrum of pathomorphological changes is detected. This is mainly demyelination, gliosis, edema and degeneration of axons, expansion of perivascular spaces and the formation of cysts, extracellular and intracellular edema, heart attacks, angioectasias, Waller degeneration. These changes are very different in nature. The majority of the examined 54% showed a decrease in white matter density, especially expressed around the anterior (less often posterior) horns of the lateral ventricles (the phenomenon of "leukoareosis"), 32% – expansion of the ventricles of the brain and subatrophy of the cortex.

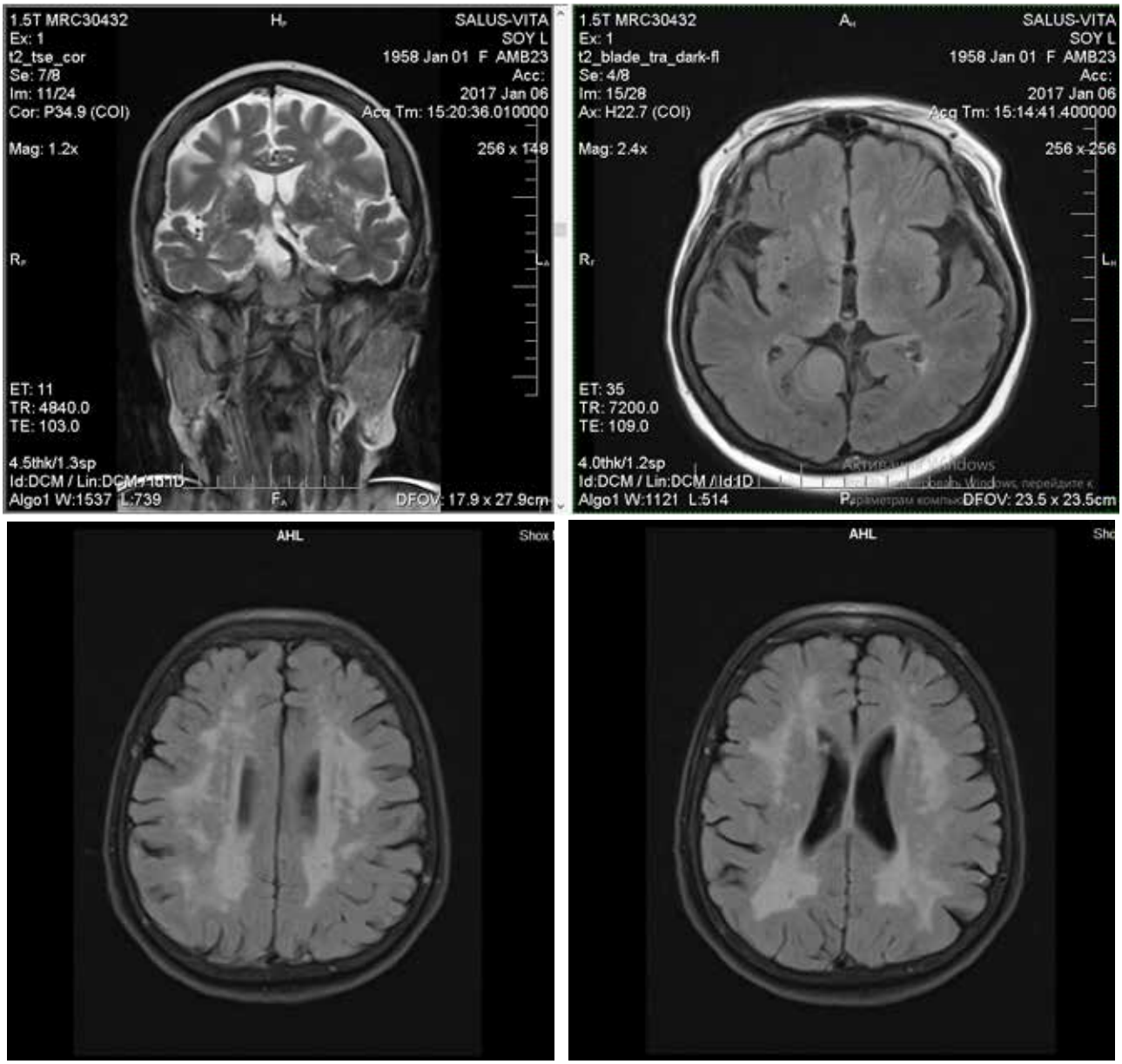


Figure 1.

It is believed that the expansion of perivascular spaces occurs with arterial hypertension as a result of pulsatile traumatisation of small vessels, which is accompanied by their elongation, crimp and atrophy of the adjacent parenchyma. The expansion of perivascular spaces and periventricular gliosis are less correlated with the severity of clinical manifestations than complete or incomplete infarctions, and neuroimaging methods in this zone usually reveal only a slight decrease in perfusion [Yakhno N. N., 2001, Pantoni L., 2010].

To determine the level of cognitive impairment, the patient was tested with MMSE, according to which a decrease in memory, attention, and violation of executive function was observed.

Patients were prescribed drugs to improve metabolism (citicolines, nootropics, neuroprotectors), vasoactive drugs, antiaggregants. Despite the treatment, the patient died 3 months after the examination and treatment.

Thus, the conducted observation showed that the course of Binswanger's disease (leukoencepha-

lopathy) can be malignant with a subsequent fatal outcome. The disease manifests itself by a rapid decrease in cognitive functions and the growth of organic lesions of the structures of the nervous system (affection of the coordinator, pyramidal and extrapyramidal systems). Instrumental methods of investigation confirmed the diagnosis. The treatment was not effective and the outcome was lethal. Systematizing the data of clinical-neurological, electroencephalographic and neuroimaging studies, it can be said that the presence of focal neurological symptoms, changes in cognitive functions, disorganization or desynchronization of the main rhythms on the EEG in combination with morphostructural changes in the white matter of the brain allows the life diagnosis of Binswanger's disease to be in vivo in patients suffering from hypertensive disease.

**References:**


1. Akiguchi I., Tomimoto H., Suenaga T., Wakita H., Budka H. "Alterations in glia and axons in the brains of Binswanger's disease patients". Stroke 28 (7),1997.– P. 1423–9. PMID9227695.
2. Akiyama H., Meyer J. S., Mortel K. F., Terayama Y., Thornby J. I., Konno S. Normal human aging: factors contributing to cerebral atrophy. J. Neurol Sci 1997.– 152.– P. 39–49.
3. Aronson S. M., Perl D. P., eds. Clinical neuropathological conference. Dis Nerv Syst 1974.– 35.– P. 286–91.
4. Ashburner J., Friston K. J. Voxel-based morphometry – the methods. Neuroimage 2000.– 11.– P. 805–821.
5. Luo F., Guo Y., Peng R.et al. Polypill-Based Therapy: A Promising Therapeutic Strategy. Heart Lung Circ. 2017. Mar 6. pii: S1443–9506(17)30088–4. doi: 10.1016/j.hlc.2017.02.004.
6. Gupta S., Singh P., Sharma B., Sharma B. Neuroprotective Effects of Agomelatine and Vinpocetine Against Chronic Cerebral Hypoperfusion Induced Vascular Dementia. CurrNeurovasc Res. 2015.– 12(3).– P. 240–52.
7. Bai F., Watson D. R., Yu H., Shi Y., Yuan Y., Zhang Z. Abnormalresting-state functional connectivity of posterior cingulatecortex in amnestic type mild cognitive impairment. Brain Res. 2009.– 1302.– P. 167–174.
8. Baldwin R. C., Walker S., Jackson A., Simpson S. W., Burns A. Further investigation of deep white matter lesions is necessary. Br Med J 1999.– 318.– 738 p.
9. Collins D. L., Zijdenbos A. P., Kollokian V., et al: Design and construction of a realistic digital brain phantom. IEEE Trans Med Imaging 1998.– 17.– P. 463–468.
10. Damoiseaux J. S., Rombouts S. A., Barkhof F., Scheltens P., Stam C. J., Smith S. M., et al. Consistent resting-state networks across healthysubjects. Proc Nat AcadSci USA. 2006.– 103.– P. 13848–13853.

# Section 6. Technical science

*Kuropyatnyk Oleksiy Andriiovych,*
*graduate student, National University*
*Odessa Maritime Academy*
*E-mail: kuropyatnyk83@gmail.com*

## REDUCTION OF $NO_X$ EMISSION IN THE EXHAUST GASES OF LOW-SPEED MARINE DIESEL ENGINES

**Abstract:** The article analyzes the effect of the exhaust gas recirculation (EGR) system on the emission of $NO_X$ in the exhaust gases of marine low-speed diesel engines. Tests have proven that EGR in the range of 4.7 … 18.8% provides reduction of $NO_X$ emission to 13.3 … 3.3 $gNO_X/(kW\,h)$ accordingly, depending on the crankshaft rotation speed and engine load. It is shown that the decrease in $NO_X$ concentration in exhaust gases (in comparison with $NO_X$ concentration without the use of EGR) can reach 37.9 … 53.5%. The use of the EGR system as the main way of reducing the $NO_X$ emission level is proposed, which provides the needed decrease in emission level in accordance with the requirements of international organizations.

**Keywords:** low-speed marine diesel, emission of nitrogen oxides in the exhaust gases, exhaust gas recirculation system.

**Introduction**

Shipbuilding industry today shows increase in the deadweight tonnage of virtually all types of ships that is most pronounced in container carriers, bulk carriers and tankers. In order to avoid loss of speed of the ship and to ensure proper performance of shipboard operations it is necessary to the increase propulsive output proportionally to the increase in the deadweight tonnage. The output of the main engines (power of which transmits to the ship propeller that is essential for movement of the ship) of the leading diesel-building companies such as Mitsubishi, MAN Diesel, Wartsila-Sulzer goes up to 56000 … 81000 kW, and auxiliary engines (which are driven by ship electric generators) – to 2500 … 4200 kW. The main engine daily fuel consumption, with an average specific fuel rate of 175 … 188 g/(kW h), can be approximately 235 … 350 ton/day, and for auxiliary engines (up to 4 engines on the modern ships, up to 3 of which can work simultaneously), up to 8 … 10 ton/day. And 16 … 24 ton/h of exhaust gases, which contain toxic components, are emitted into the atmosphere. All the toxic components that are formed in ship engines can be divided into two groups. The first group includes products of incomplete combustion of fuel – carbon monoxide, hydrocarbons, aldehydes, soot. The second group is the toxic components formed as a result of complete oxidation of the chemical elements that are mixture of fuel and air – these are nitrogen oxides ($NO_X$) and sulfur oxides ($SO_X$).

Presently, a large number of techniques that reduce emissions of $NO_X$ in exhaust gases exist. Depending on the type of diesel engines (structure and operating conditions), strictly defined options are considered to be optimal for the purpose of mini-

mizing of $NO_X$ emission. For example, for marine diesel engines with a capacity of more than 10000 kW, Mitsubishi and MAN Diesel recommend to use EGR system. Still, further research required to determine the optimum rate of gas recirculation, as well as the effect of EGR system on the main parameters of the diesel. Taking this into account, the purpose of this research was to determine the effect of the rate of recirculation of exhaust gases (as one of the methods for reducing $NO_X$ emissions) of a marine low-speed diesel engine on its environmental, economic and energy parameters.

**Relevance of research**

The most harmful emissions in almost all modes of operation of the diesel engines (regardless of their type, class size and structural differences) are, obviously, nitrogen oxides. The rates of nitrogen oxides in total emissions is 30…80% by mass and is 60…95% by equivalent toxicity. Nitrogen oxides released to the atmosphere along with aerosols and organochlorine compounds destroy the ozone layer, which is located at an altitude of 25 km and absorbs 99% of the sun and ultraviolet rays. NO and $NO_2$ that are emitted in the operation of marine engines and plants are most important to ensuring environmental standards.

Nitrogen oxides are the only pollutants that cannot be eliminated by changing the grade of fuel (as it is possible to reduce $SO_X$ emissions this way), since they are most often formed by the combination of nitrogen (which is necessarily in the liquid fuel composition) with oxygen (contained in the air in the diesel cylinder). Marine diesels, which are in operation, require constant search for effective ways to reduce the toxicity of exhaust gases, most important of which are emissions of nitrogen oxides. Reduction of $NO_X$ concentration in exhaust gases is achieved through the use of various technological and design solutions, one of which is exhaust gas recirculation (EGR). This determines the relevance of research to determine the optimum operating conditions for exhaust gas recirculation systems [1].

**Research objective**

The amount of nitrogen oxides in the exhaust gases of marine diesel engines is regulated by the requirements of the MARPOL International Convention, Annex VI. EGR systems received wide spread in both stationary and ship engines in the last decade. These systems are developed and installed for new ships. Extensive experience in the technical operation of these systems does not currently exist, and recommendations for their use are mainly based on theoretical calculations and modeling of the processes occurring in this process. Therefore, the research objective was to determine the influence of the exhaust gas recirculation system on the environmental, energy and economic performance of the 7UEC60LS low-speed marine diesel engine of Mitsubishi with a regular ERG system.

One of the features of the operation of marine vessels is their accountability to international classification societies (for example, Lloyd's Register of Shipping – England, Bureau Veritas – France, Det Norske Veritas & Germanischer Lloyd – Germany, The American bureau of shipping – USA). And one marine vessel can be under the supervision of several societies at once. On the basis of empirical experience, statistical accounting and scientific research, these organizations develop their own Rules for the Classification of Marine Vessels and maintain a system of continuous monitoring of compliance with these rules on classified ships. This limits the ability to perform structural changes in the engines of vessels (both thermal and mechanical engines, and systems that ensure their operation) without appropriate coordination with these supervisory authorities. The crew of ship, in the performance of its functional duties, is deprived of the possibility of independently re-equipping both the power plant itself and the systems that serve it. Therefore, the task of ship mechanics and representatives of research organizations is to determine the optimal operating conditions for the ship's power plant without introducing any improvements and upgrades of its structure.

**Research results**

Tests of the effect of the exhaust gas recirculation system on the environmental, energy and economic performance of the internal combustion engine were performed on a Mitsubishi 7UEC60LS marine low-speed diesel engine, operated by a two-stroke cycle with a regular ERG system.

The main characteristics of the diesel engine:

– diameter of the cylinder – 600 mm;
– piston-stroke – 2400 mm;
– number of cylinders – 7;
– nominal power – 12600 kW;
– rotation speed corresponding to the nominal power – 82 rpm.

Schematic diagram of the Mitsubishi 7UEC60LS marine diesel engine with the exhaust gas recirculation system on which the tests were performed is shown in (Fig. 1).

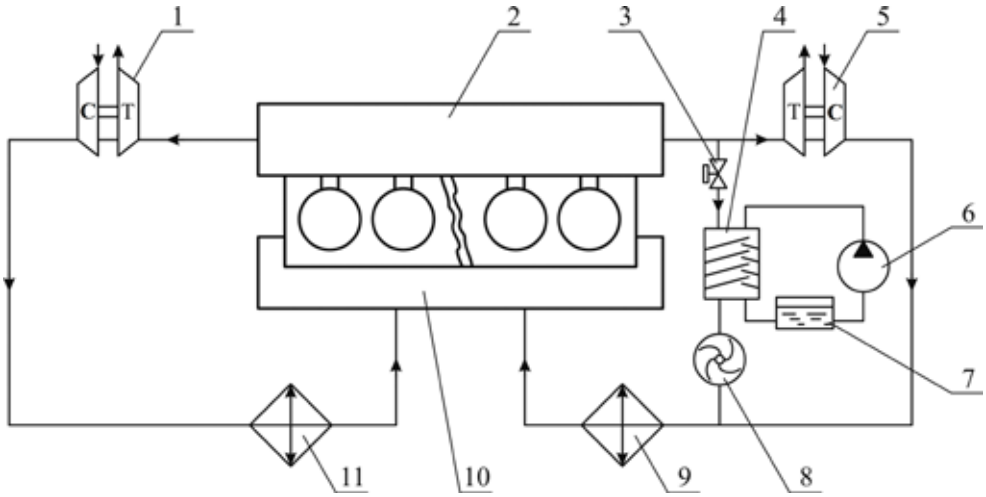


Figure 1. Schematic diagram of EGR system for a marine low-speed diesel engine: 1, 5 – turbocharger; 2 – outlet manifold; 3 – EGR valve; 4 – scrubber; 6 – water pump; 7 – water tank; 8 – electric gas turbocharger; 9, 11 – air cooler; 10 – air manifold T, C – gas turbine and turbocharger compressor

The exhaust gases from the diesel cylinders enter the common exhaust manifold 2 and then to the gas turbochargers 1 and 5, after which they are vented to the atmosphere through the gas outlet pipe. The gas turbochargers take air from the engine room and, after compression, direct it through the coolers 9 and 11 in air manifold 10. The gas turbocharger 5 is equipped with an exhaust gas recirculation system that consists of a control valve 3, a gas scrubber 4, a gas turbocharger 8, tank 7 and water pump 6. In the case of the exhaust gas recirculation system, the quantity is regulated by the valve 3. The exhaust gases are cleaned and pre-cooled in the scrubber 4, they are fed for mixing with air by the additional turbocharger 8 (coming from the exhaust gas turbocharger 5) and fed to the intercooler 9, the air receiver 10 and further to the cylinder of a diesel engine. A fan with constant flow geometry is used as a gas turbocharger 8 [2].

In experimental research conducted onboard the vessel, $NO_x$ values in exhaust gases were measured, Specific fuel oil consumption (SFOC), and effective diesel engine power ($N_e$) for various rates of exhaust gas recirculation.

Portable gas analyzers are most expedient in monitoring the concentration of harmful components [4]. German gas analyzer Testo350XL was used in this research to determine the concentration of $NO_X$ (as well as the $O_2$ concentration) in the exhaust gases, which can determine the concentrations of the following substances: CO, $O_2$, $N_2$, $NO_X$, $CH_4$, $SO_2$, as well as measure temperature, humidity, speed and the differential pressure of the medium.

The Testo 350XL gas analyzer provides the specified parameters in the temperature range of –40… 1200 °C, which completely covers the interval of the exhaust gas temperatures of the diesel engine at all modes of its operation. Using the Testo 350XL gas analyzer, it is possible to determine the content of nitrogen oxides ($NO_X$), as well as oxygen ($O_{2,\,Gas}$) and nitrogen ($N_{2,\,Gas}$) in outgoing gases in the range of 0…3000 $mln^{-1}$ with an accuracy of 1 $mln^{-1}$.

The rate of recirculation of exhaust gases during the tests varied in the following values: EGR = 4.7%, EGR = 9.8%, EGR = 14.6%, EGR = 18.8%, and was calculated using the following formula:

$$\mathrm{EGR} = \frac{\alpha_{\mathrm{EGR}}}{\alpha},$$

where α is rate of excess air without EGR system operating;

α EGR is rate of excess air with EGR system.

To determine the EGR rates of excess air, α and α EGR were determined in consideration with the volume concentrations of oxygen and nitrogen in the exhaust gases when the diesel engine is operating without EGR – $O_{2,Gas}$, $N_{2,Gas}$ and with EGR – $O^{EGR}_{2,Gas}, N^{EGR}_{2,Gas}$

$$\alpha = \frac{1}{1-3{,}76\dfrac{\mathrm{O}_{2,\,\mathrm{Gas}}}{\mathrm{N}_{2,\,\mathrm{Gas}}}}, \qquad \alpha_{\mathrm{EGR}} = \frac{1}{1-3{,}76\dfrac{\mathrm{O}^{\mathrm{EGR}}_{2,\,\mathrm{Gas}}}{\mathrm{N}^{\mathrm{EGR}}_{2,\,\mathrm{Gas}}}}.$$

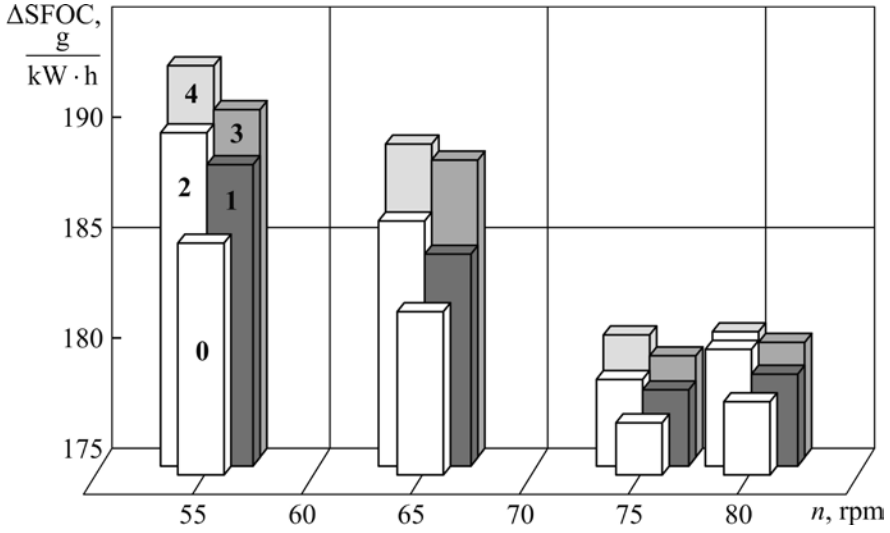


Figure 2. Change in SFOC, g/(kW h) of the Mitsubishi marine diesel engine 7UEC60LS, depending on the crankshaft rotation speed n, rpm and EGR rate,%: 0 – without circulation (EGR = 0%;) 1 – EGR = 4.7%; 2 – EGR = 9.8%; 3 – EGR = 14.6%; 4 – EGR = 18.8%

The tests were performed on the following operation modes of diesel: 55, 65, 75 and 80 rpm, which corresponded to the following values of the relative power of the diesel: $0.3N_{enom}$, $0.5N_{enom}$, $0.77N_{enom}$ and $0.93N_{enom}$. $N_{enom}$ stands for the nominal power corresponding to its excess air ratio – α. The ship diagnostic system Doctor was used to determine the power of the diesel. In addition, for each operation mode of the diesel engine, the hourly fuel consumption was measured [3].

The results, which reflect the change in the specific effective fuel consumption be, nitrogen oxide concentration NOX in the exhaust gases and the relative decrease in the effective power $\frac{N_{2EGR}}{N_2} \cdot 100$, of the Mitsubishi marine diesel engine 7UEC60LS, depending on the crankshaft rotation speed *n*, and the EGR rate are shown in (Fig. 2–4).

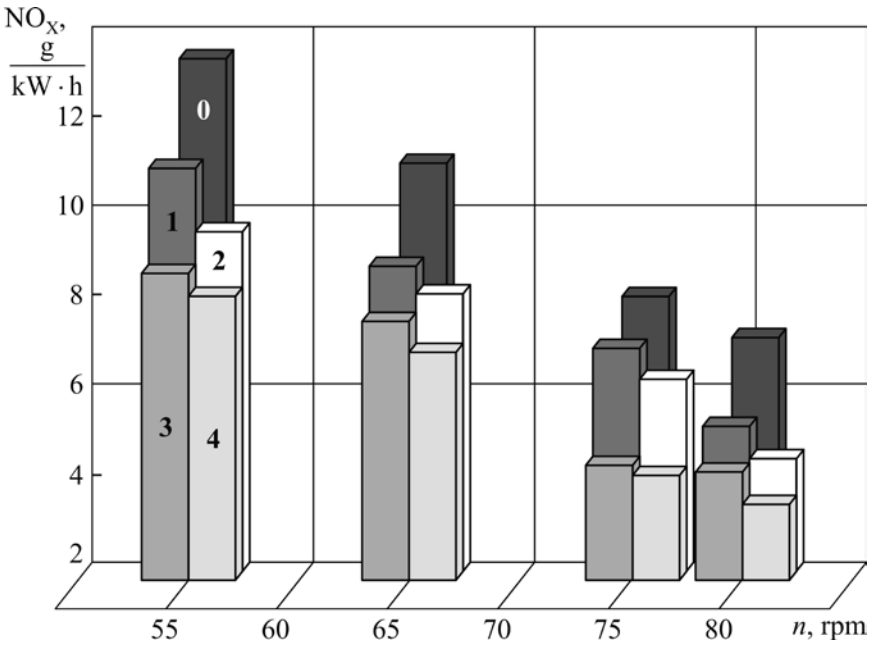


Figure 3. Change in the concentration of nitrogen oxides NOX, g/(kW h) in the exhaust gases of the Mitsubishi marine diesel engine 7UEC60LS depending on the crankshaft rotation speed n, rpm and EGR rate,%: 0 – without circulation (EGR = 0%;) 1 – EGR = 4.7%; 2 – EGR = 9.8%; 3 – EGR = 14.6%; 4 – EGR = 18.8%

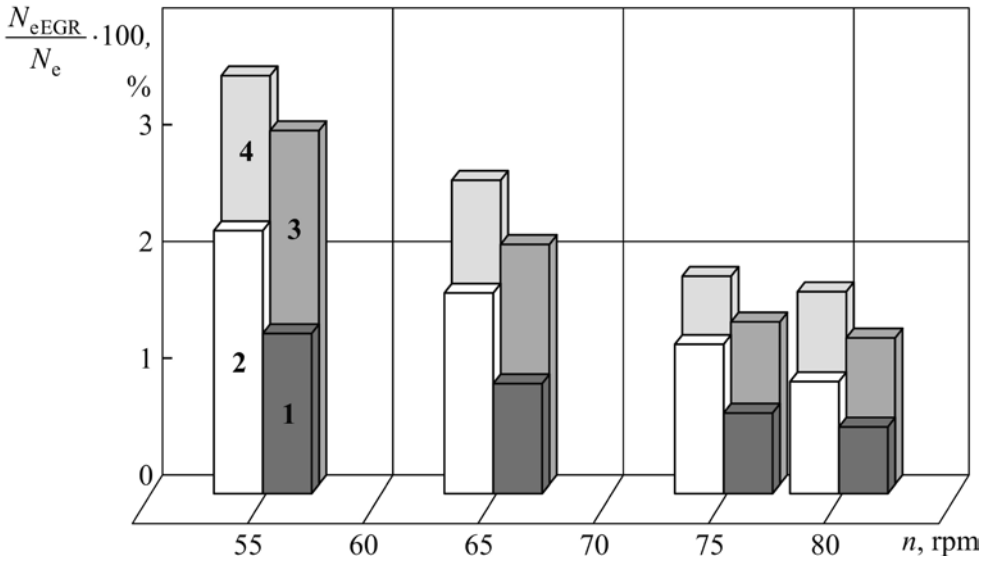


Figure 4. Relative reduction in the effective power $\frac{N_{eEGR}}{N_e} \cdot 100$, %, of the Mitsubishi marine diesel engine 7UEC60LS depending on the crankshaft rotation speed n, rpm and EGR rate: 1 – EGR = 4.7%; 2 – EGR = 9.8%; 3 – EGR = 14.6%; 4 – EGR = 18.8%

**Conclusion**

In order to meet the required environmental performance of marine diesel engines (most importantly, emissions of $NO_X$ in exhaust gases) forces the use of additional technological solutions. One such solution is the addition to marine diesel engines of EGR systems, which ensure that the part of exhaust gas passes through the cylinder. EGR system reduces

the amount of air intended for fuel combustion, so the amount of exhaust gases returning to the diesel cylinder maintains a reliable autoignition and subsequent combustion of the fuel.

The use of EGR system improves the environmental performance of the marine diesel, in particular, reduces the level of $NO_X$ emissions. It has been experimentally established that a change in the rate of recirculation of exhaust gases in the range 4.7 ... 18.8% ensures a reduction in the NOx concentration in exhaust gases to 13.3 ... 3.3 $gNO_X/(kW\,h)$ respectively, depending on the rotational speed and diesel load, which in experiments varied in the interval $n_{work}=(0.67 \dots 0.975)\, n_{nom}$ and $N_{ework}=(0.3 \dots 0.93)\, N_{enom}$. Decrease in $NO_X$ concentration in exhaust gases is in the range of 19.5 ... 48.8%, with large values corresponding to the load interval (0.77 ... 0.93) of (0.77 ... 0.93) $N_{enom}$, which is the most common operating modes of the diesel engine.

The use of the exhaust gas recirculation system helps to reduce the energy and economic performance of the low-speed marine diesel engine. Conducted tests established the following:

Specific fuel oil consumption (SFOC), which characterizes the economy of the diesel engine, increases in proportion to the increase in the rate of recirculation of exhaust gases and for different speeds of the diesel engine in percentage terms is 0.85 ... 2.01% for EGR = 4.7% and 2.16 ... 4.34% for EGR = 18.8%;

The effective power of the diesel engine, which characterizes its energy performance, decreases as the rate of recirculation of the exhaust gases increases. In modes close to the nominal load (for example for $n_{work}=0.975n_{nom}$, when $N_{ework}=0.93N_{enom}$, the drop in the effective power value is 1.2%, and for $n_{work}=0.67n_{nom}$, when $N_{ework}=0.3N_{enom}$ modes it is 3.43%.

Despite the deterioration in the economic and energy performance of diesel, the use of the EGR method on ships has broad prospects, because its use ensures the fulfillment of international requirements for protecting the ambient air from pollution and contributes to the maintenance of environmental safety of ship power plants.

## References:


1. Sagin S. V., Kuropyatnyk O. A. The Use of Exhaust Gas Recirculation for Ensuring the Environmental Performance of Marine Diesel Engines // Naše more, 2018. – Vol 65. – Iss. 2. – PP. 78–86. DOI 10.17818/NM/2018/2.3
2. Sagin S. V., Kuropyatnik A. A. Application of the system of recirculation of exhaust gases for the reduction of the concentration of nitric oxides in the exhaust gases of the ship diesels // American Scientific Journal, 2017. – No. 15. – Iss. 2. – P. 67–71.
3. Куропятник А. А. Снижение концентрации оксидов азота в выпускных газах судовых дизелей // Universum: Технические науки.2018. – Вып. 3(48). – С. 67–71.
4. Yoo J., Prikhodko V., Parks J. E., Partridge W. P., Perfetto A., Geckler S. High-speed multiplexed spatiotemporally resolved measurements of exhaust gas recirculation dynamics in a multi-cylinder engine using laser absorption spectroscopy // Applied spectroscopy.2016. – Vol. 70. – Iss. 4. – P. 572–584. DOI: 10.1177/0003702816636802.

*Mamataliev Adurasul,*
*Ph D., in technique, senior scientist*
*"Phosphate fertilizer" laboratory,*
*Institute of General and Inorganic Chemistry*
*of the Academy of Sciences of the Republic of Uzbekistan*
*Tashkent, Uzbekistan*
*E-mail: abdirasul.86@mail.ru*

*Namazov Shafoat,*
*Doctor of science, professor, academic,*
*chief of "Phosphate fertilizer" laboratory,*
*Institute of General and Inorganic Chemistry*
*of the Academy of Sciences of the Republic of Uzbekistan*
*Tashkent, Uzbekistan*
*E-mail: igic@mail.ru*

*Kurbanov Jakhongir,*
*Junior scientific researcher*
*"Phosphate fertilizer" laboratory,*
*Institute of General and Inorganic Chemistry*
*of the Academy of Sciences of the Republic of Uzbekistan*
*Tashkent, Uzbekistan*
*E-mail: jahon_17@mail.ru*

# NITROGEN POTASSIUM CONTAINING DIFFICULT FERTILIZERS ON THE BASE OF MELT AMMONIUM NITRATE AND POTASSIUM CHLORIDE

**Abstract:** With the aim of modifying ammonium nitrate, reducing its explosive properties, the process of obtaining nitrogen and potassium fertilizers based on it has been studied by introducing into its melt the potassium chloride produced by the Dehkanabad potash fertilizer plant. The composition of the fertilizers obtained is determined. The main indicator of the modification is the strength of the granules. if for pure ammonium nitrate it is equal to 1.6 MPa, then for fertilizer with the ratio N: $K_2O$ = 1: 0.5 it is 7.53 MPa and at a ratio of N: $K_2O$ = 1: 1 it is 8.36 MPa.

**Keywords:** ammonium nitrate, melt, potassium chloride, nitrogenpotassium fertilizer, density, viscosity and strength of granules.

**Introduction**

Ammonium nitrate is the most popular and effective nitrogen fertilizer in the world. In 2007, the world capacity of its production amounted to 43 million tons per year [1]. In Uzbekistan, the total capacity of the three plants producing of ammonium nitrate (JSC "Chirchik-Maxam", "Navoiazot" and "Ferganaazot"), exceeded 1 million 750 thousand tonnes per year. It used in agriculture for all types of cultures and on any type of soil.

But it has very serious drawback – the risk of explosive [2].

Thereby have been tightened requirements for quality of ammonium nitrate and the conditions of its storage. Before manufacturers assigned the problem – to provide transferring to production of fertilizers based on ammonium nitrate, preserving agrochemical efficiency with significantly greater resistance to external influences and, accordingly, less explosive.

As substances – additives, reducing the level of potential danger of ammonia slit, are used:

1) carbonate-containing compounds of natural and technogenic origin (chalk, calcium carbonate, dolomite);

2) potassium-containing substances (potassium chloride and potassium sulfate);

3) substances containing the same name cation – ammonium (ammonium sulfate, ortho-and polyphosphate of ammonium);

4) other ballast substances that do not carry a payload, but which determine only the mechanical dilution of ammonium nitrate (plasterboard, phosphogypsum and others) [3].

The first group of additives used in the production of so-called calcium ammonium nitrate [4–6]. Nowadays 31 company in Europe and 5 enterprises in Russia produced it. But its application is effective only in European's acidic soils. It is uneffective in Uzbekistan's alkaline carbonate soils. Besides, calcium ammonium nitrate in flour state is also explosive.

From the second group of additives is more used potassium chloride for the production of potassium-ammonium nitrate. Potassium-ammonium nitrate is produced a lot of in some foreign countries, with containing 16–16.5% N and 25–28% $K_2O$ [7]. It produced by following methods: 1) by mechanically mixing the dry components or wetted ammonium nitrate and potassium chloride; 2) evaporation of solutions of ammonium nitrate and potassium chloride; 3) addition to concentrated solution or melt of ammonium nitrate micronized potassium chloride followed by melt granulation in granulation towers. In Russia, production of nitrogen-potassium fertilizer on the base of ammonium nitrate and potassium chloride first time was produced at JSC "Nevinnomissk Vneshtreydinvest" in 1999. The method of obtaining the composition of fertilizer are protected by patent of the Russian Federation [8]. For production used the ammonium nitrate melt with concentration of 85–92% $NH_4NO_3$ and granulation mixture conducted in granulating drum. Besides produces more homogeneous fertilizer composition.

Startup in Uzbekistan Dehkanabad potassium plant, the capacity of which will soon come up to 360 thousand tonnes of $K_2O$ per year by form of potassium chloride, it opens perspective plans for production of nitrogen-potassium fertilizer on the basis of ammonium nitrate. Potassium sulfate is not produced in Uzbekistan. At same time we have observed large deficit of chlorine-free fertilizers.

Substances of third group used at JSC "Cherepovets Azot", where in 2002 was organized production of stabilized ammonium nitrate with composition of 32% N, 5% $P_2O_5$ capacity of 400 thousand tonnes of fertilizers per year by additive liquid complex fertilizer containing 11% N and 33% $P_2O_5$ to nitrate melt obtaining from superphosphoric acid that is used in the additive mixture of ammonium ortho- and polyphosphates.

This addition increased the temperature of nitrate decomposition on 22–24 °C, slowed the speed of its thermal decomposition, increased granule strength, reduced porosity of product, made nitrate more resistant to repeatedly repeated phase transformations, and most importantly-reduced ability to detonation of ammonium nitrate [9–12]. But superphosphoric acid is not produced in Uzbekistan. In addition, it is very expensive.

Having good prospects of fourth group is of additives to ammonium nitrate: gypsum and phosphogypsum [13–19]. In these works, developed technology of obtaining thermostable fertilizers based on ammonium nitrate by addition to its melt

dihydrate, hemihydrate phosphogypsum and natural gypsum. The product with 5 percent additive phosphohemihydrate and containing 33.6% N has twice the strength of granules than pure nitrate, retained 100% friability for 4 months, 7 withstanding thermal cycles at temperatures without 20–60.

The product has a significantly higher thermal stability compared with pure ammonium nitrate (the activation energy of pure ammonium nitrate 160 kJ/mol, with maximum amount of additive phosphogypsum was 240 kJ/mol).

So we decided to test the process of obtaining nitrogen potassium containing fertilizers by additive to melt of ammonium nitrate perspective additives-potassium chloride production plant Dehkanabad potash fertilizers.

**Materials and Methods**

For conduct of laboratorial experiments for investigation of obtaining nitrogenpotassium containing fertilizers was used granulation ammonium nitrate (34.5% N) production of JSC "Maxam-Chirchik", crystalline potassium chloride (60% $K_2O$), production of plant Dehkanabad potassium fertilizers.

Model laboratory apparatus consisted of two-liter cylindrical reactor made from stainless steel 12X18H10T equipped with stirrer and motion by motor. At first, the reactor was charged with amount of granulated ammonium nitrate and exposed it to melt. The temperature in reactor was 175–180°C. Then to ammonium nitrate melt added calculated amount of potassium chloride and the mixture was thoroughly stirred for 15 minutes.

The weight ratio of ammonium nitrate to potassium chloride by N: $K_2O$ was in the range from 1: 0.1 to 1: 1 [20–23]. After 15 minutes of reaction the components in melt is poured into porcelain dish and intensively stirred with glass rod. As cooling formed solid particles of round shape. The mass was cooled and then seeded in particle size.

Particles with size 2–3 mm were analyzed on strength of granule accordingly by State Standard (SSt) 21560.2–82. Then products are grained and analyzed for nitrogen, potassium and sulfur by known methods [24]. Studied dissolution rate of granules with size 2 mm. These granules was put into glass with 100 ml of distilled water and observing visually, fixed time of its complete dissolution. Temperature was 25°C and tested five-times. It was also tested the extent to which the conversion takes place in the melt of ammonium nitrate mixture of ammonium nitrate and potassium chloride. The degree of conversion of $NH_4NO_3$ was determined by the method described in [25].

We determined the rheological properties of melts obtained nitrogenpotassium containing complex fertilizers. Density was measured by bottle method and viscosity was measured by using a glass capillary viscometer (GCV-2) with a diameter of 0.77 mm. Experiments spent in the following way. Samples of ammonium nitrate with additive potassium chloride melted, mixed thoroughly, cooled to room temperature and milled. The obtaining powders were injected into the pycnometer, and the viscometer, which are then placed in the thermostat filled with glycerin.

Table 1.– The composition and properties of nitrogenpotassium and nitrogenpotassiumsulfur containing complex fertilizers

| **Ratio of mass N: $K_2O$** | **Content of components, mas.%** | | **Degree of conversion $NH_4NO_3$,%** | **Strength of granules, MPa** | **Time of full dissolution, sec** |
|---|---|---|---|---|---|
| | **N** | **$K_2O$** | | | |
| ***1*** | ***2*** | ***3*** | ***4*** | ***5*** | ***6*** |
| 100: 0.0 | 34.5 | – | – | 1.6 | 46.8 |
| 1: 0.1 | 32.41 | 3.24 | 5.96 | 4.37 | 63.9 |

| *1* | *2* | *3* | *4* | *5* | *6* |
|---|---|---|---|---|---|
| 1: 0.2 | 30.53 | 6.04 | 11.43 | 5.13 | 69.8 |
| 1: 0.3 | 29.40 | 8.82 | 16.84 | 6.99 | 92.4 |
| 1: 0.5 | 26.80 | 13.40 | 22.96 | 7.53 | 110.4 |
| 1: 0.7 | 24.60 | 17.22 | 27.37 | 7.91 | 120.2 |
| 1: 0.8 | 23.60 | 18.90 | 29.84 | 8.14 | 134.2 |
| 1: 1.0 | 21.90 | 21.90 | 32.55 | 8.36 | 137.0 |

The temperature in thermostat was raised to the predetermined value. The powder in the pycnometer and viscometer was melted. If melting level in the pycnometer not reached the level, added the new portion of powder. If melting level exceeds the mark, the surplus of melt was removed with cotton at the end of the wire. The temperature in the thermostat was controlled with the contact thermometer. The melt was kept at predetermined temperature for 5–7 minutes and then made measurements.

The laboratory tests results are shown in (Table 1).

**Results and its discussion**

It is seen, that confirm the content of nutrients proximity fertilizer samples prepared in the laboratory and on model set. Nitrogen and potassium contents according to ratio of N: $K_2O$ is from 21.90 to 32.41 and from 3.24 to 21.90%, respectively.

When mixing the fusion of ammonium nitrate with potassium chloride, the process of conversion of ammonium nitrate to potassium nitrate occurs. The degree of conversion of ammonium nitrate essentially depends on the amount of potassium chloride in the mixture. With a decrease in the N: $K_2O$ mass ratio from 1: 0.1 to 1: 1, the degree of $NH_4NO_3$ conversion increases from 5.96 to 32.55%.

Strength granules of potassium-ammonium nitrate also depends from amount of potassium chloride. When amount of potassium chloride rise from 1: 0.1 to 1: 1, strength granules of NK-complex fertilizers increased from 4.37 to 8.36 MPa. This confirms that interaction of the ammonium nitrate and potassium chloride formed product with reduced ability to detonation.

Table 1 show, that time of full dissolution of pure ammonium nitrate is 46.8 seconds. With the increase in the proportion of potassium chloride in mixture of nitrate granules time full dissolution of nitrogen-potassium fertilizer steady rising and reaching 137.0 seconds for sample in ratio of N: $K_2O$ = 1: 1. It means that, obtaining fertilizer will be considerably (3 times) more slowly wash out from soil than pure ammonium nitrate.

Hygroscopic point, kinetics of water vapor sorption and sorption moisture capacity, and granules of nitrogenpotassium containing complex fertilizers on the base of ammonium nitrate melt and potassium chloride were defined in.

Ammonium nitrate when the moisture 3.5% strongly caking and loses friability, and samples of nitrogenpotassium fertilizer retain the appearance and friability with moisture content of 5–6%. When humidity 7%, they will be lose ability to sieving. Therefore, we still recommend packed potassium and ammonium nitrate in paper or plastic bags [23].

In further researches determined rheological properties of melts obtained fertilizers. The results are shown in (Table 2). The data of (Table 2) are shown, the density and viscosity of the melt of ammonium nitrate considerably increased with increasing amount of additives. Pure ammonium nitrate at 165°C does not melt and, of course, does not fluid. Potassium chloride additive reduces its melting point. Mixture of ammonium nitrate and potassium chloride in ratio N: $K_2O$ of from 1: 0.1 to 1: 0.4 starts melting at 165°C and while the melt has high viscosity but flowing easily. Increasing the proportion

of potassium chloride from 0.1 to 0.5 at temperature 175 °C, that increases density and viscosity of a nitrate-chloride melt from 1.487 to 1.532 g/cm$^3$ and from 5.98 to 12.73 cps, respectively.

Table 2.– The rheological property of melt nitrogenpotassium and nitrogen-potassiumsulfur content fertilizers

| The weight ratio N: $K_2O$ | Density (g/sm$^3$) at temperature, °C | | | | | Viscosity (cps) at temperature, °C | | | | |
|---|---|---|---|---|---|---|---|---|---|---|
| | 165 | 170 | 175 | 180 | 185 | 165 | 170 | 175 | 180 | 185 |
| 100: 0.0 | –* | 1.450 | 1.448 | 1.446 | 1.437 | –* | 5.71 | 5.34 | 5.02 | 4.83 |
| 1: 0.1 | 1.508 | 1.496 | 1.487 | 1.479 | 1.468 | 6.52 | 6.27 | 5.98 | 5.76 | 5.44 |
| 1: 0.2 | 1.515 | 1.502 | 1.496 | 1.488 | 1.477 | 8.16 | 7.95 | 7.65 | 7.35 | 6.91 |
| 1: 0.3 | 1.527 | 1.514 | 1.505 | 1.492 | 1.483 | 9.78 | 9.63 | 9.37 | 8.92 | 8.36 |
| 1: 0.4 | 1.543 | 1.530 | 1.511 | 1.503 | 1.490 | 11.34 | 11.28 | 11.06 | 10.51 | 9.82 |
| 1: 0.5 | –* | 1.551 | 1.532 | 1.513 | 1.497 | –* | 12.91 | 12.73 | 12.16 | 11.26 |

–* ***temperature of melt 170 °C***

It should be noted that in all investigated ratios of N: $K_2O$ based on interaction of ammonium nitrate and potassium chloride exchange reaction occurs, in resulting are formed large crystals of potassium nitrate. Potassium nitrate crystals strongly clog hole injectors granulation tower. Therefore, in production granulation melt of potassium and ammonium nitrate we are recommended to carry out in drum granulator.

**Conclusion**

With the aim of eliminating the explosive properties of ammonium nitrate, new nitrogen and potassium-containing fertilizers have been obtained from it by introducing potassium chloride into its melt, produced by the Dehkanabad potash fertilizer plant. The compositions and properties of new fertilizers obtained in a wide range of changes in the mass ratio N: $K_2O$ (from 1: 0.1 to 1: 1) have been studied.

The most popular agricultural fertilizers are nitrogen-potassium fertilizers, in which the ratio N: $K_2O$ is 1: 0.5. Thus, at a ratio of N: $K_2O$ = 1: 0.5, using a 99.8% nylon smelting, we obtain a product with a content of 26.8% N and 13.4% $K_2O$, the strength of its pellets is 7.53 MPa, which is much exceeds the strength of granules of pure ammonium nitrate (1.6 MPa).

## References:

1. Chernyshov A. K., Levin B. V., Tugolukov A. V., Ogarkov A. A., Ilin V. A. Ammonium nitrate: properties, production, application. M. Infochem. 2009.– 544 p.
2. Lavrov V. V., Shvedov K. K. The explosive risk of ammonium nitrate fertilizer and on its bases // Scientific and technical news: CC "Infochem". Special Issue. 2004.– No. 4.– P. 44–49.
3. Levin B. V., Sokolov A. N. Problems and technology in the production of complex fertilizers on bases of ammonium nitrate // World of sulfur, N, P and K. 2004.– No. 2.– P. 13–21.
4. Baranius V., Barutsky Y., Krause A., Paul D., Stuemer K. N. Industrial plants for the production of calcium ammonium nitrate // Journal of UCS named after Mendeleev D. I. 1983.– V. 28.– No. 4.– P. 439–445.
5. Zhmay L., Hristianova E. Ammonium nitrate in Russia and in the world. Current situation and prospects // World of sulfur, N, P and K. 2004.– No. 2.– P. 8–12.

6. Postnikov A. V. Production and use of calcium ammonium nitrate // Chemicals used in agriculture. 1990.– No. 9.– P. 68–73.
7. Pozin M. E. Technology of mineral salts. – Volume 2 – Leningrad: Chemistry.1970.– 1558 p.
8. Patent of Russia 2154620. Method for producing nitrogen-potassium fertilizer // Duhanin V. F., Serebryakov A. I.– 08.20.2000.
9. Ilin V. A. Development of technology of complex nitrogen-phosphate fertilizers based on ammonium nitrate: Author's abstract of Ph.D. in technics. Ivanovo state chemical-technological university.– Ivanovo.2006.– 17 p.
10. Patent of Russia 2223932. Method for producing complex nitrogen-phosphorus fertilizers // Ilin V. A., Patohin O. I., Glagolev O.L and others.– 20.02.2004.
11. Glagolev O. L. Practical experience of AS-72 unit working at JSC "Cherepovets Azot" on flexible circuit production of ammonium nitrate and products on its basis // World of sulfur, N, P and K.2004.– No. 2.– P. 21–23.
12. lyin V. A., Rustambeyov M. K., Akayev O. P., Nenajdenko G. N. Study the thermal stability of the complex nitrogenous phosphatic fertilizers // Problems of stabilization of fertility and productivity in the VerxneVolga.– Moscow.2006.– P. 128–136.
13. Pak V. V., Pirmanov N. N., Namazov Sh. S., Reymov A. M., Beglov B. M. Nitrogen sulfur fertilizers based on ammonium nitrate melt and phosphogypsum // Chemistry and Chemical Engineering.2011.– No. 2.– P. 21–24.
14. Pak V. V., Pirmanov N. N., Namazov Sh. S., Reymov A. M., Beglov B. M., Seytnazarov A. R. Nitrogen sulfur fertilizers based on ammonium nitrate melt and gypsum // Chemistry and Chemical Engineering.2012.– No. 3.– P. 5–8.
15. Moskalenko L. V., Kolesnikov V. P., Reznichenko O. A., Sygankova S. S. Use of phosphogypsum in preparation of fertilizers based on ammonium nitrate – // Materials VII of the International scientific–pract. conf. "Ecology and life".– Penza.2004.– 131 p.
16. Reznichenko O. A., Moskalenko L. V. Estimate influence of phosphogypsum composition on strength of ammonium nitrate granules // Proceedings of VIII regional scientific and engineering conf. "University sciences – to Northern Caucasus region".– Stavropol.2004.– P. 40–41.
17. Kolesnikov V. P., Moskalenko L. V. Thermographic study of modification reactions of fertilizer produced on the basis of ammonium nitrate // Chemical industry today.2006.– No. 7.– P. 18–21.
18. Kolesnikov V. P., Moskalenko L. V. Development of thermostable fertilizers based on ammonium nitrate // Coll. of 2nd All-Russian scientific and engineering. conf. "New technologies in nitrogen industry".– Nevinnomyssk.– 8–13 October.2007.– Stavropol.– P. 70–71.
19. Moskalenko L. V. Development of technology for thermostable fertilizers based on ammonium nitrate. Author's abstract of Ph.D. in technics, Nevinnomyssk Institute of Technology.– Moscow.2007.– 16 p.
20. Beglov B. M., Namazov Sh. S., Seytnazarov A. R., Mamataliev A. A. Potassium and ammonium nitrate–based concentrated solutions and melts of ammonium nitrate and potassium chloride // Chemical Industry.2013.– V. 90.– No. 6.– P. 267–278.
21. Mamataliev A. A., Seytnazarov A. R., Namazov Sh. S. Beglov B. M. Potassium and ammonium nitrate–based solution of ammonium nitrate and potassium chloride // Chemical technology. Control and management.2013.– No. 4.– P. 5–11.

22. Mamataliev A. A., Seytnazarov A. R., Reymov A. M., Namazov Sh. S. Potassium and ammonium nitrate–based melt of ammonium nitrate and potassium chloride // Chemical technology. Control and management.2013.– V. 49.– No. 1.– P. 5–10.
23. Mamataliev A. A., Seytnazarov A. R., Namazov Sh. S., Beglov B. M. Physico-chemical properties and commodity properties of potassium and ammonium nitrate-based concentrated solutions, melt of ammonium nitrate and potassium chloride // Chemistry and Chemical Engineering.2014.– No. 3.– P. 20–26.
24. Vinnik M. M., Erbanova L. N., Zaytsev P. M. Methods of analysis of phosphate rock, phosphorous and complex fertilizers, food phosphates // – Moscow.– Chemistry.1975.– 213 p.
25. Friedman S. D., Skum L. S. The solubility of potassium chloride in nitroammophos // Chemical Industry.1971.– No. 1.– P. 44–47.

*Ortikova Safie Saidmambievna,*
*Ph D., student,*
*the Laboratory of Phosphate Fertilizers*
*Institute of General and Inorganic Chemistry*
*Academy of Sciences of Uzbekistan,*
*E-mail: ortikova.sofiya@mail.ru*
*Namazov Shafaat Sattarovich,*
*doctor of science, professor,*
*Chemistry Academy of Sciences of Uzbekistan,*
*head of Phosphate Fertilizers Laboratory*
*Institute of General and Inorganic*
*E-mail: igic@rambler.ru*

# COMPOSITION AND PHYSICOCHEMICAL PROPERTIES OF NITROGEN-PHOSPHORUS- SULPHUR-CALCIUM CONTAINING FERTILIZERS

**Abstract:** In this study scientific data on investigation of composition and hygroscopic points of nitrogen-phosphorus-sulphur-calcium containing (NPSCa) fertilizer based on interaction of off-balanced ore from Central Kyzyl-Kum phosphorite by partially ammoniated mixes of sulphuric and phosphoric acid slurry, have been summarized. In consideration of relative content acceptable and water soluble form of $P_2O_5$ in products, optimal ratio of ammoniated mixes of sulphuric and phosphoric acid slurries to mineralized mass (ASPS: MM) for fertilizer is 100: 25 and 100: 30 with weight ratio of $SO_3$: $P_2O_5$ = 1.2; 1.65; 2.60 and pH = 2.5 and 3.0.

**Keywords:** mineralized mass, ammonized sulphuric and phosphoric acid, fertilizer, moisture, hygroscopic point, relative acceptable form of $P_2O_5$.

**Introduction.** In Uzbekistan for production of highly qualified phosphate fertilizers namely ammophos (10% N; 46% $P_2O_5$) and suprephos (8–15% N; 20–24% $P_2O_5$) there is used washed and calcinated phosconcentrate (26% $P_2O_5$) obtained by thermic enrichment of Kyzyl-Kum phosphorite. Output of Kyzyl-Kum phosphorite complex producing the phosconcentrate is 716 thousand tonnes per year (or 186.16 thousand tonnes $P_2O_5$). Whereas value of mined phosphate ore containing at average of 17.12% $P_2O_5$ is 1874.6 thousand tonnes based on 320.93 thousand tonnes $P_2O_5$. However, the released amount of phosphorite concentrate can not provide the capacity joint stock company (JSC) "Ammophos-Maxam". At the same time, JSC "Samarkandkimyo" and JSC "Kokand superphosphate" producing calcium nitrate-phosphate (6% N and 16% $P_2O_5$) and single ammonized superphosphate (1.5% N and 13.5% $P_2O_5$) are needed in phosphate raw more. Although approved powers these three plants in the aggregate are 612.6 thousand tonnes $P_2O_5$ per year. Moreover, problem is degenerated due to that at present working many-stage processing flowsheet (grinding, dry separation with preparation powdered phosphorite, washing off chlorine, deslimation, dry and calcinating to release $CO_2$) is ineffective. Increasing $P_2O_5$ concentration in washed and calcinated phosconcentrate (25.77%)

as compared with its initial concentration in ore (17.12%) is 8.65% based on loss of $P_2O_5$ (134.77 thousand tonnes $P_2O_5$ or 42% with total $P_2O_5$ in ore) with reject so-called "Off-balance ore". Of them 9.6% is during the dry separation, 28.3% – throughout the washing and 4.1% – within dry and burning process. As these are mineralized mass (12–14% $P_2O_5$), sludge phosphorite (10–12% $P_2O_5$) and dust like fraction (18–20% $P_2O_5$).

The present study has information on usage of off-balanced phosphorite ore – mineralized mass, which is not as a waste but cheap raw to generate standard fertilizer. In this paper given results on activation of MM by ASPS with various ratios of $SO_3$: $P_2O_5$.

**Objects and methods of research.** As the certain raw material was MM containing (weight.%): 14.33 $P_2O_5$; $P_2O_{5acceptable.}$ by citric acid: $P_2O_{5toatl}$ = 9.01; 43.02 CaO; 1.19 MgO; 1.38 $Fe_2O_3$; 1.18 $Al_2O_3$; 2.22 $SO_3$; 14.70 $CO_2$; 13.23 insoluble residue; $CaO_{total.}$: $P_2O_{5total.}$ = = 3.0. The content in the waste of $Ca_5F(PO_4)_3$ (fluorineapatite) constitutes 34.70% but $CaCO_3$ (calcium carbonate) – 30.4%. Before using, MM is milled in the porcelain mortar. Wet-processing phosphoric acid form joint stock company "Ammophos-Maxam" with composition (weight.%): 14.32 $P_2O_5$; 0.86 CaO; 0.29 MgO; 1.32 $Fe_2O_3$; 0.32 $Al_2O_3$; 1.31 F; 0.38 $SO_3$. It is necessary to note that pH of ASPS with various ratios of ($SO_3$: $P_2O_5$ = 1.2, 1.65, 2.65) was in a range 2.0; 2.5; 3.0; 3.5 and weight ratio of the ASPS: MM equal from 100: 10 to 100: 60.

After feeding, interaction process lasted in 30 min. The temperature of reaction mass was held up at level of 60 °C by contact thermometer. Further obtained slurry was dried in oven at 90–100 °C till constant weight. After that, dried samples was cooled, milled and subjected to chemical analysis to determine different form of $P_2O_5$ and CaO, as well as nitrogen according to procedure [1]. Acceptable form of $P_2O_5$ was defined by solubility both 2% solution of citric acid and 0.2M solution of ethylenediamine tetra-acetic acid (EDTA). While acceptable form of CaO was determined by citric acid only and nitrogen by Kjeldahl. pH of finished product was determined on a basis of 10% water suspension. Moisture of the probes was carried out according to the procedure in [2]. Static strength of granule with size 2–3 mm was conducted according to State standard [3] on device MIP-10–1. Hygroscopic point of the fertilizer with indicated size was determined by exsiccator method to [4, 5] under atmospheric moisture capacity equal to 70, 80, 90 and 100% at 25 °C.

**Results and its discussion.** Figure shows dependency of relative form of phosphorus by citric acid, 0.2 M solution of EDTA and water.

As it is seen from fig. there was occurred activation of MM, that is, unacceptable form of $P_2O_5$ transferred into acceptable for plant form when processing phosphorite by ammoniated mixes of phosphoric and sulphuric acids.

At Figure 1 (a) there were revealed the area of optimal value of relative and water form of $P_2O_5$ depending on the $SO_3$: $P_2O_5$ = 1.2. So, A, B, C, D, E, F points belong to relative acceptable and water form of $P_2O_5$in the fertilizers obtained with ASPS: MM= = 100:25 at pH 2.5 and 3.0. At that time, G, H, I, J, K, L point belong to area of relative acceptable and water form of $P_2O_5$ in the fertilizers generated based on ASPS: MM = 100:30 at pH 2.5 and 3.0.

In consideration of relative acceptable and water form of $P_2O_5$ in products with ASPS: MM = = 100: 25; 100: 30 and $SO_3$: $P_2O_5$ = 1.2 for pH = = 2.5 are the following composition (weight.%): 21.84–22.34 $P_2O_{5total}$; 8.99–9.62 N; 17.25–19.13 $CaO_{total.}$; $P_2O_{5acceptable\ by\ citric\ acid:}$ $P_2O_{5total.}$ = 76.14–80.26%; $P_2O_{5acceptable\ by\ EDTA}$: $P_2O_{5total.}$ = 70.01–72.83%; $P_2O_{5water.}$: $P_2O_{5total}$ = 35.76–41.23%; $CaO_{acceptable.}$: $CaO_{total.}$ = 62.89–65.68%; pH = 5.80–5.95.

When $SO_3$: $P_2O_5$ = 1.2 and pH 3.0 ASPS: MM equal to 100: 25 and 100:30 content (weight.%): 21.68–22.14 $P_2O_{5total.}$; 9.22–9.99 N; 17.46–19.34 $CaO_{total.}$; $P_2O_{5acceptable\ by\ citric\ acid}$: $P_2O_{5total.}$ = 75.23–78.86%; $P_2O_{5acceptable\ by\ EDTA}$: $P_2O_{5total.}$ = 69.51–72.36%; $P_2O_{5water.}$: $P_2O_{5total.}$ = 33.95–38.89%; $CaO_{acceptable.}$: $CaO_{total.}$ = 61.84–64.37%; pH = 6.20–6.38.

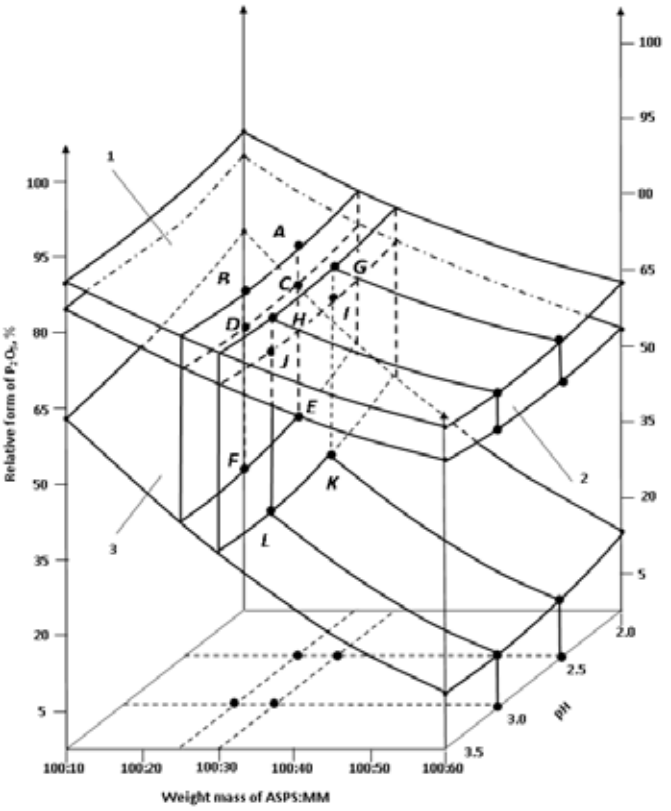


a)

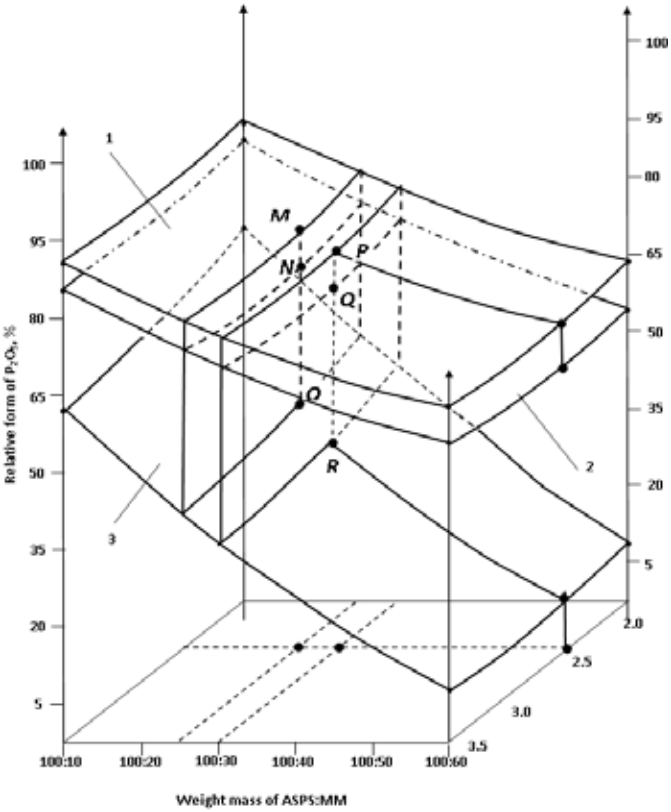


b)

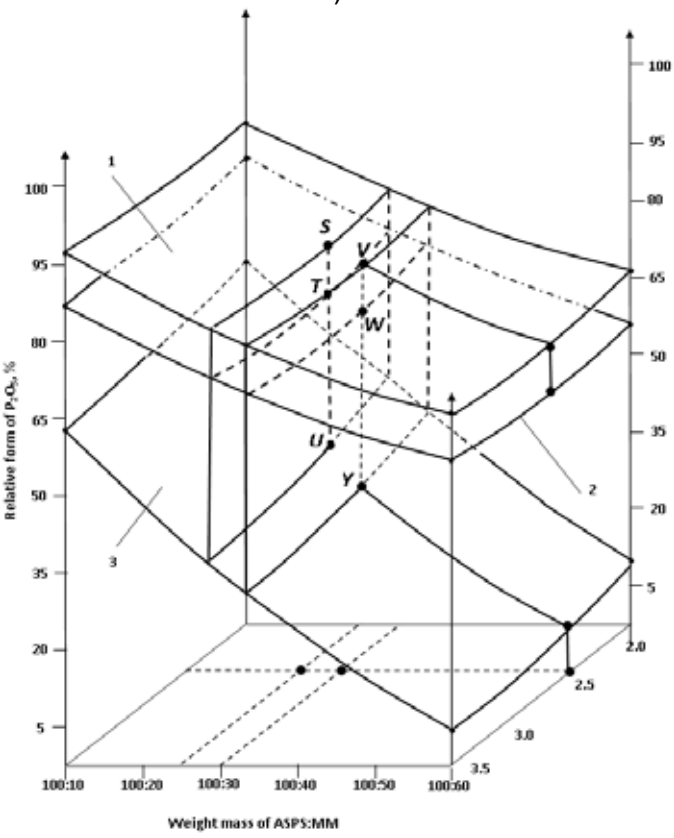


c)

Figure 1. Dependency of relative form of P2O5 by 2% solution of citric acid (1), 0.2M solution of EDTA (2) and water (3) upon the weight ratio of ASPS : MM and pH 2.0, 2.5, 3.0, 3.5, obtained with SO3 : P2O5 = 1.2 (a), 1.65 (b) and 2.6 (c)

Yet, $SO_3$: $P_2O_5$ = 1.65 (Figure 1 (b)) at pH 2.5 M, N, O, P, Q, R points lie on the line of relative acceptable and water form $P_2O_5$ in the products with ratio of ASPS: MM = 100: 25 and 100:30 have content (вес.%): 20.48–20.66 $P_2O_{5total.}$; 10.17–10.77 N; 16.29–18.36 $CaO_{total.}$; $P_2O_{5acceptable\ by\ citric\ acid:}$ $P_2O_{5total.}$ = = 77.49–81.46%; $P_2O_{5acceptable\ by\ EDTA}$: $P_2O_{5total.}$ = 71.53–74.59%; $P_2O_{5water.}$: $P_2O_{5total}$ = 30.42–36.59%; $CaO_{acceptable}$: $CaO_{total.}$ = 64.00–66.79%; pH = 6.00– – 6.19.

Table 1.– Composition and static strength of NPSCa fertilizers

| Numbering of fertilizers samples No | Weight ratio of ASPS: MM | Composition, weight,% | | | Initial moisture, % | Static strength, MPa | Hygroscopic point, % |
|---|---|---|---|---|---|---|---|
| | | N | $P_2O_{5total}$ | $CaO_{total}$ | | | |
| When $SO_3$: $P_2O_5$ = 1.20 and pH = 2.5 | | | | | | | |
| 1 | 100:25 | 8.92 | 22.63 | 16.78 | 1.92 | 3.85 | 68.61 |
| 2 | 100:30 | 8.29 | 22.20 | 18.64 | 1.89 | 3.92 | 72.52 |
| When $SO_3$: $P_2O_5$ = 1.20 and pH = 3.0 | | | | | | | |
| 3 | 100:25 | 9.99 | 22.14 | 17.46 | 1.12 | 3.70 | 71.06 |
| 4 | 100:30 | 9.22 | 21.68 | 19.34 | 1.48 | 3.68 | 74.73 |
| When $SO_3$: $P_2O_5$ = 1.65 and pH = 2.5 | | | | | | | |
| 5 | 100:25 | 10.77 | 20.66 | 16.29 | 1.52 | 3.50 | 72.07 |
| 6 | 100:30 | 10.17 | 20.48 | 18.36 | 1.86 | 3.20 | 73.18 |
| When $SO_3$: $P_2O_5$ = 2.60 and pH = 2.5 | | | | | | | |
| 7 | 100:25 | 12.04 | 16.81 | 14.62 | 1.21 | 2.49 | 74.01 |
| 8 | 100:30 | 11.43 | 16.85 | 16.46 | 1.19 | 2.38 | 75.26 |

The rest optimal lines across through S, T, U, V, W, Y points belonging to $SO_3$: $P_2O_5$ = 2.6, pH 2.5 and ratio of ASPS: MM = 100: 25 and 100:30 with composition (weight.%): 16.81–16.85 $P_2O_{5total}$; 11.43– –12.04 N; $P_2O_{5acceptable\ by\ citric\ acid:}$ $P_2O_{5total.}$ 78.93–83.34%; $P_2O_{5acceptable\ by\ EDTA:}$ $P_2O_{5total.}$ 73.65–76.86%; $P_2O_{5water.}$: $P_2O_{5total.}$ 28.43–34.03%; 14.62–16.46 $CaO_{total}$; $CaO_{acceptable.}$: $CaO_{total.}$ 69.50–73.46%; pH 5.90–6.10 (Figure 1 (c)).

In order to study physic-chemical and commodity properties there were selected probes of granular NPSCa fertilizers composition and properties given in Table 1. It should be note that mentioned above products in condition Central Asian region, where average monthly minimal atmospheric moisture capacity equal to 46%, average annual – 60%, but maximal average monthly is 74%, during the storage they do not absorb moisture in the course of year.

In our point of view according to scale of N. E. Pestov on rate of hygroscopicity the fertilizers prepared in vitro belong to hygroscopic and weak hygroscopic substances [4]. Besides, the fertilizers investigated have sufficient friability with their initial moisture and static strength.

## References:

1. Vinnik M. M., Erbanova L. N., Zaytsev P. M., Ionova L. A., Makarevich V. M., Nepomnyashcaya N. A., Osherovich R. Kh. Methods of analysis of phosphate raw, phosphorus and complex fertilizers, feed phosphates // – Moscow: Chimiya, 1975.– 218 p. (in Russian).

2. GOST 20851.4–75. Fertilizer mineral. Tests on water determination // – Moscow: IPK. 2000.– 6 p. (in Russian).
3. GOST 21560.2–82. Mineral fertilizers. Testing method // – Moscow: State standard, 1982.– 30 p. (in Russian).
4. Pestov N. E. Physicochemical properties granular and powder chemical products // – Moscow, AN SSSR, 1947.– 239 p. (in Russian).
5. Pozin M. E., Kopyilyov B. A., Tumarkina E. S., Bel`chenko G. V. Handbook for practical activity on inorganic chemistry technology // Leningrad: Goshimizdat, 1963.– 376 p. (in Russian).

*Sagin Sergii Victorovych,*
*Candidate of Technical Sciences,*
*associate professor of National University*
*"Odessa Maritime Academy",*
*E-mail: saginsergii@gmail.com*

# IMPROVING THE PERFORMANCE PARAMETERS OF SYSTEMS FLUIDS

**Abstract:** Complex tribotechnical and optical research of systems fluids (fluids that are used for lubrication and cooling of metal surfaces) have been performed. The relations between the properties of the boundary lubricating layer of systems fluids (thickness and degree of ordering of molecules) and the tribological characteristics of the contacting surfaces (resistance to normal load and Friction torque) were established. Tests have shown that the thickness of the boundary layer of lubricating coolant liquids can reach 13.5 … 15.8 mkm, which contributes to an increase in the elastic-damping properties of lubricating coolant liquids and provides a reduction in the frictional torque of tribocoupling.

**Keywords:** lubricating coolant liquids, frictional boundary layer, boundary layer thickness, Friction torque.

**Introduction**

Sea endurance of a ship and need to ensure the operation of all structural elements of the ship power plant (main and auxiliary engines, steam and oil boilers, auxiliary machinery) makes it necessary to carry large volumes of working substances on board the ship. Along with fuel, oil, fresh and drinking water this includes lubricating coolant liquids (LCL). They are used to compensate for temperature and mechanical stresses during machining of high-strength parts (primarily cylinder bushings, pistons and connecting rods of engines, as well as main and intermediate shafts of auxiliary mechanisms). Repair and restoration work with the use of LCL, can take a long time, while the LCL usage can be measured in tens and hundreds of liters per workpiece. LCL amount during repairs in the sea is limited by the volumes of the corresponding technical tanks and by the lack of the ability to replenish it. LCL that can be synthesized on the ship, as well as those that have high lubricating power, have the clear advantage.

**Relevance of research**

When compared to the standard lubricants, one of the disadvantages of LCL is their low lubricity, which makes it necessary to supply LCL to the contact zone with increased pressure and in a large volume. The first requires more power of auxiliary equipment and the second increases its deterioration. Both limit the use of LCL in ship power plants, as it requires not only their increased reserves, but also increases the necessary productivity of the purification mechanisms that perform their regeneration [1]. Therefore, the actual objective of this research is to increase the performing parameters of the LCL (most importantly their antifriction parameter), which can be achieved by activating the intermolecular interactions of LCL and increasing the elastic-damping properties of the lubricating layer separating the contact surfaces.

**Research objective**

The composition of modern LCL includes special chemical compounds that fulfill the functions of surface-active agents. These compounds and elements, due to polymolecular forces, adsorb the boundary level of the liquid on the metal surface, which is characterized by the orientational order of the molecules. The research objective was to determine the influence of the thickness of the

orientational boundary layer of the liquid on the antifriction properties of the metal surface-LCL-metal surface complex, and to develop an experimental express method allowing LCL grading according to their performance parameters.

**Research results**

The most common research techniques that determine the properties of a lubricant in the boundary friction mode are techniques performed using rheometers and friction machines [2].

Tribotechnical researches were performed on a friction machine. The main check parameter was the friction torque [3]. Also, the setting pressure and the time of stable operation of the steel-steel friction pair (as the most common for the marine diesel engine components) were evaluated during functioning under normal load when various LCL were fed to the tribocoupler. The results of the tests are shown in figures 1, 2 and in table 1. The setting moment corresponds to a sharp change in the character of the corresponding graphical dependence (line 2 in Fig. 1, *a, b, c*). LCL of various brands and manufacturers (which are referred to as «1», «2», «3» for commercial reasons) were subjected to the tests, as well as LCL Greterol (granted by Vladimir Vasilyevich Teregerya, candidate of sciences (engineering), professor of Vladimir State University).

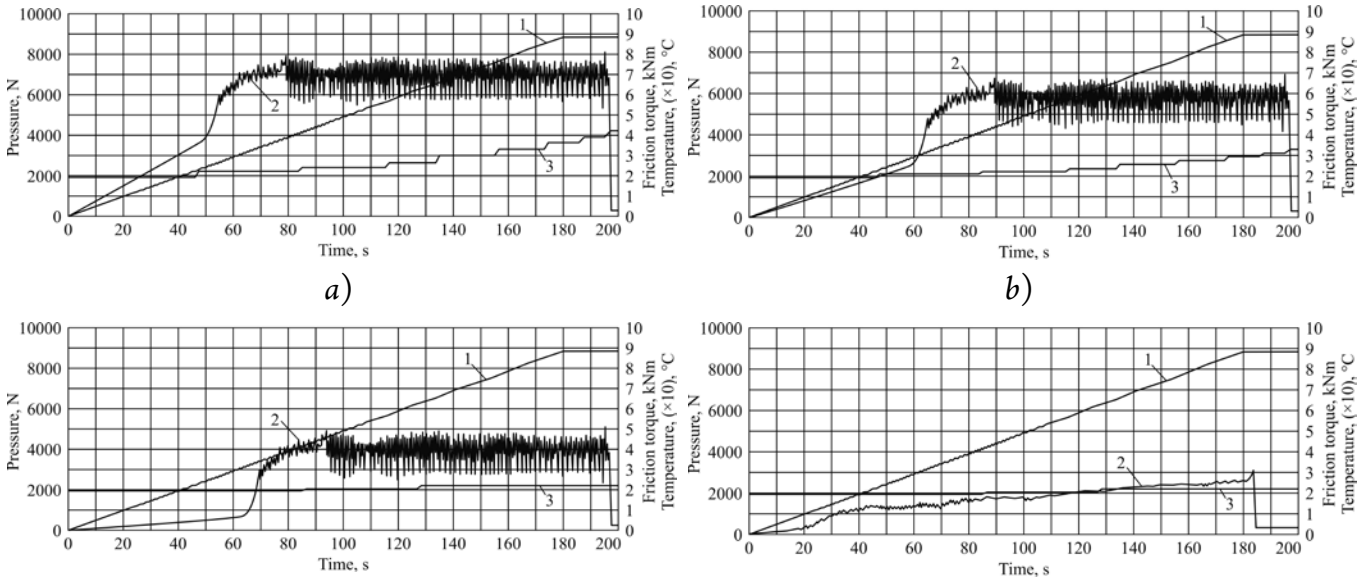


Figure 1. Test results of various LCL on the friction machine: a – «1»; b – «2»; c – «3»; d – Greterol; 1 – applied force, 2 – friction moment, 3 – temperature in the contact zone

For most of the tested materials, the setting pressure was 3.0 … 5.0 kN, and the operating time before setting begins was 75 … 95 s. The maximum compressive force produced by the friction machine was 7.0 kN. When working with LCL Greterol (in a wide spectrum of it concentration changes in water), this amount of compressive force was not enough to destroy the boundary lubricating layer, so the setting moment of it was not recorded (Fig. 1, d). The sinusoidal section on the oscillogram corresponds to the destruction of the boundary layer LCL and to the direct contact of the surfaces. A step-like increase in temperature corresponds to an increase in the number of direct contact between surfaces and an increase in the intensity of their wear. Note that both the sinusoidal variation of the frictional moment and the abrupt temperature rise in the friction zone were observed only for LCL «1», «2», «3». When researching LCL Greterol, these occurrences were not recorded.

The boundary friction (under which LCL operates) is characterized by the anisotropy of some of its parameters, in particular, optical parameters (that is the intensity of absorption of transmitted light). Observation of the changes of this parameter was carried out using the mechanical device, with it the scheme shown in (figure 2) [4].

The light beam from the light source (2) was focused by the lens (1) and directed by a parallel beam through the polarizer (3) to the researched liquid (5). Glass was used to perform the scanning procedure for the boundary layer along the thickness, a wedge-shaped cuvette (4) made of polished quartz. The cuvette was filled with the researched LCL. The molecules of LCL formed a boundary layer with an ordered molecular structure near the quartz surface. During the experiment, the cuvette moved in a direction perpendicular to the direction of the light. The intensity of transmitted light was fixed with a photoelectronic device (6) and transmitted to a personal computer (7) [3].

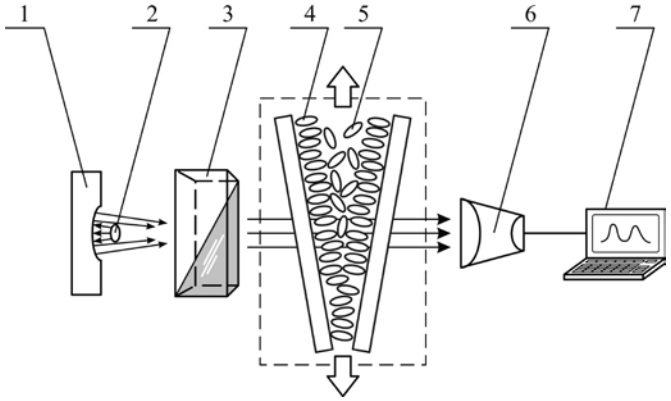


Figure 2. The scheme of the device that determines the anisotropy of the optical characteristics of the boundary layer LCL: 1 – focusing lens; 2 – light source; 3 – polarizer; 4 – wedge-shaped cuvette; 5 – researched liquid; 6 – photoelectronic device; 7 – personal computer

Scanning was carried out using a mechanical device that allowed the cuvette to move without opening the chamber and record the movement with an accuracy of 0.1 mm, which corresponded to a change in the thickness of the gap in the cuvette 1 … 2 nm. The layer thickness was scanned in the range 3 … 20 mkm, which corresponded to the assumed thickness of the boundary layer LCL. The temperature during the experiments was maintained in the range of (20 ± 2)° C. The results of the research are shown in figure 3 and in (table 1).

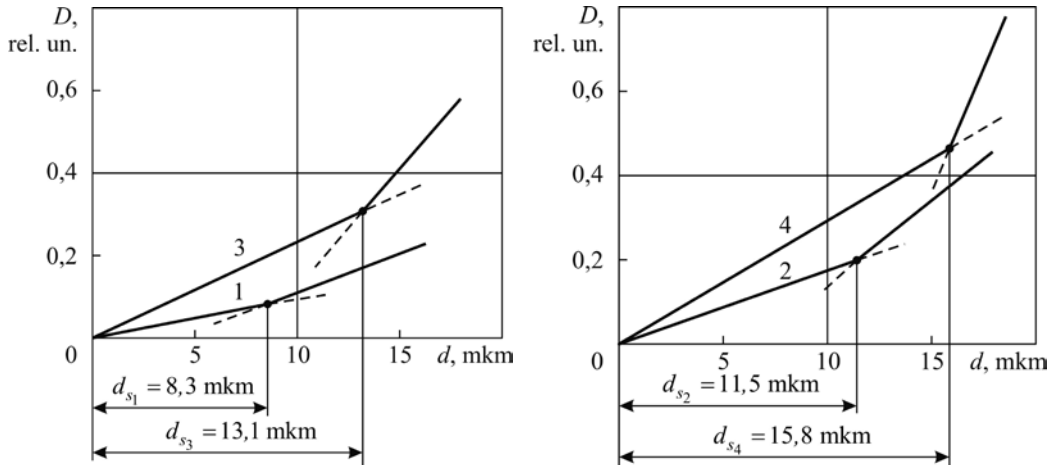


Figure 3. Dependences of the optical density of LCL D (relative units) on the thickness of their multimolecular layer d (mkm): 1 – «1»; 2 – «2»; 3 – «3»; 4 – Greterol

Table 1. – LCL Research Results

| LCL Type | Parameter | | |
|---|---|---|---|
| | Setting load, kN | Operating time (before setting), s | Thickness of boundary layer, $d_s$, mkm |
| Water + LCL «1» | 3.2 | 77 | 8.0…8.3 |
| Water + LCL «2» | 4.3 | 84 | 11.0…11.5 |
| Water + LCL «3» | 5.1 | 94 | 11.2…13.1 |
| Water + LCL Greterol (density 0.5…4%) | exceeds 7.0 | exceeds 185 | 13.5…15.8 |

The performed research made it possible to experimentally determine the dependences of the optical density of different LCL $D$ (relative units) on the thickness of their multimolecular layer $d$ (mkm) – (figure 3).

These dependences can be characterized by two sections – the first corresponds to the optical density of LCL in the boundary layer, the second – to the bulk phase. The inflection point of the correspondence $D = f(d)$ coheres to the thickness of the boundary layer $d_s$, and the initial section is the ordering degree of the LCL molecules in the boundary layer.

The results show that different LCL have unequal tribotechnical characteristics, most important of which are the load at which surface setting occurs and the operating time before setting. We consider that this is due to the different molecular structure of LCL. Among them exists LCL, which consist of long molecular chains with branched groups that aid the formation of oriented molecular structures in their boundary layers. Ordered boundary layers of LCL (as well as in any lubricant) are characterized by a thickness and a degree of order. The conducted research shows that LCL, which possess a more ordered structure of the multimolecular boundary layer, provide the best tribotechnical characteristics of the contacting surfaces [5].

To ensure lubrication functions, LCL include surface-active agents. Moreover, in the "metal-lubricant liquid-metal" triad additional wedging forces arise due to the orientational ordering of molecules in the boundary layers of the liquid. Such forces increase the carrying capacity of the multilayer LCL layer and prevent contact of surfaces. At the same time, these layers have clear "Non-Newtonian" properties and, under certain conditions, acquire the properties of liquid crystals. It is primarily due to an increase in the orderliness of molecules in the boundary layers of the LCL – a property that is completely absent in the bulk phase and is ineffective under hydrodynamic lubrication [6].

Greterol is a type of LCL and its surface active agent is potassium oleate, which is a typical lyotropic liquid crystal, and upon adsorption of its micelles, a 13.0…16.5 μm thick boundary layer is formed on the metal surface that blocks the metal surface and protects it from direct contact with another surface. In addition, we note that the thickness of the boundary layer of LCL Greterol is higher than that of other similar researched LCL. That is why this LCL provides the best tribotechnical characteristics of friction units, primarily the temperature resistance of the lubricating-cooling layer.

Sizes of the boundary layer of researched LCL differ from each other (Table 1). Water-and-Greterol LCL has the greatest thickness of the layer. Moreover, an increase in the concentration of the latter from 0.5 to 4% increases only the thickness of the layer, while the tribological parameters of the friction node remain practically unchanged with such a change in the concentration (in all cases the setting moment was not recorded).

Lower concentration of LCL Greterol relative to water should be noted as well (the recommended

concentration of LCL Greterol is 0.5 … 4%, and for the other researched LCL it is 10 … 25%), which, among other parameters, makes it possible to use Greterol more economically. The rational use of LCL contributes both to increased reliability in the machining of parts, and to increase the economical operation of the ship power plant, similar to when motor oils and fuels are used.

**Conclusion**

The main points of conclusion are:

1. Some chemicals (metal salts of fatty acids) added to LCL as surface-active agents contribute to the formation molecules order in thin lubricant films of these substances. Depending on the type of surfactants used, the thickness of the LCL boundary layer (for the samples studied) is in the range 8.0 … 15.8 mkm.

2. A direct dependence of the thickness of the boundary layer LCL (which is formed at the metal surface) on the tribological characteristics of the friction of triad of metal-LCL-metal exists. With increasing thickness of the boundary layer of LCL, its ability to withstand normal loads, and also 2.5 … 3 times the time of stable operation of the friction unit, increases more than 2 times. Therefore, the thickness of the boundary layer of LCL contributes to the increase in the elastic-damping properties of LCL, which provides a reduction in friction torque in tribocoupling.

3. Given the relationship between the thickness of the boundary layer of LCL and the elastic-damping properties of LCL, an optical method for determining the dichroism of light absorption in the boundary layer can be used as an express method for estimating the tribological characteristics of LCL. This method is characterized by the relative simplicity of the hardware design and carrying out the experiment, and by the thickness of the defined boundary layer, LCL allows them to be ranked according to tribotechnical characteristics (without corresponding long and energy-intensive studies).

**References:**


1. Сагин С. В., Аблаев А. А., Гребенюк М. Н. Снижение энергетических затрат при механической обработке деталей движения двигателей внутреннего сгорания // Проблемы техники. 2013. – № 4. – С. 75–87.
2. Kiriyan S. V., Altois B. A. Rheology of motor oils with quasi-liquid crystalline layers in friction triad // Friction and Wear. 2010. – Vol. 31. – Iss. 3. – P. 312–318.
3. Sagin S. V., Solodovnikov V. G. Estimation of Operational Properties of Lubricant Coolant Liquids by Optical Methods // International Journal of Applied Engineering Research. 2017. – Vol. 12. – Num. 19. – P. 8380–8391. Research India Publication (Index Scopus)
4. Поповский А. Ю., Сагин С. В. Оценка эксплуатационных свойств смазочно-охлаждающих жидкостей судовых технических средств // Автоматизация судовых технических средств: наук.-техн. сборник. 2016. – Вып. 22. – С. 66–74.
5. Zablotsky Yu. V., Sagin S. V. Maintaining Boundary and Hydrodynamic Lubrication Modes in Operating High-pressure Fuel Injection Pumps of Marine Diesel Engines // Indian Journal of Science and Technology. – May 2016. – Vol. 9(20). – P. 208–216. DOI: 10.17485/ijst/2016/v9i20/94490
6. Sagin S. V., Semenov O. V. Motor Oil Viscosity Stratification in Friction Units of Marine Diesel Motors / American Journal of Applied Sciences, 2016. – Vol.13. – Iss. 2. – P. 200–208. DOI: 10.3844/ajassp.2016.200.208

# Section 7. Chemistry

*Juraev Ilkhom Ikromovich,*
*Lecturer of chemistry department*
*of Navoiy State Mining Institute,*
*External doctoral candidate of chemistry department*
*of National University of Uzbekistan*
*named after Mirzo Ulugbek,*
*Tashkent, Vuzgorodok*
*E-mail: kimyo8585@mail.ru*

*Smanova Zulaykho Asanaliyevna,*
*Head of analytical chemistry subdepartment*
*of chemistry department of National University of Uzbekistan,*
*Named after Mirzo Ulugbek, Uzbekistan*
*E-mail: Smanova.chem@mail.ru,*

*Rakhimov Samariddin Bakhtierovich,*
*External doctoral candidate of chemistry department*
*of National University of Uzbekistan*
*Named after Mirzo Ulugbek,*
*Uzbekistan, Tashkent, Vuzgorodok*

## STRUCTURE AND PROPERTIES OF PYRIDILAZO-CONTAINING DERIVATIVES

**Abstract:** The structure and composition of the azo coupling compounds synthesized at the Department of Analytical Chemistry of the National University of Uzbekistan named after Mirzo Ulugbek have been studied. Pyridilazo-containing derivatives were studied by IR and electron spectroscopy, and analytical active and functionally active groups were identified. The optimum conditions for the complexing of copper ions (II) with synthesized reagents are determined. A photometric method for determining copper (II) in various water samples has been developed.

**Keywords:** copper, complex formation, structure, 4-(6-$CH_3$–2-pyridilazo)-m-phenilendiamine.

One of the most formidable challenges to the researchers of organic reagents synthesis is finding a common principle for choosing analytical reagents with high selective ability and sensitiveness. Elaborate study of three-dimensional and electronic structure of reagents, metals and changes occurring at their complexing is necessary to resolve this problem.

Revelation of aforementioned properties should help in outlining of the main direction of synthesis and physico-chemical researches aiming at obtaining

valuable analytical reagents. In the study of new synthesized reagents, complexing is studied primarily on copper ions as they have properties peculiar to them. Studied reagents were synthesized at analytical chemistry subdepartment of chemistry department of National University of Uzbekistan named after Mirzo Ulugbek.

The aim of this study is to synthesize new pyridilazo-containing organic reagents 4-(6-$CH_3$–2- pyridilazo)-5- $CH_3$-resorcinol (6-$CH_3$-PAO); 4-(6-$CH_3$–2- pyridilazo)-m-aminophenol (6-$CH_3$-PAPh); 4-(6-$CH_3$–2-pyridilazo)-m-phenylenediamine (6-$CH_3$-PAPhDA); 4-(6-methyl-2-pyridilazo)-5-diethylaminophenol (PADEAPh) and finding analytical reagents with better selective properties to determine copper ions. Variation of azo coupling compound was achieved by adding analytical-active components to the structure of reagent. It was assumed that π-electronic structure of the reagents and the successive replacement of the ligand center –OH in azo coupling compound by -$NH_2$ will radically change both the nature of the interaction and the electronic characteristics of the excited configurations and the delocalization of mobile π-electrons inside the reagent molecule and their complexes with a copper ion. As a result, synthesized azo reagents based on 6-$CH_3$-aminopicoline are more selective and have higher analytical selectivity.

It was shown by the carried out studies that the sequential introduction of the -$NH_2$ group (transition of resorcinol through *m*-aminophenol to *m*-phenylenediamine) ensures high selectivity of some synthesized reagents (6-$CH_3$-PAPh, 6-$CH_3$-PAPhDa) to copper and sets the task a comparative discussion of the electronic characteristics of the compounds formed, depending on the structure of the ligands. The synthesis was carried out through a series of successive steps, described in the literature [1]. The yield of reagents was 70–75%. After air drying, 6-$CH_3$-PAO and 6-$CH_3$-PAPh have become dark-brown powders and 6-$CH_3$-PAPhDA – resinous substance. Purified by repeated reprecipitation from absolute alcohol, 6-$CH_3$-PAPhDA was analyzed for carbon, hydrogen and nitrogen content, while the calculated values correspond to experimental values [2]. All synthesized reagents are readily soluble in alcohol, acetone, dimethylformamide and poorly soluble in water and diethyl ether. The individuality of all azo compounds was proved by thin layer chromatography in the butanol-hydrochloric acid-water system (100:15:27) [3].

To study the structure and composition of the azo compounds, the infrared spectra (IRS) of the reagents were recorded on the «Avatar system 360 FT-IR» spectrometer produced by Nikolet (USA) using the method of sample pressing with potassium bromide.

In the area of 3000–3600 $cm^{-1}$ of 6-$CH_3$-PAO in IRS a very wide intensity related to the valence vibration of the associated -OH group is visible. Intensity in the area of 1100$cm^{-1}$ is the deformation vibration of phenolic hydroxyl. The group of intensities in the area of 1500, 1600 $cm^{-1}$ is the stretching vibration of –C=C-, -C=N-, -N=N-, in the molecule of reagent. Comparison of 6-$CH_3$-PAPh IS and 6-$CH_3$-PAO IS revealed that 6-$CH_3$-PAPh spectrum in the area of 3000–3600cm-1 has two intensities of –OH and –$NH_2$ primary groups. Changes of intensity form of 6-$CH_3$-PAPh is attributed to –$NH_2$ primary group. Other intensities in 1500, 1610 $cm^{-1}$ are similar to intensities of 6-$CH_3$-PAO reagent [4–6].

However, in 3000–3600 $cm^{-1}$ area of 6-$CH_3$-PAPhDA instead of one wide intensity zone, as in 6-$CH_3$ –PAO spectrum, a split of intensity in 3200, 3330, 3380, 3490 $cm^{-1}$ areas was found, attributed to symmetrical and asymmetric valence vibrations of the primary –$NH_2$ group. Therewith, 1100 $cm^{-1}$ area lacks intensity attributed to deformation vibrations of –OH group at 6-$CH_3$-PAO and 6-$CH_3$-PAPh reagents [6].

To determine the existing forms of synthesized azo reagents in aqueous solution, the light absorption spectra of the reagents were taken from the acidity of the medium: in 10%, 2 n, 0.1n $H_2SO_4$, pH=7 and 0.1 n NaOH on SF-46 from 210–600 nm. Analysis of the light absorption spectra of azo reagents shows

the bathochromic shift of the light absorption maxima attributed to different dissociation of the reagents depending on the acidity of the medium. In neutral and weak-alkaline media, the reagents are in a more reactive ionic state. Consequently, 6-$CH_3$-PAO and 6-$CH_3$-PAPh reagents interact with many metal ions to form brightly colored complex compounds. Apparently, the replacement of one –OH group by –$NH_2$ group (transition from 6-$CH_3$-PAO to 6-$CH_3$-PAPh) is almost unseen in qualitative terms. Yet, the replacement of both hydroxyl groups by –$NH_2$ sharply increases the selectivity and reduces the number of interacting ions (transition from 6-$CH_3$-PAPh to 6-$CH_3$-PAPhDA). Due to its selective properties 6-$CH_3$-PAPhDA reagent was used in the analysis of copper and cobalt in standard samples of steels, soils, donor blood and polymeric metal complexes, the results of which were published in [7–9].

The electronic structure of this azo reagent confirms that 6-$CH_3$-PAPhDA interacts only with cobalt, palladium and copper ions. The use of this reagent made it possible to apply the developed methods for photometric determination of copper [10].

**Determination of copper content in industrial sample**

Developed photometric method for determining copper with 6-$CH_3$-PAPhDA reagent turned out to be sensitive and sufficiently selective. Therefore, during the analysis of the industrial sample, M-138–2 sample was choosen. A weighted proporion of sample (0.500 grams) was dissolved in nitric acid diluted by 1:1 without heating, and after vigorous release, nitrogen oxides were gradually heated to complete removal of nitrogen oxides. After cooling, the solution was diluted to 500 ml. Copper was determined from an aliquot of this solution.

**Method of determination:** a certain amount of sample solution, 2.0 ml of a 0.1% of 6-$CH_3$-PAPhDA reagent solution, 10 ml of universal buffer solution were placed in a measuring cone with a capacity of 25 ml, adding masking agents ($F^-$ 1:800, $CH_3COO^-$ 1:200) and the volume was brought to the mark with distilled water. Optical density was measured on «КФК-2» photoelectric colorimeter at l=1 cm relative to the blank test solution.

The obtained test results of M-138–2 sample, containing Cu 89.820% and their mathematical processing showed that the relative standard deviation does not exceed 0.0148; the relative error is 0.84%, and developed photometric method for determining copper (II), is characterized by high accuracy, selectivity and low boundaries of the concentrations determined.

## References:


1. Иванов В. М. Гетероциклические азотсодержащие азосоединения.– М.: Наука, 1982.– С. 129–136.
2. Мансурходжаев У. М. Синтез, свойства и применение в неорганическом анализе азосоединений // Энцикл.инж.-химика, 2009.– № .5.– С. 76–87.
3. Мансурходжаев У. М., Толипов Ш. Т., Джиянбаева Р. Х. О синтезе новых азокрасителей на основе анабазина, пиридина, хинолина и антипирина. Научные Труды ТашГУ. Вып 435. 1973.– С 30–33.
4. Накамото К. Инфракрасные спектры неорганических и координационных соединений.– М.: Мир, 1966.– С. 198–208.
5. Казицина Л. А., Куплетская Н. Б. Применение УФ-, ИК-, ЯМР-спектроскопии в органической химии.– М.: Высш.шк., 1971.– С. 214–234.
6. Беллами Л. Новые данные по ИК-спектрам сложных молекул.– М.: Мир 1971.– 318 с.
7. Сманова З. А., Мансурхужаев У. М. Экстракционно-фотометрическое определение металлов с азореагентом 2-(5-метилпиридилазо)-2-гидрокси-5-метоксибензолом Вестник НУУз. 2005.– № 4.– С. 124–126.

8. Мансурходжаев У. М., Нематов О. Н. Раздельное фотометрическое определение никеля и кобальта при их совместном присутствии // Вестник НУУз.– Ташкент. 2006.– № 5.– С. 54–59.
9. Сманова З. А., Мансурходжаев У. М., Курбаналиева Р. А. 4-(–метил-2-анабазиназо)-м-фенилендиамин как аналитический реагент // Узб.хим.журн. 1995.– № 3.– С. 9–11.
10. Сманова З. А., Мансурхужаев У. М. Оғир металларни янги реагент ёрдамида аниклаш «Аналитик киме ва экологиянинг долзарб муаммолари» илмий-амалий конференция материаллари. Самарканд 2006.– С. 92–93.
11. Сманова З. А., Турабов Н. Т., Мансурхужаев У. М. Фотометрическое определение никеля. Тезислар туплами. Техносфера, инсон. 2004.– С. 66–68.

*Solikhova Ozoda,*
*assistant professor,*
*Tashkent Chemical Technological Institute,*
*Tashkent, Uzbekistan*
*Organic chemistry and technology*
*of basic organic synthesis department,*
*Tashkent Chemical Technological Institute,*
*E-mail: yaxshiyeva67@mail.ru*

# USAGE OF α-ALUMINUM OXIDE IN THE PROCESS OF ACETYLENE HYDROGENATION IN ETHANE-ETHYLENE FRACTION IN THE STUDY OF PALLADIUM CATALYST

**Abstract:** The research shows the purification processes of ethane-ethylene fraction of pyrolysis gas from acetylene hydrocarbons, which are based on the reaction of catalytic alkynes hydrogenation. The hydrogenation reaction happens after the usage of metallic or oxide catalysts. A contact containing 0.04 wt.% of palladium on α-aluminum oxide with specific surface area of 9 $m^2/g$ was used as a catalyst to research the kinetics of the acetylene hydrogenation processes. The results show that palladium content in supported hydrogenation catalyst affects the selectivity, the total catalytic activity and the duration of the catalyst operation, with the optimum palladium content of 0.2–0.3%. The introduction of alkaline and alkaline-earth elements into the composition of the catalyst does not have a noticeable effect on its properties. The addition of sulfur compounds to the catalyst composition leads to a decrease in its activity during the acetylene hydrogenation, without affecting the activity in the ethylene hydrogenation.

**Keywords:** industrial catalyst, acetylene hydrogenation, ethane-ethylene fraction, hydrogen conversion, acetylene conversion, pilot plant.

Light olefins (ethylene and propylene) are still mainly produced with pyrolysis. Pyrolysis plants today are capable of producing 113 million tons/year of ethylene that is 100% of world production and 38.6 million tons/year of propylene that is a bit more than 65% of world production. The distribution of feedstock produced by pyrolysis is as follows: ethane – 27.6% (wt.), liquefied gases – 14.0% (wt.), straight-run gasoline (naphtha) – 53.1% (wt.), hydrotreated kerosene-gasoil fractions – 5.3% (wt.). Separation of hydrocarbon stream into fractions: methane-hydrogen, ethane-ethylene, propane-propylene, etc. occurs at cooling at temperature of 110–130 °C and pressure from 0.5 to 5.0 MPa. Among them, ethylene and propylene have greatest value due to being used for the production of polymer materials. Due to the fact that the presence of alkynes can lead to the breakage of polymer chain and decrease in the molecular weight of a polymer, the production of polyethylene, polypropylene of various grades and ethylene oxides, requires the feedstock to have a high degree of purity (not more than 10 ppm of acetyl). The ethane-ethylene fraction is subjected to catalytic hydrogenation to purify it from the acetylene impurity. Active palladium catalysts based on γ-aluminum oxide, active carbon (MA-15, PU-2, KhPU-1, G-58I) are the most commonly used for this process. Today the search for

a catalyst comparable with known and widely used industrial catalysts in activity, but with a higher mechanical strength and selectivity, is important.

The ethane-ethylene fraction is subjected to catalytic hydrogenation to remove the acetylene impurity. The purification process of ethane-ethylene fraction (EEF) of pyrolysis gas from the admixture of acetylene hydrocarbons is based on the reaction of catalytic hydrogenation of alkynes. The hydrogenation reaction takes place in the presence of metallic or oxide catalysts. To research the kinetics of the acetylene hydrogenation process, a contact containing 0.04 wt.% of palladium on α-aluminum oxide with a specific surface area of 9 $m^2/g$ was used as a catalyst. Tests of the finished catalyst were carried out at temperatures of 40–60 °C and pressure of 2.3–2.5 MPa and a molar ratio of hydrogen and acetylene of 1.6–1.9. The selectivity of acetylene hydrogenation on this catalyst was 90%.

**Experiment:** an important stage in development and implementation of a new catalyst is the test of its main characteristics in conditions that are as close as possible to the industrial. This is necessary to predict the stability of its operational properties, such as activity, selectivity and performance life, which is of particular importance in the case of the use of expensive metal – palladium.

An estimation of activity and selectivity of test samples and their comparison with industrial catalysts during tests in four-level reactors (laboratory, pilot, experimental and industrial) lead to the completion of our task. Comparative tests of test sample and industrial catalyst G-58I on laboratory, pilot and experimental plants were carried out using a real industrial gas mixture – ethane-ethylene fraction of the composition: ethylene, approximately 55%, ethane 43%, acetylene 0.3%, hydrogen – 0.9%, the rest were methane, propylene, propane, carbon monoxide, etc. In the contact gas, the acetylene content should not exceed 10 ppm. We performed comparative tests on 32 test samples and industrial catalyst G-58I: at minimum temperatures of the acetylene hydrogenation process, at which its complete destruction occurs (not higher than 1 ppm), hydrogen conversion and selectivity corresponding to these temperatures, the formation of a green oil as a result of the course of the ad hoc reactions of oligomerization of ethylene and acetylene at the acid sites of the inner surface of the carrier.

The results obtained on the experimental samples confirm the presence of two types of active centers on the inner surface of the given palladium catalyst, one of which is responsible for the acetylene hydrogenation and is present on a fresh catalyst, the second for the ethylene hydrogenation, its percentage on the surface increases during operation, which means that the selectivity of the hydrogenation process decreases. As a result of the treatment of G-58I catalyst with hydrogen sulphide, part of the active centers responsible for ethylene hydrogenation and acetylene does occur, the overall activity of the catalyst decreases. The rate of the hydrogenation reaction of ethylene increases with increasing content of palladium in the catalyst. As in the case of acetylene hydrogenation, an increase in the rate of ethylene hydrogenation with an increase in the palladium content from 0.03 to 0.1 wt.% can be observed. It should be noted that at the same value of the palladium content in the test sample and the industrial catalyst G-58I (0.5 wt.%), the hydrogenation rate of ethylene at the latter is greater, and the hydrogenation rate of acetylene is, on the contrary, less. Consequently, the selectivity of a sample with a palladium content of 0.5% during the acetylene hydrogenation in the ethane-ethylene stream is higher than the selectivity of G-58I.

**Results and discussion:** comparative tests of test samples and industrial catalyst G-58I on the laboratory, pilot and experimental plants were carried out using a real industrial gas mixture, where ethane-ethylene fraction of the composition is as follows: ethylene, approximately 55%, ethane – 43%, acetylene – 0.3%, hydrogen – 0.9%, the rest are methane, propylene, propane, carbon monoxide, etc. In the contact gas, the acetylene content should not exceed

10 ppm. Kinetic studies of the process of acetylene hydrogenation and ethylene were carried out in a laboratory plant. The temperature dependences of the rate constants of the hydrogenation reactions of acetylene and ethylene for test samples and industrial catalyst G-58I were presented. From the results of comparative tests on a pilot plant and kinetic studies on a laboratory installation, one can conclude that:

– reaction of acetylene hydrogenation is of the first order in acetylene, zero in hydrogen;

– reaction of ethylene hydrogenation – first order in hydrogen and zero in ethylene;

– the rate of hydrogenation reactions of acetylene and ethylene depends on the content of palladium in the catalyst; for test samples it was found that the optimal content is 0.2–0.3 wt.%, it has almost no effect on the reaction rate after 0.5 wt.%;

– additions of sodium sulfide and sodium formate reduces the speed of acetylene hydrogenation reaction, practically without affecting the rate of ethylene hydrogenation, which explains the decrease in the selectivity of the "seeded" test samples;

– activity of test samples in the acetylene hydrogenation prepared by the ethanolamine method is higher than in other samples and industrial catalyst G-58I;

– the best of the brands used for the preparation of test samples of the copper support, was a fresh circular one with a specific surface area up to 3.0 $m^2/g$ and a bulk density of 790 $kg/m^3$;

– no formation of green oil was noted on the experimental samples prepared by the ethanolamine method.

**Conclusion:** We can conclude that acetylene hydrogenation on palladium catalyst has the first order in acetylene and zero order for hydrogen; the order of the reaction of ethylene hydrogenation by hydrogen is equal to one, and by ethylene – to zero. The reaction takes place in the kinetic region at temperatures of 50–70 °C. The characteristics of the corundum carrier are determined by the performance life of the catalyst, its selectivity, the course of side processes (oligomerization of acetylene and ethylene with the formation of a green oil), its mechanical strength. The results show that palladium content in supported hydrogenation catalyst affects the selectivity, the total catalytic activity and the duration of the catalyst operation, with the optimum palladium content of 0.2–0.3%. The introduction of alkaline and alkaline-earth elements into the composition of the catalyst does not have a noticeable effect on its properties. The addition of sulfur compounds to the catalyst composition leads to a decrease in its activity during the acetylene hydrogenation, without affecting the activity in the ethylene hydrogenation.

## References:

1. Накацудзи Хироси, Хада Масахико, Йонэдзава Тэйндзиро. Теоретическое изучение каталитических свойств палладия. Реакция гидрирования ацетилена «Секубай, Catalyst» 2004.– т. 28.– № 2.– 139 с.
2. Nakatsuji H., Hada M. Theoretical research on the catalytic activities of palladium for the hydrogenation reaction of acetylene / "Quantum Chem.: Challenge Transit. Metals and Coord. Chem.: Proc. NATO Adv. Res. Workshop and 40th Int. Meet. Soc.Chem. Phys., Strasbourg, Sept. – P. 16–20." Dordrecht e.a. 2006.– P. 477–487.
3. Beeск O. Catalysis and the adsorption of H on metal catalysts // Dis. Faraday Soc. 2003.– v. 8.– № 118.
4. Tan W., Peng S., Tan C. Исследование кинетики последовательной гидрогенизации ацетилена // «Инъюн хуасю, Chin. J. Appl. Chem.» 2005.– T. 5.– No. 1.– C. 47–51.

*Turakulov Jakhongir Ulugbekovich,*
*Institute of General and Inorganic Chemistry*
*of Uzbek Academy of Science*
*E-mail: joxa86@mail.ru*

# COMPLEX COMPOUNDS OF CALCIUM ACETATE WITH NITROCARBAMIDE

**Abstract:** synthesized homogeneous coordination compounds of calcium acetate with nitrocarbamide. The composition, individuality, methods of coordination of acetate groups and the molecule of nitrocarbamide are established.

**Keywords:** coordination compounds, synthesis, IR spectroscopy, X-ray phase analysis, calcium acetate, nitrocarbamide.

**Introduction.** Rapid development of the chemistry of coordination compounds is due to their application in various fields. The coordination compounds of metals, possessing a number of specific properties, have found wide practical use in many branches of the national economy. For example, in the chemical technology of using multi-ligand coordination compounds is associated with the optimization of the separation processes of the components of the mixture. In analytical chemistry with the help of different ligand coordination compounds, it is possible to lower the detection limit and hang the selectivity of determining a large number of elements and substances. In biochemical systems, the synthesis of some different ligand coordination compounds can serve as models of processes occurring in living organisms. Molecules of nitrocarbamide (NTC) and anion of acetate acid ($CH_3COO^-$) contain donor atoms and promote the formation of coordination compounds with metal ions. In [1–3], coordination compounds of a number of metal carboxylates with amides were synthesized and studied. In the literature there is no information on homogeneous complex compounds of calcium acetate with nitrocarbamide.

**Objects and methods of research.** Synthesis, IR spectroscopy, X-ray phase analysis of homogeneous complex compounds of calcium acetate with nitrocarbamide are given. In the course of the present study, calcium acetate was used for the synthesis of complex compounds of $Ca(CH_3COO)_2 \cdot H_2O$ composition of the "AR" or "R" type. As the ligands used nitrocarbamide ($H_2NCONHNO_2$) brand "AR".

To carry out the synthesis of coordination compounds, we chose the most effective mechanochemical method, since it does not require scarce organic solvents. The synthesis procedure was carried out according to [4].

Analysis of synthesized compounds for calcium content was carried out according to [5]. Nitrogen was determined by the Dumas method [6], carbon and hydrogen by burning in an oxygen flow [Table 1]. To determine the individuality of the synthesized compounds, radiographs were taken on a DRON-2.0 unit with a Cu-anticathode [7]. IR absorption spectra were recorded in the 400–4000$cm^{-1}$ region on the AVATAP-360 spectrometer of Nicolet (Fig. 1–4).

The thermal analysis was carried out on the derivatograph of the Paulik-Paulik-Erdey system [6] at a rate of 10 deg / min and a 0.1 g sample with the sensitivity of the T-900, TG-100, DTA-1/10, DTG-1/10 galvanometers. The recording was carried out under atmospheric conditions with a constant removal of the gaseous medium by means of a water jet pump. The holder was a platinum crucible with a diameter of 7 mm without a cover. $Al_2O_3$ was used as a standard.

For the synthesis of complex compounds, we chose the most effective mechanochemical method, since it does not require scarce organic solvents [7].

The mechanochemical process of interaction of the initial components is carried out by intensive rubbing at room temperature in a ball mill of components taken in molar ratios of calcium acetate and carbamide 1: 2 and 1: 4, respectively. Similarly, all of the following compounds are shown in (Table 1).

In the synthesis of the complex compound $Ca(CH_3COO)_2 \cdot 2H_2NCONHNO_2$, 3.5238g(0.02 mol) of $Ca(CH_3COO)_2 \cdot H_2O$ was triturated from 4.2041 g (0.04 mol) of nitrocarbamide in a ball mill at room temperature for 0.3 hours. The yield of the product is 94.0%.

The compound of the composition $Ca(CH_3COO)_2 \cdot 4O_2NHNCONH_2 \cdot H_2O$ was synthesized by mixing 1.7619g(0.01mol) of $Ca(CH_3COO)_2 \cdot H_2O$ with 4.2013 g (0.04mol) of nitrocarbamide in a ball mill at room temperature in continuation 3 hours. The yield of the product is 96.0%.

Table 1.– Results of elemental analysis of homogeneous coordination compounds of calcium acetate with nitrocarbamide

| Compounds | Elements in percent | | | | | | | |
|---|---|---|---|---|---|---|---|---|
| | Mg,% | | N,% | | C,% | | H,% | |
| | Found | Calculated | Found | Calculated | Found | Calculated | Found | Calculated |
| $Ca(CH_3COO)_2 \cdot 2H_2NCONHNO_2$ | 11.03 | 10.94 | 23.03 | 22.95 | 19.82 | 19.68 | 2.81 | 2.75 |
| $Ca(CH_3COO)_2 \cdot 4H_2NCONHNO_2 \cdot H_2O$ | 7.01 | 6.91 | 29.06 | 28.96 | 16.72 | 16.56 | 3.54 | 3.47 |

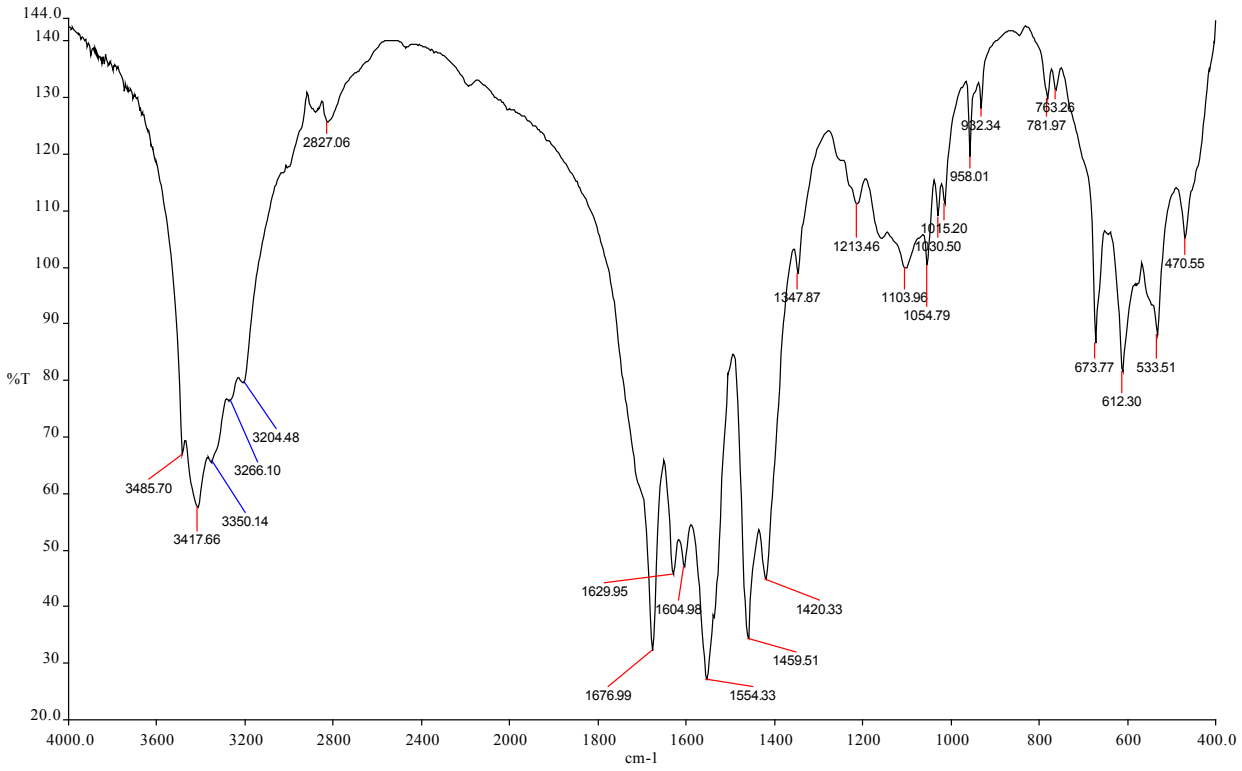


Figure 1. IR absorption spectrum of a homogeneous coordination compound of calcium acetate with nitrocarbamide – $Ca(CH_3COO)_2 \cdot 2H_2NCONHNO_2$

Table 2. – Interplanar distances and relative intensities of calcium acetate lines, nitrocarbamide and their homogeneous complexes

| Compounds | d, Å | I,% | d, Å | I,% | d, Å | I,% | d, Å | I,% | d, Å | I,% |
|---|---|---|---|---|---|---|---|---|---|---|
| $Ca(CH_3COO)_2 \cdot 2H_2NCONHNO_2$ | 16.94 | 6 | 4.42 | 22 | 3.15 | 20 | 2.25 | 12 | 1.779 | 10 |
| | 15.19 | 8 | 4.35 | 22 | 3.09 | 24 | 2.22 | 6 | 1.747 | 8 |
| | 12.96 | 6 | 4.21 | 37 | 3.07 | 22 | 2.20 | 16 | 1.721 | 6 |
| | 10.12 | 6 | 4.11 | 8 | 3.00 | 16 | 2.15 | 29 | 1.687 | 12 |
| | 8.89 | 27 | 4.06 | 18 | 2.92 | 45 | 2.09 | 10 | 1.651 | 8 |
| | 7.73 | 100 | 4.02 | 24 | 2.85 | 12 | 2.06 | 18 | 1.637 | 10 |
| | 7.35 | 18 | 3.99 | 16 | 2.77 | 67 | 2.03 | 10 | 1.612 | 8 |
| | 6.79 | 4 | 3.82 | 51 | 2.63 | 29 | 2.00 | 6 | 1.598 | 6 |
| | 6.15 | 6 | 3.69 | 31 | 2.58 | 27 | 1.959 | 18 | 1.542 | 4 |
| | 5.88 | 6 | 3.60 | 10 | 2.53 | 22 | 1.946 | 27 | 1.538 | 6 |
| | 5.56 | 51 | 3.54 | 6 | 2.50 | 18 | 1.900 | 8 | 1.499 | 4 |
| | 5.08 | 10 | 3.39 | 78 | 2.48 | 47 | 1.875 | 6 | | |
| | 4.86 | 22 | 3.31 | 98 | 2.36 | 4 | 1.846 | 20 | | |
| | 4.56 | 6 | 3.22 | 24 | 2.31 | 6 | 1.810 | 4 | | |
| $Ca(CH_3COO)_2 \cdot 4H_2NCONHNO_2 \cdot H_2O$ | 13.77 | 5 | 4.86 | 2 | 2.70 | 2 | 1.95 | 3 | 1.562 | 1 |
| | 13.35 | 4 | 4.71 | 39 | 2.63 | 2 | 1.91 | 1 | 1.551 | 1 |
| | 12.31 | 4 | 4.48 | 100 | 2.59 | 11 | 1.90 | 3 | 1.534 | 1 |
| | 11.36 | 5 | 4.29 | 19 | 2.53 | 10 | 1.85 | 3 | 1.528 | 1 |
| | 10.35 | 2 | 4.11 | 2 | 2.45 | 4 | 1.84 | 1 | 1.520 | 1 |
| | 9.84 | 1 | 3.99 | 13 | 2.40 | 2 | 1.801 | 4 | 1.505 | 1 |
| | 9.38 | 2 | 3.93 | 2 | 2.37 | 4 | 1.786 | 2 | 1.489 | 1 |
| | 9.07 | 2 | 3.84 | 23 | 2.33 | 3 | 1.766 | 1 | 1.483 | 1 |
| | 8.22 | 2 | 3.82 | 2 | 2.29 | 1 | 1.741 | 2 | 1.467 | 1 |
| | 7.84 | 1 | 3.63 | 6 | 2.26 | 1 | 1.734 | 1 | 1.450 | 1 |
| | 7.50 | 2 | 3.55 | 3 | 2.22 | 1 | 1.717 | 1 | 1.440 | 8 |
| | 7.23 | 2 | 3.51 | 3 | 2.20 | 6 | 1.701 | 1 | 1.426 | 1 |
| | 6.93 | 2 | 3.48 | 3 | 2.18 | 8 | 1.687 | 1 | 1.419 | 1 |
| | 6.64 | 3 | 3.40 | 3 | 2.15 | 4 | 1.664 | 2 | 1.415 | 1 |
| | 6.36 | 2 | 3.34 | 1 | 2.12 | 1 | 1.653 | 2 | 1.406 | 1 |
| | 6.13 | 2 | 3.28 | 17 | 2.10 | 2 | 1.647 | 2 | 1.401 | 1 |
| | 5.96 | 1 | 3.18 | 33 | 2.09 | 1 | 1.633 | 1 | 1.387 | 1 |
| | 5.85 | 1 | 3.08 | 25 | 2.07 | 2 | 1.627 | 1 | 1.383 | 2 |
| | 5.67 | 2 | 3.04 | 5 | 2.06 | 2 | 1.612 | 1 | 1.371 | 1 |
| | 5.52 | 2 | 2.94 | 8 | 2.03 | 1 | 1.600 | 1 | | |
| | 5.32 | 1 | 2.87 | 2 | 2.02 | 1 | 1.595 | 1 | | |
| | 5.20 | 2 | 2.82 | 4 | 2.00 | 2 | 1.585 | 3 | | |
| | 4.97 | 1 | 2.75 | 3 | 1.96 | 10 | 1.570 | 1 | | |

**Results and its discussion.** Comparison of interplanar distances and relative intensities of calcium acetate monohydrate, nitrocarbamide and their complex compounds showed that the new homogeneous coordination compounds differ from each other, as well as from the original components, hence the compounds have crystal lattices (Table 2).

In the infrared absorption spectrum of an uncoordinated molecule of nitrocarbamide, frequencies at 3437 – $\nu_{as}(NH_2)$, 3352 – $\delta(NH_2)$, 3182 – $\nu(NH_2)$, 1704 – $\nu(C=O)$, 1615 – $\delta(NH_2)$, $\nu(CO)$, 1530 – $\nu_{as}(NO_2)$, 1466 – $\nu(CN)$, 1340 – $\nu_s(NO_2)$, 1108 – $-\rho(NH_2)$, 1027 – $\nu_s(CN)$, 785 – $\delta(NH_2)$, 543 – $-\delta(NCO)$.

The following frequencies were detected in the IR absorption spectrum of the complex compound $Ca(CH_3COO)_2 \cdot 2H_2NCONHNO_2$: 3486, 3429, 3316, 3255, 3064, 2851, 2414, 1661, 1634, 1603, 1569, 1484, 1416, 1352, 1217, 1152, 1057, 1028, 946, 789, 726, 610, 534 and 434 $cm^{-1}$ (Fig. 1).

The following frequencies were observed in the IR absorption spectrum of the complex compound $Ca(CH_3COO)_2 \cdot 4H_2NCONHNO_2 \cdot H_2O$: 3485, 3431, 3322, 3256, 2840, 1668, 1631, 1606, 1471, 1443, 1411, 1352, 1218, 1152, 1028, 981, 946, 789, 725, 610, 576 and 534 $cm^{-1}$ (Fig. 2).

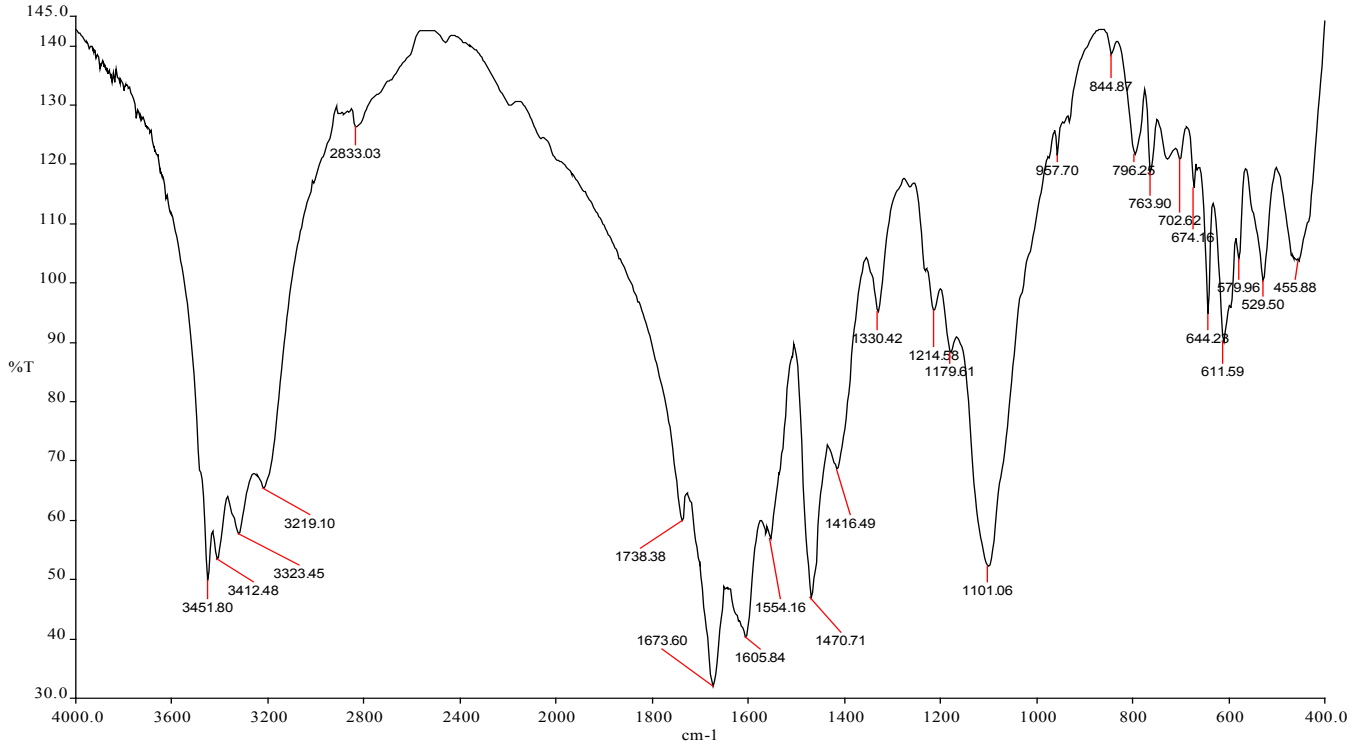


Figure 2. IR absorption spectrum of a homogeneous coordination compound of calcium acetate with nitrocarbamide – $Ca(CH_3COO)_2 \cdot 4H_2NCONHNO_2 \cdot H_2O$

Comparison of the IR absorption spectra of the free molecules of nitrocarbamide and their complex compounds with calcium acetate showed that with the transition to a coordinated position, the values of certain amide frequencies vary significantly. In the complex compounds of the compositions $Ca(CH_3COO)_2 \cdot 2H_2NCONHNO_2$, $Ca(CH_3COO)_2 \cdot 4H_2NCONHNO_2 \cdot H_2O$, the frequencies of the preferential stretching vibration of the C = O bond were 1726 $cm^{-1}$, respectively. While the frequencies of stretching vibrations of the C-N bond of the amide fragment were found at 1484 and 1471 $cm^{-1}$. These changes indicate the coordination of nitrocarbamide molecules through the oxygen atom of the carbonyl group. Water molecules are retained by the presence of hydrogen bonds.

On the heating curve of the compound $Ca(CH_3COO)_2 \cdot 2H_2NCONHNO_2$, seven endothermic effects were found at 122, 195, 247, 317, 411, 527, 828 and two exothermic effects at 603 and 722 °C. The character of the subsequent thermal effects is accompanied by a stepwise decomposition

of the anhydrous compound. In the temperature ranges 80–144, 144–240, 240–285, 285–356, 356–474, 474–552, 552–660, 660–760, 760–860 °C, the weight loss is respectively 1.76; 15.29; 15.88; 14.12; 2.35; 2.71; 3.53; 3.53; 7.06%. The total mass loss in the temperature range 120–800 °C on the TG curve is 66.23%, which corresponds to the formation of calcium oxide.

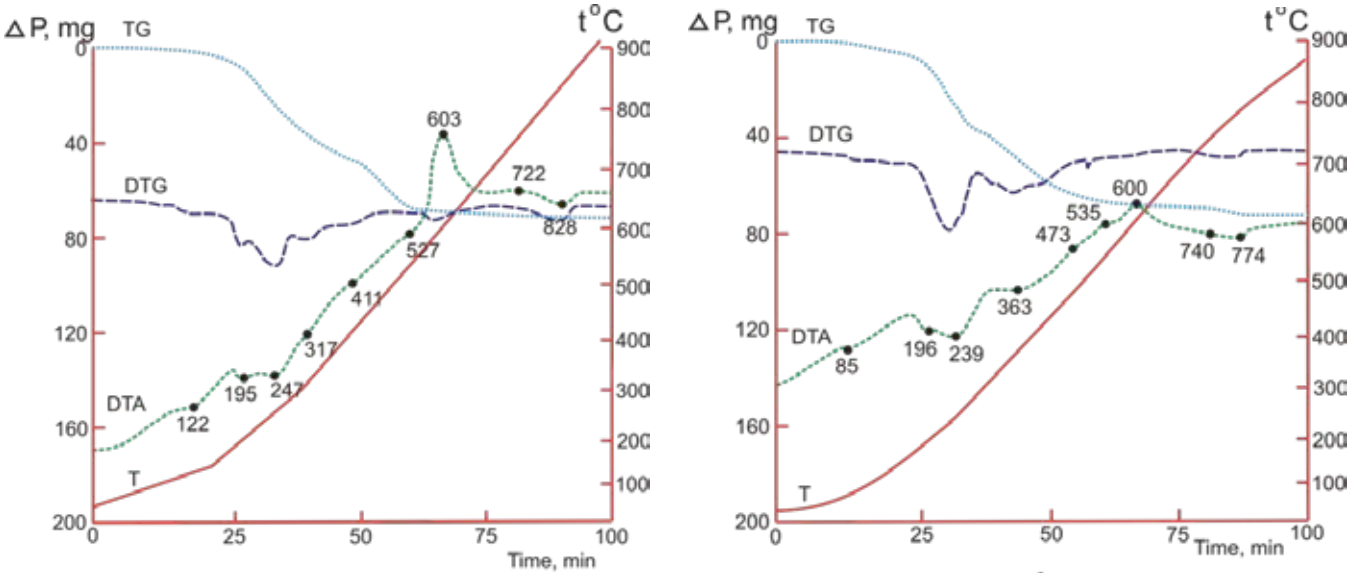


a) b)

Figure 3. Derivatograms: I–$Ca(CH_3COO)_2 \cdot 2H_2NCONHNO_2$; II – $Ca(CH_3COO)_2 \cdot 4H_2NCONHNO_2 \cdot H_2O$

The heating curve of the complex compound $Ca(CH_3COO)_2 \cdot 4H_2NCONHNO_2 \cdot H_2O$ is characterized by seven endothermic effects at 85, 196, 239, 363, 473, 740, 774 °C and two exothermic effects at 535 and 600 °C. The appearance of the first endoeffect is due to the removal of the water molecule. The nature of other thermal effects is associated with a stepwise decomposition of the complex. The mass loss in the temperature range 60–126 °C is 3.04%; 3.02% is calculated. In the temperature ranges 126–204, 204–314, 314–405, 405–504, 504–566, 566–660, 660–750, 750–790 °C the mass loss is 9.09; 27.27; 16.67; 8.59; 2.53; 1.21; 2.53; 2.40%, respectively. The total loss in the temperature range of 60–790 °C on the TG curve is 73.23%, with the formation of calcium oxide.

The synthesis conditions have been developed, homogeneous calcium acetate compounds with nitrocarbamide are isolated in the solid state. The composition, individuality, ways of coordination of apical ligands and acetate fragments and thermal behavior are established. The structure of synthesized complex compounds of calcium acetate with nitrocarbamide is proposed. The new synthesized complexes can be used as stimulator in the cotton grows. The results obtained can be used as reference data for researchers working in the field of coordination chemistry.

## References:

1. Lukachina V. V. Ligand–ligand interaction and stability of multiligand complexes.– Kiev, Naukova Dumka, 1988.– 181 p.
2. Azizov T. A., Azizjonov Kh. M., Suleymanova G. G., Azizov O. T., etc. Mixed–amide complex compounds of some metal carboxylates // Chemical Technology. Article reports of International Conference in Chemical Technology.– Moscow, 2007.– P. 220–221.

3. Meldebekova S. U., Azizov T. A. Pseudoamide complex compounds of nickel (II) acetate // Uzbek chemical journal. Tashkent, 2002.– No. 5. P. 23–28.
4. Direct synthesis of coordination compounds. Ed. acad. NAS Ukraine Skopenko V. V.– Kiev: Vent, 1997.– 175 p.
5. Prishibl P. Complex in chemical analysis. Moscow: IL, 1960.– P. 175–304.
6. Klimova V. A. Basics of the micromethod of analysis of organic compounds.– Moscow: Chemistry, 1967.– 19 p.
7. Kovba P. M., Trunov V. K. X–ray phase analysis.– Moscow: MSU, 1976.– 232 p.

*Fayzullaev N. I.,*
*Shukurov B. Sh.,*
*Samarkand state university*
*E-mail: x-toshpulatov@samdu.uz*

# CATALYTIC AROMATIZATION OF METHANE WITH NON-MO-CONTAINED CATALYSTS

**Abtsract:** In this aricle catalytic aromatization of methane was studied with $(MoO_3)_x \cdot (ZrO_2)_y \cdot (ZnO_2)_z$ content nanocatalyst. Effect of nature different d-elements and their promoter property of catalyst on catalytic dehydrogenaromatization reaction. Interaction between $MoO_3$ and bentonite acidic centers was investigated. Based on obtained results possible mechanism for preparation aromatic hydrocarbons.

**Keywords:** methane, dehydroaromtaization, bentonite, sol-gel technology, nanocatalyst, acidic center, mechanism scheme.

**Introduction**

Effective using of natural gas has been staying problematic for a long time.

Main component of natural gas is methane and its quantity reaches up to 95%. Today methane is used to heat houses, in production of ammonia and hydrogen. Researches to prepare benzene from methane directly started in 90$^{th}$ of previous century [1–4]. Product of dehydroaromatization of methane without oxidants are aromatic hydrocarbons. Arenes, mainly benzene, toluene, ethylbenzene and xylene are important proucts in petroleum chemistry.

Today aromatic hydrocarbons are prepared from catalytic reforming of petroleum fractions. But as decreasing petroleum stock there is requirement to find alternative sources of the preparation of arenes. Alternative sources of preparation of aromatic hydrocarbons are natural gas and biogas. Aromatization of alkanes can be carried out for two different purposes: obtaining liquid fuel with high octane number and aromatic hydrocarbons for petroleum chemistry synthesis [5].

Benzene formation reaction from methane molecule $6CH_4 \rightarrow C_6H_6 + 9H_2$ is highly exothermic ($\Delta H = 523$ kJ/mol), and requires effective catalyst and high temperature to go the process. As a main component of natural gas, methane is thermodynamic stable and durable effects of many reagents. Energy of C-H bond is 398 kJ/mol. Direct synthesis on the basis of methane is very difficult, but its products are more active than methane and reacts easily.

Today Mo-containing mono- and polymetal systems catalysts are good catalysts for methane dehydroaromatization reaction, and zeolites are used in the research to prepare motor oil and aromatic hydrocarbons from natural gas, petroleum. satellite gas and gas condensates [6]. Reaction takes place in presense of zeolite contained catalysts. No oxidant present in the process. Taking into account above mentioned current work aims to study direct catalytic aromatization of natural gas and effect of different factors.

**Experimental part**

Methane conversion absence of oxidants takes place at 600–800 °C and $P = 0{,}1$ Mpa pressure, volumetric rate of methane is 500–1500 hour$^{-1}$. Ratio of methane: argon = 1:1 and in flow reactor.

Reactants and proucts of the reaction were studied with chromatography. Chromatogram of reaction mixture is given in (Fig. 2).

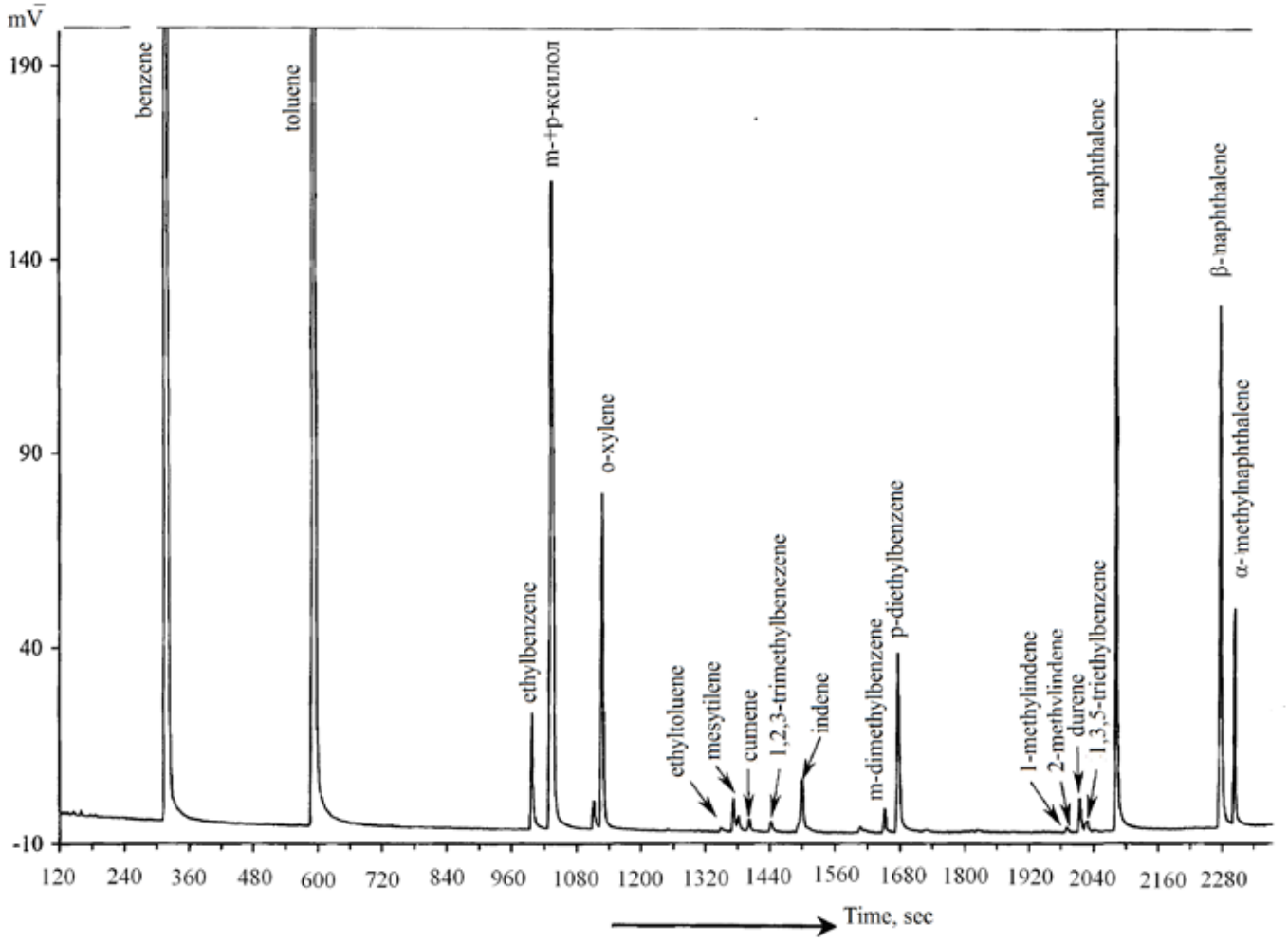


Figure 2. Chromatogram of liquid products of the catalytic aromatization of methane in the presence of selected catalysts

Today Mo-containing mono- and polymetal modified systems catalysts are good catalysts for methane dehydroaromatization reaction. Recently sol-gel method is used at the synthesis of organic-inorganic matrices at low temperatures. This method has advantage because of simplicity of apparatus, cost effectiveness, ecological safer, and adaptive technological features.

Nanocatalysts represent high catalytic activity, selectivity and stability. High effectiveness of nanocatalysts come from charge, energy, mass and information transfer and movement, and this process takes place in nanostructure and reaction in nanosystems. Application of novel nanocatalysts with high effectiveness made it possible improvement of ecological characteristics of industry and technological processes, decrease of waste into the atmosphere, creation of new products and materials. Using nanoparticle catalysts in catalysis depends on the following two points. Firstly, as decreasing of the particles most atoms place on the surface, for this reason nanoparticle catalysts gain high surface area and show high activity in heterogeneous reactions. Secondly, many features of nanoparticles depend on their size (size effectiveness), because of this by changing size of nanoparticle we may change the activity as well as control selectivity. Decreasing size of nanoparticles increases the rate of the reaction.

This method has advantage because of simplicity of apparatus, cost effectiveness, ecological safer, and adaptive technological features. For this reason we chose nanocatalyst with several polyfunctional properties for methane dehydroaromatization process prepared with sol-gel technology with the following content $(MoO_3)_x \cdot (ZrO_2)_y \cdot (ZnO_2)_z$.

Nanocatalyst preparation for methane catalytic aromatization with sol-gel technology is given in (Fig. 3).

Synthesis scheme of core-shell $(MoO_3)_x \cdot (ZrO_2)_y \cdot (ZnO_2)_z$ nanoparticle:

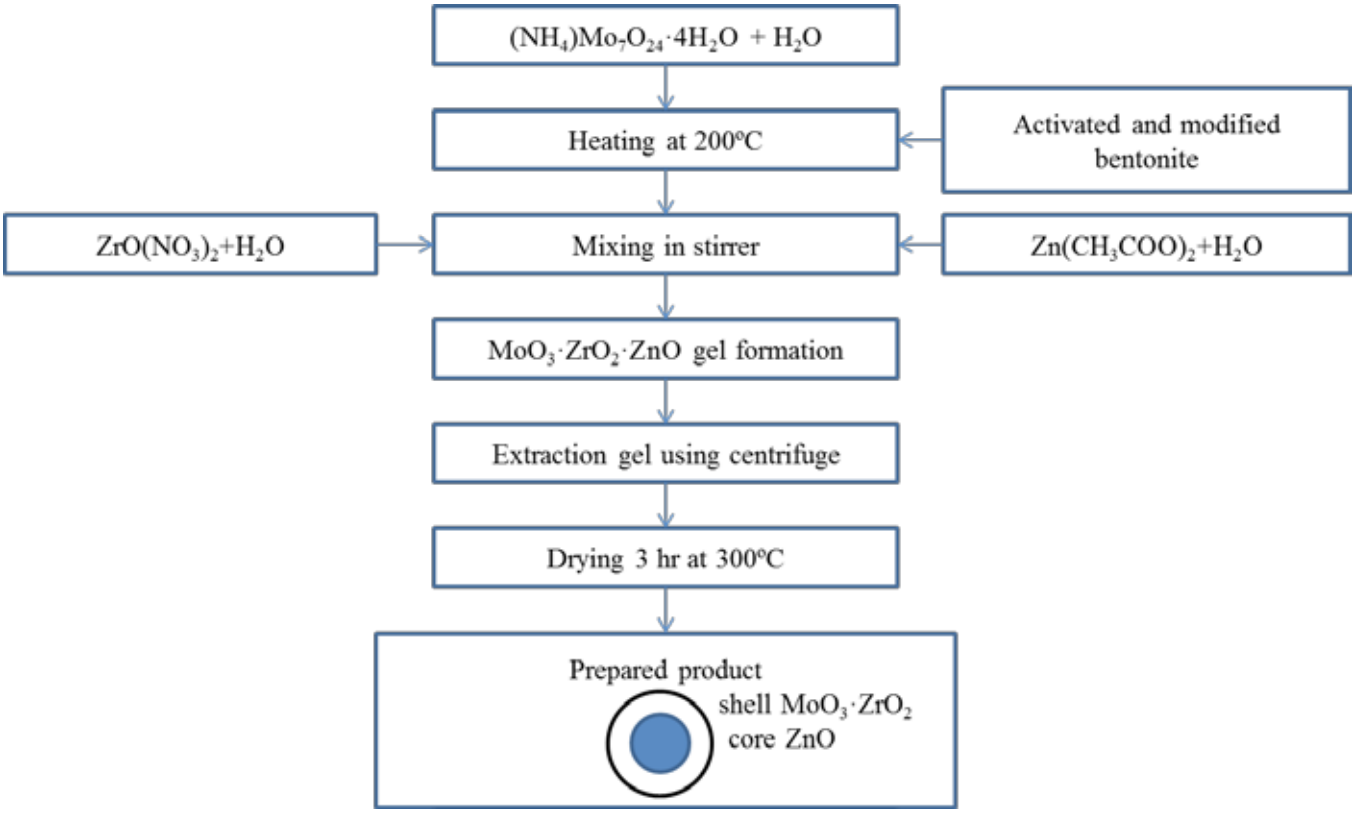


Figure 3. Synthesis scheme of core-shell $(MoO_3)_x \cdot (ZrO_2)_y \cdot (ZnO_2)_z$ nanoparticle

Structure of catalyst active site and state were characterized with electron microscopy and electron diffraction.

**Experimental results and their discussion**

One of drawbacks of non-oxidative methane aromatizion reaction at 700–800 °C is deactivation of catalysts because of coke formation. To keep stability of catalysts different metals are added (Cu, Zr, Pt, Zn, Fe, Co ва ҳ.з) as promoters.

It is known from the literatures that Mo-contained catalysts show high activity in methane aromatization reaction. Core-compound (carrier) of the catalyst made from local raw material – bentonite. Preliminary experiments shown that pure bentonite at the following methane aromatization reaction conditions at 750 °C and $V_{methane}$ = 1000 $hour^{-1}$ has no catalytic effect and no arenes formed. As adding Mo-nanoparticles to bentonite methane conversion to aromatic hydrocarbons observed. Experiments show that optimal concentration of Mo in bentonite is 50% and such catalyst show selectivity and high throughput.

In the formation of aromatic hydrocarbons catalyst with 5% Mo and modification it increases

its catalytic activity. For this reason we studied effect of copper, zinc, gallium, zirconium, manganese, iron, nickel and cobalt metals on the catalyst. Experiments shown that Zr, Zn and Ga modified bentonite catalysts increase the yield of methane aromatization reaction. Experiments shown that zirconium doped catalyst has highest result. Experimental results is shown in (Fig. 4).

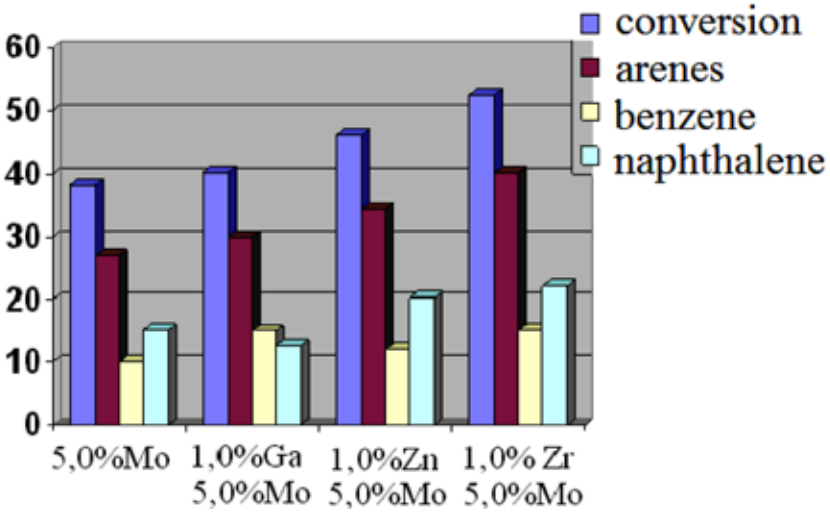


Figure 4. promoter effect of different metals on molybdenum based catalyst

As seen from (Fig. 4), bentonite based catalyst content 1.0% Zr and 5.0% Mo has high catalytic activity. Moreover increase of zirconium concentration from 0.25% to 2%, the optimal concentration found 1.0%. To achieve maximum reaction yield we studied Ga and Zn doped catalysts. Doping Zr–Mo contained catalysts with zinc and gallium increases their catalytic activity. Yield of aromatic hydrocarbons is highest with $(MoO_3)_x \cdot (ZrO_2)_y \cdot (ZnO_2)_z$/ bentonite catalyst.

Table 1.– Effect of temperature on Mo, Zr and Zn nanoparticle modified catalysts for methane catalytic aromatization reaction ($V_{CH_4}$ = 1000 hour$^{-1}$)

| T. °C | $X_{gas}$.% | Reaction products | | | | | | | $Y_{Ap.}$% | $S_{Ap.}$% |
|---|---|---|---|---|---|---|---|---|---|---|
| | | $H_2$ | $C_nH_{2n+2}$ | $C_nH_{2n}$ | $C_6H_6$ | $C_7H_8$ | $C_8H_{10}$ | $C_{10}H_8$ | | |
| *1* | *2* | *3* | *4* | *5* | *6* | *7* | *8* | *9* | *10* | *11* |
| **5.0% Mo/bentonite** | | | | | | | | | | |
| 650 | 18.6 | 2.45 | 85.27 | 3.58 | 3.53 | 0.01 | 0.10 | 5.07 | 8.7 | 46.8 |
| 675 | 26.4 | 3.95 | 76.74 | 2.41 | 5.67 | 0.05 | 0.30 | 10.88 | 16.9 | 64.0 |
| 700 | 31.5 | 4.97 | 72.60 | 1.03 | 6.99 | 0.10 | 0.60 | 13.71 | 21.4 | 67.9 |
| 750 | 38.3 | 8.68 | 65.69 | 0.73 | 9.92 | 0.11 | 0.90 | 15.97 | 26.9 | 70.2 |
| **5.0% Mo-0.5% Zr/ bentonite** | | | | | | | | | | |
| 650 | 21.8 | 1.79 | 84.47 | 2.84 | 3.58 | 0.01 | 0.20 | 7.11 | 10.9 | 50.0 |
| 675 | 32.6 | 4.49 | 74.29 | 2.22 | 4.71 | 0.06 | 0.50 | 13.73 | 19.0 | 58.3 |
| 700 | 39.4 | 6.52 | 66.51 | 1.77 | 8.17 | 0.10 | 0.80 | 16.13 | 25.2 | 64.0 |
| 750 | 49.7 | 8.81 | 50.91 | 1.08 | 12.6 | 1.25 | 1.5 | 17.35 | 32.4 | 65.2 |
| **5.0% Mo-1.0% Zr/ bentonite** | | | | | | | | | | |
| 650 | 31.6 | 1.87 | 79.25 | 2.38 | 6.69 | 0.11 | 0.23 | 9.47 | 16.5 | 52.2 |
| 675 | 43.8 | 5.20 | 65.55 | 2.25 | 10.6 | 0.75 | 0.59 | 15.07 | 27.0 | 61.6 |

| *1* | *2* | *3* | *4* | *5* | *6* | *7* | *8* | *9* | *10* | *11* |
|---|---|---|---|---|---|---|---|---|---|---|
| 700 | 48.6 | 7.72 | 54.72 | 2.06 | 15.5 | 1.08 | 1.22 | 17.65 | 35.5 | 73.0 |
| 750 | 52.5 | 10.8 | 47.85 | 0.92 | 15.2 | 1.32 | 1.87 | 21.98 | 40.4 | 77.0 |
| **5.0% Mo-1.5%Zr/ bentonite** | | | | | | | | | | |
| 650 | 21.6 | 1.57 | 85.82 | 2.21 | 3.87 | 0.12 | 0.20 | 6.21 | 10.4 | 48.2 |
| 675 | 28.3 | 2.86 | 75.27 | 2.07 | 8.65 | 0.59 | 0.30 | 10.26 | 19.8 | 70.0 |
| 700 | 36.7 | 5.27 | 66.63 | 2.20 | 9.8 | 0.72 | 0.50 | 14.88 | 25.9 | 71.0 |
| 750 | 44.6 | 6.57 | 59.57 | 2.06 | 11.4 | 0.96 | 0.70 | 18.76 | 31.8 | 71.3 |

*Note: T – reaction temperature; Xconversion; $Y_{An}$ – yield of aromatic hydrocarbons; $S_{An}$ – selectivity of aromatic hydrocarbon formation*

Effect of temperature on the rate of methane non-oxidative aromatization reaction, yield of the reaction, selectivity and conversion of reactants were studied. Results of the experiment is given in (Table 1).

Maximal amount of aromatic hydrocarbons was obtained with the catalyst of following content: $(MoO_3)_x \cdot (ZrO_2)_y \cdot (ZnO_2)_z$/bentonite. Yield od aromatic hydrocarbons is 40.4% with the catalyst at $V_{CH_4}$ = 1000 hour$^{-1}$, T = 750 °C. Effect of several factors (volumetric rate, temperature, contact time, height of catalyst layer, mass relationship of catalyst active components) on selected catalysts has been studied. Effect of volumetric rate on the rate of aromatization reaction with the $(MoO_3)_x \cdot \cdot (ZrO_2)_y \cdot (ZnO_2)_z$/bentonite catalyst is given in (Table 2).

Table 2.– Effect of volumetric rate on the rate of aromatization reaction with the $(MoO_3)_x \cdot (ZrO_2)_y \cdot (ZnO_2)_z$/bentonite catalyst is given in Table 2. (T = 750 °C)

| $V_{CH_4}$ | X.% | Reaction products.% | | | | | | | A.% | C.% |
|---|---|---|---|---|---|---|---|---|---|---|
| | | $H_2$ | Alkane | Alkene | $C_6H_6$ | $C_7H_8$ | $C_8H_{10}$ | $C_{10}H_8$ | | |
| 500 | 56.8 | 32.65 | 12.15 | 12.01 | 9.68 | 0.73 | 1.01 | 16.06 | 27.48 | 48.38 |
| 1000 | 52.5 | 10.83 | 47.85 | 0.92 | 15.23 | 1.32 | 1.87 | 21.08 | 40.4 | 77.0 |
| 1500 | 49.6 | 8.55 | 50.32 | 1.15 | 15.71 | 1.27 | 2.05 | 17.44 | 7.5 | 73.5 |

It can be seen from the (Table 2) that increase in volumetric rate from 1000 to 1200 hour$^{-1}$ conversion of reactants and yield of aromatic hydrocarbons decreases.

Catalytic activity of the catalyst depends on not only its content, but also thermometric preparation process. When working on catalyst thermomechanically high disperse particles with excess energy form. During in-process for 2–3 hour at 500–600 °C on 1.0% zirconium contained catalyst no change observed in aromatization characteristics. Increase in temperature at 700–750 °C improves aromatization quality of the catalyst. Moreover, cracking and dehydrogenation products formation also decreased.

In addition to catalyst activity and selectivity, another important parameter is its stability of working without lost of high aromatization quality. During aromatization process of hydrocarbons coke forms on the surface of catalyst, and this negatively effects efficiently and its activity gradually decreases. For this reason it requires regeneration of catalysis. Regeneration of catalysis carried out at 650°C and under air stream for 8 hours with gradual increase of oxygen content. After regeneration the catalyst gains its initial full activity.

In lower alkanes aromatization reaction catalysis preparation technology also effects catalyst activity and effectiveness. After zirconile nitrate sorption of bentonite, it thermally worked at 500–650 °C for 2 hours and its catalytic activity studied. At that stage its catalytic activity has not changed. When catalyst

worked at 700–750 °C for 3 hours its aromatization activity dramatically increased. At 750 °C yield of aromatic hydrocarbons reached to 5.2%.

Experiments shown that increase in temperature and volumetric rate leads more coke formation, furthermore because of covering of catalytic active sites with coke catalytic activity decreases. In order to hinder coke formation and decreasing we added 0.2% cobalt to Mo contained bentonite and coke formation dropped. As a result catalysts working time and stability increased.

Increasing volumetric rate of reactants causes conversion and benzene and naphthalene content in products decrease. Moreover $C_2 - C_5$ – olefin and alkylaromatic hydrocarbons content increases. Decrease in volumetric rate follows increase in oligomerizarion and dehydrocyclization reaction activity of olefins and this increases the yield of aromatic hydrocarbons. Increase in methane partial pressure also causes increase of aromatic hydrocarbons yield. From this conclusion, we may propose that aromatic hydrocarbon formation has unique mechanism and not depend on used catalyst content.

Aromatic hydrocarbon formation from methane has very complex mechanism and process takes place with several steps. Calculations shown that at the first step adsorption complex from methane and active site interaction (Fig. 5a) and it dissociates methyl and hydrogen radical. Adsorption complex does not change methane molecule geometry but C –H bonds polarizes. `at transition state (Fig. 5b) hydrogen atom of methane places between carbon and molybdenum linked oxygen atom. Dissociated hydrogen atom form OH gropu with oxygen atom and methyl radical interacts with molybdenum atom forming chemical bond.

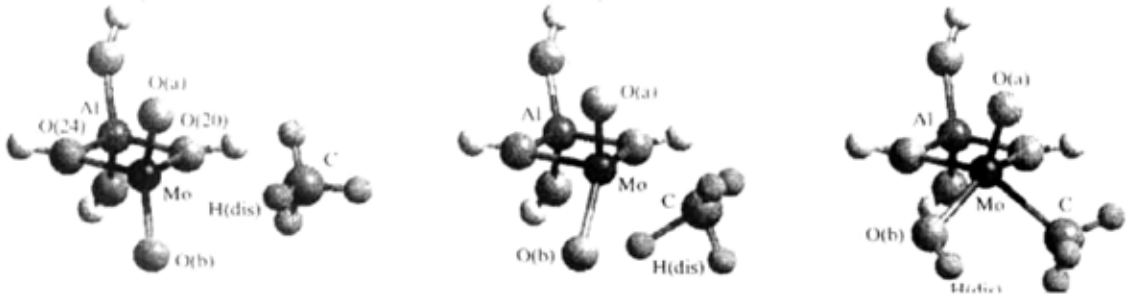


Figure 5. Interaction of active site with methane molecule forming a) adsorption complex; b) transition state and; c) covalent bond

OH amd $CH_3$ groups makes stable methane addition products and forms covalent bond with molybdenum atom (Fig. 5c). There $MoO_3$ interacts with acidic centers of bentonite forming following complex ions:

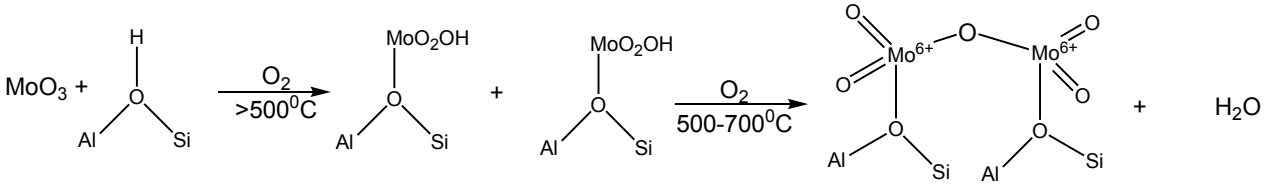


Scheme 1. Formation if $[Mo_2O_5]^{2+}$ dimers at Bronsted acidic surfaces

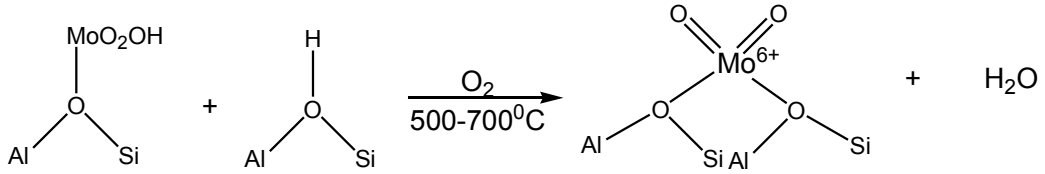


Scheme 2. Formation of $[MoO_2]^{2+}$ cation at Bronsted bridge area

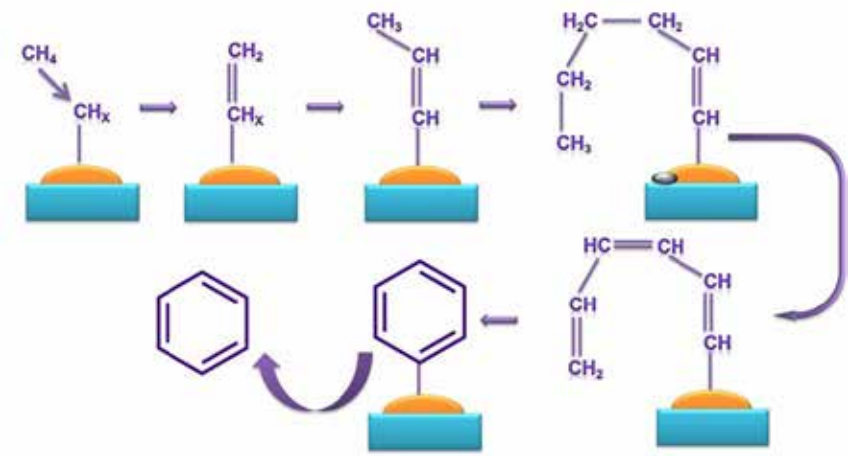

Scheme 3. Benzene formation scheme

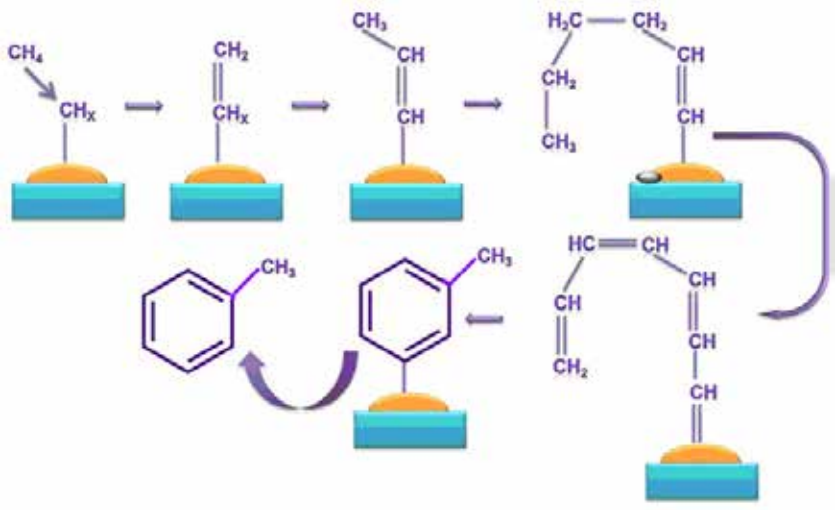

Scheme 4. Toluene formation scheme

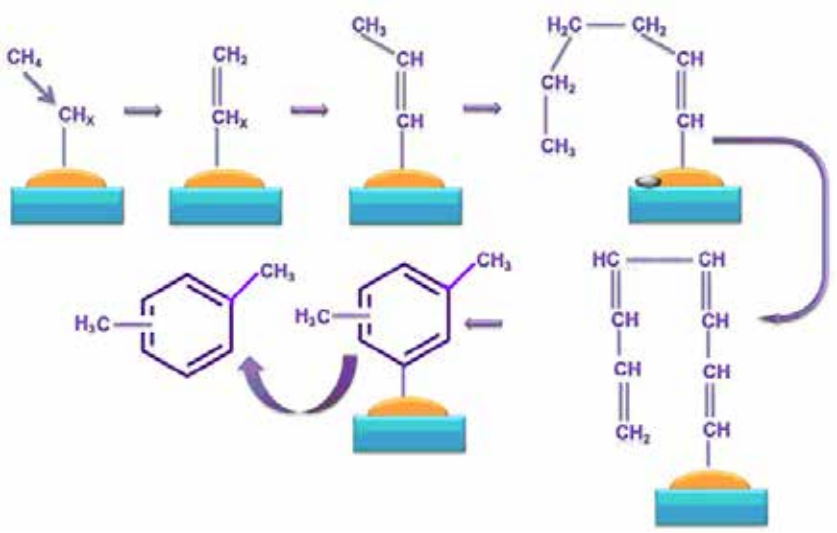

Scheme 5. Xylenes formation schemes

Figure 6. Schematic representation of methane dehydroaromatization

Based experiment results and references we propose the following scheme aromatic hydrocarbon formation form methane:

Based on knowledge about reaction mechanism, reaction elementary steps, rate constants and kinetic equations containing absorption coefficients can be drawn. Application knowledge about reaction mechanism one can draw different kinetic equations for one reaction. After identification of kinetic parameters conclusion can be made about satisfactory equation.

**Conclusions**

1) Appropriate polyfunctional nanocatalyst $(MoO_3)_x \cdot (ZrO_2)_y \cdot (ZnO_2)_z$ with sol-gel technology methane dehydroaromatization process.

2) With selected $(MoO_3)_x \cdot (ZrO_2)_y \cdot (ZnO_2)_z$/ bentonite catalyst yield of aromatic hydrocarbon at $V_{CH_4}$ = 1000 hour$^{-1}$, T = 750 °C found 40.4%.

3) Different d-metals nature and their promoter characteristics for methane catalytic dehydroaromatization reaction catalyst activity.

4) Based on experimental results mechanism of aromatic hydrocarbon formation from methane proposed.

## References:


1. Госсен Л. П., Величкина Л. М. Экологические проблемы использования нефтегазовых запасов и получения высококачественных нефтепродуктов // Нефтехимия. 2012.– Т. 52.–№ 2.– С. 154–158.
2. Туктин Б., Шаповалова Л. Б., Егизбаева Р. И., Комашко Л. В. Неокислительная конверсия метана в ароматические углеводороды на монометаллических молибденсодержащих катализаторах // Известия НАН РК. Серия химия и технология. 2013.– № 6.– С. 40–45.
3. Файзуллаев Н. И., Туробжонов С. М. Метан ва нефтнинг йўлдош газларини каталитик ароматлаш // Кимё ва кимё технологияси. 2015.– No. 2.– Б. 3–11.
4. Туктин Б., Шаповалова Л. Б., Егизбаева Р. И., Шаповалов А. А. Неокислительная конверсия метана в ароматические углеводороды на $Mo/A1_2O_3$ и $Mo–Co/A1_2O_3$ катализаторах, промотированных бентонитом ZSM // Известия НАН РК. Серия химия и технология. 2013.– № 6.– С. 46–51
5. Мамонов Н. А. Фадеева Е. В., Григорьев Д. А., Михайлов М. Н., Кустов Л. М., Алхимов С. А. Металл–бентонитные катализаторы дегидроароматизации метана // Успехи химии – 2013.– Т. 82, № 6.– С. 567–585.
6. Vosmerikova A. V., Zaikovskii V. I., Kozlov V. V. Methane conversion into aromatic hydrocarbons over Ag–Mo/ZSM-5 catalysts // Reaction kinetics and catalysis letters. 2011.– Vol. 52ю – № 3.– P. 427–433.

*Shukurullaev Botir Amanbaevich,*
*Institute of General and Inorganic Chemistry,*
*Academy of Science of the Republic of Uzbekistan,*
*Senior Research Associate, a doctorate candidate*
*E-mail: ximtex.botir86@mail.ru*

*Yusupov Farhod Makhkamovich,*
*doctor of Engineering Science,*
*Head of the laboratory "Chemical Technology"*
*Institute of General and Inorganic Chemistry,*
*Academy of Science of the Republic of Uzbekistan,*
*E-mail: ximtex.botir86@mail.ru*

# COMMERCIAL OIL SLUDGE AS A SOURCE OF BINDER FOR ASPHALT-CONCRETE ROADS AND THEIR QUALITY

**Abstract:** Qualitative indicators of resulting resinaceous binder as density, softening temperature, dropping, viscosity, molecular weight, penetration and others were high enough. The obtained product meets the normative requirements of petroleum bitumen for road asphaltic coating and can be used instead of Jarkurgan oil.

**Keywords:** oil, oil sludge, bitumen, binder, sulfonating, viscosity, penetration.

Analysis of the published literature showed that, it is very important to find new sources of petroleum bitumen for construction of broad front of new buildings and new motor roads in accordance with the needs of the Republic, which is rapidly developing after independence. Thereby our choice has focused on oil sludge, whose reserves are estimated at millions of tons, they currently do not have proper application and in many cases are not disposed of, but buried as oil wastes [1–3].

According to the research of many types of reservoir oil sludge, it is established that the ratio of petroleum products, water and mechanical impurities (particles of sand, clay, rust, etc.) varies within very wide limits. Hydrocarbons are 5–90%, water is 1–52% and solid impurities are 0.8–65%. As a consequence, such significant change in the composition of oil sludge determine the range of changes in their physical-chemical characteristics, which are very broad.

Table 1.– Natural composition of various oil sludge

| Name of composition | Types of oil sludge,% of mass | | | |
|---|---|---|---|---|
| | Reservoir | | | |
| | From kerosene | From diesel | From slurry-basin-terminal | From oilfields |
| Carbohydrates | 88–93 | 86–90 | 85–90 | 82–90 |
| Mineral impurities | 3.8–4.5 | 5.7–6.1 | 9.5–10.2 | 8.5–10.7 |
| Crystallization water | 1.5–3.2 | 2.9–3.4 | 3.5–4.6 | 2.2–3.0 |

The compositions for various types of oil sludge are confirmed by the data of their analysis and average intervals of their hydrocarbons content are presented.

Table 2. – Group Composition of oil sludge

| Name of group hydrocarbon composition | Types of oil sludge,% | | | |
|---|---|---|---|---|
| | Subterranean | Bottom | Reservoir | Commercial |
| High-molecular paraffin | 42–50 | 32–35 | 30–35 | 25–40 |
| Condensed aromatic | 8–10 | 20–25 | 10–12 | 20–25 |
| Naphthene-Aromatic | 15–17 | 20–22 | 25–35 | 15–17 |
| Asphaltene-resinous | 13–15 | 10–15 | 15–20 | 30–35 |

The densities of oil sludge range from 930–1300 kg / m, and the congelation temperature from –3 °C to + 80 °C. The flash point is in the range from 35 to 120 °C. When water enters the volume of petroleum derivatives, stable water-oil emulsions form, which are stabilized by the natural stabilizers contained in the petroleum products from a number of asphaltenes, resins and paraffins. The upper layer of oil sludge is a watered oil, which contains up to 5% finely dispersed impurities and belongs to the class of water-in-oil emulsions. The composition of this layer includes 70–80% of oil, 6–25% of asphaltenes, 7–20% of resins, and 1–4% of paraffins. The water content does not exceed 5–8%. The organic part of the freshly formed upper layer of the oil sludge is fairly often similar in composition and properties to the original petroleum product stored in the tanks.

The oil of Southern Uzbekistan (Jarkurgan) is a good raw material for obtaining road bitumen [4], which contains up to 90% of excise resins, high sulfur (more than 3%), paraffin (about 3%) and small amounts of light fractions.

The quality of the Jarkurgan oil processed to road bitumen is as follows:

Density, d204 0.9584;
Molecular weight 396;
Sulfur,% of mass 4.0;
Neutral resins,% of mass 28.1;
Excise resins, volume% 92;
Asphaltenes content,% of mass 1.9;
Coke content,% of mass 8.87;
Nitrogen,% of mass 0.5;
Paraffin with destruction,% of mass 2.93;
Congelation temperature, °C 2;
Flash temperature, °C 96;
Acid number, mg KOH/g 0.45;
Relative viscosity, at 100 °C 3.7.

It can be seen from the given data, that the Jarkurgan oil is sulphurous and paraffinic.

The bitumen obtained from Jarkurgan oil, is an externally dark, solid mass with the following characteristics:

Softening temperature in K and W, °C 88;
Penetration at 25 ° 15;
The content of insoluble in hot benzene substances,% 0.32;
Ash content,% 0.08;
Flash temperature according to Brenken, °C295;
Solubility in linseed oil in the ratio of bitumen:
oil = 1: 1 at a temperature of 270–280° full;
Solubility of bitumen alloy with linseed oil in white – alcohol in the ratio of alloy:
white – alcohol = 2: 1 full

We used oil sludge from the Feruza mine of «Shurtanneftegaz» LLC as an object of research to obtain the binder. The inquired into sample was a dark and viscous paste and had the following physicochemical parameters:

Viscosity according to VZ-3 at 50 °C, sec 28;
Density at 20 °C, kg/m$^3$ 988;
Content of oil fractions,% up to 98;
Residual water content,% up to 22

In subsequent investigations we indicate the range of the obtained results, due to the fact that the oil sludge in the initial state was a heterogeneous mass.

An analysis of the group composition and the determination of the physicochemical properties of the oil sludge yielded the following results:

Specific gravity, g/cm$^3$ 0.990 – 1.150;
Congelation temperature, °C 17–20;
Viscosity according to VZ-3 at 60 °C, sec10–12;
Hydrocarbons,%
– condensed naphthenes (asphaltenes) 20–30;
– hydrocarbons of the alto naphthalene series 15–25;
– resinous substances 5–8.

The reservoir oil sludge can be a raw material for obtaining the binder base of highways according to obtained data.

This task was solved based on the development of a technological process for the sulfonating of oil sludge on a model plant with concentrated sulfuric acid in order to create a tarry (bitumen analog) binder that could be used in sandy-gravel decking of highways [5–7].

The resulting binder from the oil sludge has similar characteristics to road bitumen.

Sulfonating of the oil sludge yielded a dark solid mass, soluble in liquid hydrocarbons – a binder with the following properties: specific gravity: 1.085–1.115 g/cm$^3$; the viscosity $\eta$ according to VZ-4 at 60 °C – 40–43 sec; softening point is 50–54 °C. The resulting binder from the oil sludge has similar characteristics to road bitumen (Table 3).

The obtained binder had sufficiently high qualitative indices (density, softening temperature, dropping, viscosity, molecular weight, penetration, etc.). This product meets the normative requirements of petroleum bitumen for road asphaltic coating and can be used instead of Jarkurgan oil.

Table 3.– Physicochemical properties of the resulting binders

| № | Sludge ratio: $H_2SO_4$ | Temperature, K | Time, min | Relative viscosity, Ø Of limber hole 5 mm, $C_{60}^5$, sec | Penetration At 298K, mm | Softening temperature (по КИШ), K | Extensibility at 298K, sm |
|---|---|---|---|---|---|---|---|
| 1. | Control of oil sludge | | | 22 | | | |
| 2. | 98: 2 | 403 | | 78 | 70 | 313 | 45 |
| 3. | 97: 3 | 403 | | 147 | 80 | 314 | 53 |
| 4. | 95: 5 | 403 | 30 | 530 | 90 | 315 | 62 |
| 5. | 90: 10 | 403 | 30 | Viscous mass | 137 | 316 | 65 |

The resulting binder was tested in road construction on the routes of SJSC "Uzavtoyul" with positive results and recommended for application in road construction, in particular, in the construction of asphalt road bases.

## References:


1. Gureev A. A. Technology of production of road bitumen. Chemistry and technology of fuels and oils, 2005.– No. 3.– P. 54–55.
2. Gureev A. A. In the book Collection of reports of the III All-Russian scientific-production conference on problems of production and application of bituminous materials, Perm (RF), 2007.– P. 35–47.
3. Konovalov A. A., Andreev A. F. In the book Collection of reports of the III All-Russian scientific-production conference on problems of production and application of bituminous materials, Perm (RF), 2007.– 313 p.
4. Khodzhaev G. H., Dmitriev P. P., Ryabova N. D. and others "Oil of Southern Uzbekistan (Jarkurgan)". In the book Oil of Uzbekistan, Publishing House of the Academy of Sciences of the Uzbek SSR.,– Tashkent, 1962.– P. 213–241.

5. Alimov A. A. Asphaltic bitumen based on commercial oil sludge. Regional Central Asian International Conference on chemical technology "HT-12",– Moscow, 2012.– P. 225–228.
6. Shukrullaev B. A., Yusupov F. M., Bekturdiyev G. M. Sulfurization of the tank oil sludge of the Angren terminal in order to obtain asphalt bitumen. Uzbek Chemistry magazine, 2002.– No. 5.– P. 54–56.
7. Shukrullaev B. A., Yusupov F. M., Khamraev S. S. Asphalt-bitumen production for paving on the basis of commercial oil sludge. Thesis of reports of International Conference "Catalytic Processes of Oil Refining: Petrochemicals and Ecology", Tashkent, 2013.– P. 236–237.

# Contents